



**Andreia Santos
Paula**

**Aplicação de métodos de otimização à cromatografia
líquida 2D**

**Application of optimization methods to the 2D liquid
chromatography**

Dissertação apresentada no Departamento de Química da Universidade de Aveiro para cumprimento dos requisitos necessários à obtenção do grau de Mestre em Química - Especialidade em Química Analítica e Qualidade, realizada sob a orientação científica do Doutor Armando da Costa Duarte, Professor Catedrático do Departamento de Química da Universidade de Aveiro, e da Doutora Regina Maria Brandão de Oliveira Duarte, Investigadora Auxiliar do Centro de Estudos do Ambiente e do Mar (CESAM) da Universidade de Aveiro.

Aos meus pais e avó.

O Júri

Presidente

Prof. Doutor Artur Manuel Soares da Silva
Professor Catedrático do Departamento de Química da Universidade
de Aveiro

Prof. Doutora Teresa Alexandra Peixoto da Rocha Santos
Professora Associada do ISEIT/Viseu do Instituto Piaget

Doutora Regina Maria Brandão de Oliveira Duarte
Investigadora Auxiliar do Centro de Estudos do Ambiente e do Mar
(CESAM) da Universidade de Aveiro

Agradecimentos

Para a realização desta dissertação tive o apoio de diversas pessoas as quais gostaria de deixar o meu *Muito Obrigada*.

Em primeiro lugar, gostaria de agradecer aos meus orientadores, Doutor Armando da Costa Duarte e Doutora Regina Maria Brandão de Oliveira Duarte pela disponibilidade, compreensão, dedicação e amizade demonstrada durante ano.

Aos meus pais e avó, por todo o apoio, educação e carinho que demonstraram nesta etapa.

Ao meu namorado por me aturar nos bons e maus momentos e por me apoiar sempre.

Aos meus amigos, especialmente à Telma, e colegas de laboratório, especialmente ao João Matos, por toda ajuda e disponibilidade demonstrada durante o desenvolvimento de todo o trabalho. Também agradeço à Sónia e à Catarina todo o apoio. Obrigada pelas gargalhadas e boa disposição.

Palavras-chave

Cromatografia líquida bidimensional abrangente; otimização; coluna de modo misto de fase reversa/troca aniónica; coluna de fase reversa de octadecil de sílica; amostras de vinho tinto.

Resumo

Esta dissertação teve como principal objectivo a aplicação de metodologias quimiométricas de otimização em cromatografia líquida bidimensional abrangente (LC×LC) por forma a determinar as condições ótimas para a separação de amostras de vinho tinto português. Para este estudo, foi utilizada, na primeira dimensão, uma fase estacionária de modo misto de fase reversa/troca aniónica (Acclaim® Mixed-Mode WAX-1, *denominação em inglês*) e, na segunda dimensão, uma fase reversa de octadecilsílica (C18). O LC×LC foi acoplado a um detector de fotodíodos, a operar na gama de comprimentos de onda de 221 a 400 nm. O modo de eluição por gradiente foi adotado para ambas as dimensões cromatográficas. O planeamento experimental D-Optimal foi considerado o mais adequado para a otimização na primeira dimensão, tendo permitido identificar entre um conjunto de 6 variáveis experimentais (% MeOH_i, [Buffer]_i, t_i, % MeOH_f, [Buffer]_f, and t_f), quais as mais importantes que afetam a qualidade de separação cromatográfica, em termos unidimensionais, de uma amostra composta de vinhos tintos portugueses. A qualidade de separação cromatográfica foi avaliada utilizando uma função de resposta cromatográfica (CRF, *sigla inglesa para "chromatographic response function"*) previamente desenvolvida por Duarte & Duarte (2010) (DCRF), concluindo-se que as variáveis mais importantes são % MeOH_i and % MeOH_f. A otimização da separação na segunda dimensão foi efectuada utilizando já o sistema LC×LC, e recorrendo ao método Simplex para o estudo das duas variáveis mais importantes que afectam a eluição por gradiente numa coluna de fase reversa C18: % MeOH_i and % MeOH_f na fase móvel. A qualidade de separação cromatográfica bidimensional foi avaliada utilizando uma CRF previamente desenvolvida por Duarte *et al.* (2010) (DCRF_{f,2D}). Nas condições ótimas estimadas para a aplicação da técnica de Mixed-Mode WAX-1×C18, para a separação de uma amostra representativa dos vinhos tintos portugueses seleccionados, foram registados 59 picos no espaço cromatográfico, em 150 minutos de tempo total de análise. Utilizando as condições de separação cromatográfica previamente otimizadas, efectuou-se a análise de 4 amostras de vinho tinto português a fim de se verificar a existência, para posterior comparação, de perfis cromatográficos diferentes.

Keywords

Comprehensive two-dimensional liquid chromatography; optimization; mixed-mode reverse phase/anion exchange column; conventional reverse phase column of octadecyl silica; red wine samples

Abstract

The main objective of this work was the application of chemometrics to the optimization of comprehensive two-dimensional liquid chromatography (LC×LC) in order to find the optimal conditions for the separation of samples of Portuguese red wines. A column with a stationary phase mixed-mode reverse phase/anion exchange (Acclaim® Mixed -Mode WAX -1) was used as the first dimension, and a reverse phase column of octadecylsilica (C18) was used as the second dimension. The LC×LC was coupled to a photodiode detector, operating in the wavelength range of 221-400 nm. A gradient elution mode was adopted for both chromatographic dimensions. The D-Optimal design was considered the most suitable for the optimization of separation in the first dimension (¹D) and it allowed from a set of 6 experimental variables (% MeOH_i, [Buffer]_i, t_i, % MeOH_f, [Buffer]_f, and t_f) the identification of the most relevant for the quality of chromatographic separation of a composite sample of selected Portuguese red wines. The quality of the chromatographic separation was evaluated using a chromatographic response function (CRF), previously developed by Duarte and Duarte (2010) (DCRF). Thus, it was concluded that the most important variables affecting the separation of the sample in the first dimension are the % MeOH_i and % MeOH_f. The optimization of separation in the second dimension (²D) was performed using now the LC×LC system, and using the Simplex method for the study of two most important variables affecting gradient elution on a reverse phase C18 column: starting and ending of the organic solvent (eg, methanol) concentration in the mobile phase. The quality of the two-dimensional chromatographic separation was evaluated using a CRF previously developed by Duarte *et al.* (2011) (DCRF_{f,2D}). Under the optimum conditions for the separation of a composite sample of Portuguese red wines by the technique of Mixed -Mode WAX-1×C18, 59 peaks were recorded in 150 minutes of total analysis time. Using conditions previously optimized a chromatographic separation of 4 Portuguese wine samples was carried out in order to compare chromatographic profiles associated with different samples

Table of contents

<i>Table of contents</i>	XV
<i>List of figures</i>	XIX
<i>List of tables</i>	XXV
<i>List of abbreviations</i>	XXIX
I Aims and structure of dissertation	1
1.1. Introduction	3
1.2. Aim of the dissertation	4
1.3. Structure of the dissertation.....	4
II Two-dimensional liquid chromatography: basic concepts	7
2.1. The emergence of comprehensive two-dimensional liquid chromatography (LC×LC).....	9
2.2. Structure of data in LC×LC.....	10
2.2.1 Removal of background and noise.....	13
2.2.2. Dealing with overlapping.....	16
2.2.2.1. Multivariate curve resolution- alternating least squares (MCR-ALS)	17
2.2.2.2. Generalized rank annihilation method (GRAM).....	18
2.2.2.3. Parallel factor analysis – alternating least squares (PARAFAC-ALS).....	18
2.2.2 Synchronization and shifts of retention time.....	20
2.3. Chromatographic responses functions (CRF)	21
III Optimization in analytical chemistry – basic concepts	29
3.1. Introduction	31
3.2. Design of experiments.....	31
3.3. Simplex algorithm	34
IV Application of LC×LC applied to the analysis of complex mixtures	37
V Experimental conditions for chromatographic analysis of wine samples	45
5.1. Chemicals	47
5.2. Description and preparation of wine samples	47
5.3. Instrumentation.....	48
5.4. Chromatographic conditions for experimental design	50
5.4.1 Optimization of one-dimensional liquid chromatography (1D-LC)	51
5.4.2. Optimization of the second dimension (² D) in LC×LC	51
5.5. Software for control and data acquisition.....	53
VI Search of optimum conditions for 1D-LC of wine samples	55
6.1. Choice of operational details and starting conditions.....	57
6.2. Conclusions and planning of following work	62

VII Search of optimum conditions of the ²D in LC×LC of wine samples	63
7.1. Choice of operational conditions details and starting conditions	65
7.2. Change from D-Optimal design to Simplex	69
7.2.1. Choice of operational details and starting conditions	69
7.2.2. LC×LC applied to the analysis of wine samples.....	72
7.3. Conclusions	76
VIII Final conclusions and further work.....	77
References.....	81
Annex A: Optimization of 1D-LC	i
Annex B: Optimization of the ²D for the LC×LC.....	xix

List of figures

Figure 1:	Simulated output at the end of the 2D of a LC \times LC system.	11
Figure 2:	Assembling the individual chromatograms in the 2D defined by a modulation time of 2 minutes.	11
Figure 3:	Three-dimensional (3D) representation of an interpolated and smoothed LC \times LC chromatogram.	12
Figure 4:	Contour plot of a LC \times LC chromatogram.	12
Figure 5:	Representation of the background signal on a simulated LC \times LC chromatogram.	13
Figure 6:	Representation of the noise on a simulated LC \times LC chromatogram.	15
Figure 7:	Representation of overlapped peaks on a simulated LC \times LC chromatogram and its corresponding one-dimensional chromatogram.	16
Figure 8:	Schematic representation of a 1D chromatogram illustrating the parameters for the estimative of resolution between unresolved peaks using equation 2.23	
Figure 9:	Several steps of an experimental design (Inspired by D.L: Massart, 1997)	32
Figure 10:	Example of Simplex optimization.	35
Figure 11:	Schematic arrangement of the LC \times LC assemblage used in this work (inset: operation positions A and B of the eight-port interfacing valve).	48
Figure 12:	Elution program applied into 1D (purple) and 2D (green).	52
Figure 13:	Response surface showing the effect of the experimental variables MeOH _i and [Buffer] _i on the values of the DCRF _f given by the D-optimal design for 1D .	60
Figure 14:	Optimum conditions chromatogram obtained by D-Optimal design.	60
Figure 15:	Chromatogram with overlapped peaks obtained by optimization in 1D .	61
Figure 16:	Response function expressed in terms of DCFR values for the initial and the final % of methanol given by D-Optimal design for the 2D .	66
Figure 17:	ANOVA of various models fitted to the results obtained following the D-Optimal design.	67
Figure 18:	ANOVA of the quadratic model suggested as the most appropriate for fitting the results obtained by the D-Optimal design.	68
Figure 19:	Chromatogram obtained by D-Optimal design for 50% of initial methanol and 5% of final methanol.	69
Figure 20:	Simplex scheme to find optimal conditions for 2D .	70

Figure 21:	Two-dimensional liquid chromatography of the composite sample obtained at optimal conditions.	71
Figure 22:	Representation of peaks for optimum condition of composite sample.	72
Figure 23:	Representation of the peaks in 2D chromatogram.	72
Figure 24:	Chromatogram of red wine sample (EA – Vinho Regional Alentejano (2010)) without any problem of dragging.	73
Figure 25:	Chromatogram of red wine sample (EA – Vinho Regional Alentejano (2010)) with dragging.	73
Figure 26:	Chromatogram of red wine sample (CICONIA – Vinho Regional Alentejano (2010)).	74
Figure 27:	Chromatogram of red wine sample (Príncipe do Dão (2009)).	74
Figure 28:	Chromatogram of red wine sample (Torre de Estremoz – Vinho Regional Alentejano (2010)).	75
Figure 29:	Chromatogram obtained by optimization in the ¹ D (10% of MeOH _i ; 40mM [PPB] _i ; 2.61 t _i ; 42.83% of MeOH _f ; 5mM [PPB] _f ; 4.93 t _f).	iii
Figure 30:	Chromatogram obtained by optimization in the ¹ D (10% of MeOH _i ; 50mM [PPB] _i ; 3 t _i ; 40.00% of MeOH _f ; 10mM [PPB] _f ; 6 t _f).	iii
Figure 31:	Chromatogram obtained by optimization in the ¹ D (5% of MeOH _i ; 40mM [PPB] _i ; 3 t _i ; 50.00% of MeOH _f ; 5mM [PPB] _f ; 4 t _f).	iii
Figure 32:	Chromatogram obtained by optimization in the 1D (10% of MeOH _i ; 46.43mM [PPB] _i ; 2 t _i ; 50.00% of MeOH _f ; 7.44mM [PPB] _f ; 4 t _f).	iv
Figure 33:	Chromatogram obtained by optimization in the 1D (10% of MeOH _i ; 50mM [PPB] _i ; 3 t _i ; 40.00% of MeOH _f ; 10mM [PPB] _f ; 6 t _f).	iv
Figure 34:	Chromatogram obtained by optimization in the ¹ D (7.46% of MeOH _i ; 40mM [PPB] _i ; 2.46 t _i ; 40.00% of MeOH _f ; 10mM [PPB] _f ; 4 t _f).	iv
Figure 35:	Chromatogram obtained by optimization in the ¹ D (9.39% of MeOH _i , 40mM [PPB] _i , 2 t _i , 40% MeOH _f , 5mM [PPB] _f , and 4 t _f).	v
Figure 36:	Chromatogram obtained by optimization in the ¹ D (10% of MeOH _i , 50mM [PPB] _i , 3 t _i , 50% MeOH _f , 5mM [PPB] _f , and 4 t _f).	v
Figure 37:	Chromatogram obtained by optimization in the ¹ D (7.75% of MeOH _i , 45.93mM [PPB] _i , 2.48 t _i , 50% MeOH _f , 10mM [PPB] _f , and 5.03 t _f).	v
Figure 38:	Chromatogram obtained by optimization in the ¹ D (5% of MeOH _i , 50mM [PPB] _i , 2 t _i , 46.55% MeOH _f , 5mM [PPB] _f , and 6 t _f).	vi

-
- Figure 39:** Chromatogram obtained by optimization in the ¹D (10% of MeOH_i, 50mM [PPB]_i, 3 t_i, 50%MeOH_f, 5mM [PPB]_f, and 4 t_f). vi
- Figure 40:** Chromatogram obtained by optimization in the ¹D (10% of MeOH_i, 40mM [PPB]_i, 2.55 t_i, 40%MeOH_f, 7.88mM [PPB]_f, and 6 t_f). vi
- Figure 41:** Chromatogram obtained by optimization in the ¹D (5% of MeOH_i, 50mM [PPB]_i, 2 t_i, 50%MeOH_f, 5mM [PPB]_f, and 4 t_f). vii
- Figure 42:** Chromatogram obtained by optimization in the ¹D (10% of MeOH_i, 50mM [PPB]_i, 2.36 t_i, 44.49%MeOH_f, 10mM [PPB]_f, and 4 t_f). vii
- Figure 43:** Chromatogram obtained by optimization in the ¹D (10% of MeOH_i, 40mM [PPB]_i, 2 t_i, 50%MeOH_f, 5mM [PPB]_f, and 6 t_f). vii
- Figure 44:** Chromatogram obtained by optimization in the ¹D (10% of MeOH_i, 50 mM [PPB]_i, 2.36 t_i, 44.49%MeOH_f, 10mM [PPB]_f, and 4 t_f). viii
- Figure 45:** Chromatogram obtained by optimization in the ¹D (5% of MeOH_i, 50 mM [PPB]_i, 2 t_i, 40%MeOH_f, 8.34mM [PPB]_f, and 6 t_f). viii
- Figure 46:** Chromatogram obtained by optimization in the ¹D (5% of MeOH_i, 40 mM [PPB]_i, 3 t_i, 50%MeOH_f, 10mM [PPB]_f, and 6 t_f). viii
- Figure 47:** Chromatogram obtained by optimization in the ²D (5% of MeOH_i, 40mM [PPB]_i, 3 t_i, 40%MeOH_f, 10mM [PPB]_f, and 4 t_f). ix
- Figure 48:** Chromatogram obtained by optimization in the ¹D (5% of MeOH_i, 40mM [PPB]_i, 2 t_i, 50%MeOH_f, 10mM [PPB]_f, and 4 t_f). ix
- Figure 50:** Chromatogram obtained by optimization in the ¹D (5% of MeOH_i, 43.21mM [PPB]_i, 2 t_i, 40%MeOH_f, 5mM [PPB]_f, and 6 t_f). ix
- Figure 51:** Chromatogram obtained by optimization in the ¹D (9.69% of MeOH_i, 50 mM [PPB]_i, 2.08 t_i, 41.23%MeOH_f, 5.41mM [PPB]_f, and 4 t_f). x
- Figure 52:** Chromatogram obtained by optimization in the ¹D (5% of MeOH_i, 40 mM [PPB]_i, 2 t_i, 50%MeOH_f, 10mM [PPB]_f, and 4 t_f). x
- Figure 53:** Chromatogram obtained by optimization in the ¹D (8.09% of MeOH_i, 40 mM [PPB]_i, 3 t_i, 50%MeOH_f, 7.05mM [PPB]_f, and 5.66 t_f). x
- Figure 54:** Chromatogram obtained by optimization in the ¹D (10% of MeOH_i, 45.49mM [PPB]_i, 3 t_i, 47.%MeOH_f, 5mM [PPB]_f, and 6 t_f). xi
- Figure 55:** Chromatogram obtained by optimization in the ¹D (10% of MeOH_i, 50mM [PPB]_i, 2 t_i, 50%MeOH_f, 10mM [PPB]_f, and 6 t_f). xi
- Figure 56:** Chromatogram obtained by optimization in the ²D (5.70% of MeOH_i, 40mM [PPB]_i, 2.89 t_i, 40%MeOH_f, 10mM [PPB]_f, and 6 t_f). xi
-

- Figure 57:** Chromatogram obtained by optimization in the 1D (5% of MeOH_i, 50 mM [PPB]_i, 3 t_i, 40% MeOH_f, 5mM [PPB]_f, and 4.97 t_f). xii
- Figure 58:** Chromatogram obtained by optimization in the 1D (10% of MeOH_i, 50 mM [PPB]_i, 2 t_i, 50% MeOH_f, 10mM [PPB]_f, and 6 t_f). xii
- Figure 59:** Chromatogram obtained by optimization in the 1D (5% of MeOH_i, 40 mM [PPB]_i, 2 t_i, 50% MeOH_f, 5mM [PPB]_f, and 6 t_f). xii
- Figure 60:** Chromatogram obtained by optimization in the 1D (5% of MeOH_i, 50mM [PPB]_i, 2.44 t_i, 40% MeOH_f, 5mM [PPB]_f, and 4 t_f). xiii
- Figure 61:** Chromatogram obtained by optimization in the 1D (6.63% of MeOH_i, 40mM [PPB]_i, 2 t_i, 49.22% MeOH_f, 5mM [PPB]_f, and 4 t_f). xiii
- Figure 62:** Chromatogram obtained by optimization in the 1D (5% of MeOH_i, 50mM [PPB]_i, 3 t_i, 50% MeOH_f, 10mM [PPB]_f, and 4 t_f). xiii
- Figure 63:** Chromatogram obtained by optimization in the 1D (10% of MeOH_i, 43.29 mM [PPB]_i, 2 t_i, 40% MeOH_f, 10mM [PPB]_f, and 4.97 t_f). xiv
- Figure 64:** Chromatogram obtained by optimization in the 1D (6.63% of MeOH_i, 40 mM [PPB]_i, 3 t_i, 40% MeOH_f, 5mM [PPB]_f, and 6 t_f). xiv
- Figure 65:** Chromatogram obtained by optimization in the 1D (10% of MeOH_i, 40mM [PPB]_i, 3 t_i, 50% MeOH_f, 10mM [PPB]_f, and 4 t_f). xiv
- Figure 66:** Chromatogram obtained by optimization in the 1D (5% of MeOH_i, 50mM [PPB]_i, 3 t_i, 48.91% MeOH_f, 5mM [PPB]_f, and 4 t_f). xv
- Figure 67:** Chromatogram obtained by optimization in the 1D (5% of MeOH_i, 50mM [PPB]_i, 2.76 t_i, 40% MeOH_f, 10mM [PPB]_f, and 6 t_f). xv
- Figure 68:** Chromatogram obtained by optimization in the 1D (5% of MeOH_i, 40 mM [PPB]_i, 2 t_i, 40% MeOH_f, 6.91mM [PPB]_f, and 4.42 t_f). xv
- Figure 69:** Chromatogram obtained by optimization in the 1D (10% of MeOH_i, 44.29 mM [PPB]_i, 3 t_i, 40% MeOH_f, 5mM [PPB]_f, and 4 t_f). xvi
- Figure 70:** Chromatogram obtained by optimization in the 1D (8.72% of MeOH_i, 40mM [PPB]_i, 2 t_i, 44.72% MeOH_f, 10mM [PPB]_f, and 6 t_f). xvi
- Figure 71:** Chromatogram obtained by optimization in the 1D (5% of MeOH_i, 50mM [PPB]_i, 3 t_i, 50% MeOH_f, 5mM [PPB]_f, and 6 t_f). xvi
- Figure 72:** Chromatogram obtained by optimization in the 1D (5.39% of MeOH_i, 40.31mM [PPB]_i, 2.91 t_i, 40% MeOH_f, 5mM [PPB]_f, and 4.03 t_f). xvii
- Figure 73:** Chromatogram obtained by optimization in the 1D (5% of MeOH_i, 50mM [PPB]_i, 2 t_i, 40% MeOH_f, 10mM [PPB]_f, and 4 t_f). xvii

-
- Figure 74:** Chromatogram obtained by optimization in the 1D (10% of $MeOH_i$, 50mM $[PPB]_i$, 2 t_i , 40% $MeOH_f$, 5mM $[PPB]_f$, and 6 t_f). xvii
- Figure 75:** Chromatogram obtained by optimization in the 2D (25% of $MeOH_i$, and 25% $MeOH_f$). xxi
- Figure 76:** Chromatogram obtained by optimization in the 2D (35% of $MeOH_i$, and 28% $MeOH_f$). xxi
- Figure 77:** Chromatogram obtained by optimization in the 2D (28% of $MeOH_i$, and 35% $MeOH_f$). xxi
- Figure 78:** Chromatogram obtained by optimization in the 2D (18% of $MeOH_i$, and 32% $MeOH_f$). xxii
- Figure 79:** Chromatogram obtained by optimization in the 2D (10% of $MeOH_i$, and 34% $MeOH_f$). xxii
- Figure 80:** Chromatogram obtained by optimization in the 2D (21% of $MeOH_i$, and 42% $MeOH_f$). xxii
- Figure 81:** Chromatogram obtained by optimization in the 2D (11% of $MeOH_i$, and 39% $MeOH_f$). xxiii
- Figure 82:** Chromatogram obtained by optimization in the 2D (15% of $MeOH_i$, and 38% $MeOH_f$). xxiii
- Figure 83:** Chromatogram obtained by optimization in the 2D (12% of $MeOH_i$, and 28% $MeOH_f$). xxiii
- Figure 84:** Chromatogram obtained by optimization in the 2D (19% of $MeOH_i$, and 39% $MeOH_f$). xxiv
- Figure 85:** Chromatogram obtained by optimization in the 2D (22% of $MeOH_i$, and 33% $MeOH_f$). xxiv
- Figure 86:** Chromatogram obtained by optimization in the 2D (17% of $MeOH_i$, and 37% $MeOH_f$). xxiv
- Figure 87:** Chromatogram obtained by optimization in the 2D (18% of $MeOH_i$, and 44% $MeOH_f$). xxv
- Figure 88:** Chromatogram obtained by optimization in the 2D (20% of $MeOH_i$, and 46% $MeOH_f$). xxv

List of tables

Table 1:	Different weights for the parameters of $DCRF_f$ equation, used for different analytical scenarios.	25
Table 2:	Survey of the studies published after 2008, inclusive, using LC×LC for the analysis of complex samples.	40
Table 3:	Experimental variables and their ranges of variation used in the optimization procedure for the 1D .	50
Table 4:	Experimental design table produced by D-Optimal design for the 1D, using the Design-Expert software version 7.00.	58
Table 5:	Optimum values of each experimental variable achieved by D-optimal design for 1D .	59
Table 6:	Experimental design generated by Design-Expert software version 7.0.0, for the 2D .	66
Table 7:	Range of percentages of methanol for the Simplex algorithm.	70

List of abbreviations

ALS	Alternating Least Squares
ANOVA	Analysis of Variance
AU	Arbitrary Units
BSA	Bovine Serum Albumin
COWA	Correlation Optimized Warping Algorithm
CAD	Aerosol-Charged Detector
CRF	Chromatographic Response Function
D-PS	Deuterated Polystyrene
DAD	Diode Array Detector
DCRF	Duarte's Chromatographic Response Function
DMF	<i>N,N</i> -dimethylformamide
ELSD	Evaporative Light Scattering Detector
ESI	Electrospray Ionization
FTIR	Fourier Transform Infrared Spectroscopy
GC×GC	Comprehensive Two-Dimensional Gas Chromatography
GRAM	Generalized Rank Annihilation Method
H-PS	Protonated Polystyrene
HILIC	Hydrophilic Interaction Liquid Chromatography
HPLC	High Performance Liquid Chromatography
HPMC	Hydroxypropylmethylcellulose
IR	Infrared
LC×LC	Comprehensive Two-Dimensional Liquid Chromatography
LCLC	Liquid Chromatography at Critical Conditions
LS	Light Sensor
MCR	Multi Curve Resolution
MS	Mass Spectrometry
NBA	3-Nitrobenzyl Alcohol
NOM	Natural Organic Matter
NP	Normal Phase
PALC	Per Aqueous Liquid Chromatography
PARAFAC	Parallel Factor Analysis
PEG	Polyethylene Glycol

List of abbreviations

PEO	Polyethylene Oxide
PL-FA	Pony-Lake Fulvic Acids
PS	Polystyrene
RI	Refractive Index
RP	Reversed Phase
SEC	Size Exclusion Chromatography
SCX	Strong Cation Exchange
SR-FA	Suwannee River Fulvic Acids
S/N	Signal-to-noise ratio
TCB	Trichlorobenzene
THF	Tetrahydrofuran
TOF	Time of Flight
UV	Ultra-Violet
WCX	Weak Cation Exchange
1D-LC	One-Dimensional Liquid Chromatography
2D-LC	Two-Dimensional Liquid Chromatophy
1D	One-Dimensional
2D	Two-Dimensional
3D	Three-Dimensional
¹ D	First Dimension
² D	Second Dimension
λ_{Exc}	Excitation Wavelength
λ_{Em}	Emission Wavelength

I

Aims and structure of dissertation

1.1. Introduction

Lately, and due to the fast progress of science in many fields, there has been a growing interest in multidimensional techniques that allow analysing complex matrices. From the many available techniques, the one chosen for this work was two-dimensional liquid chromatography (2D-LC), mostly because of its increased peak capacity, selectivity, and resolution (as compared to one-dimensional liquid chromatography (1D-LC)), and also because it is a chromatographic technique still under development.

The main goal of this thesis was to develop optimization strategies with the aid of chemometric tools for deducing the best experimental conditions, both in the first and second dimensions, for the subsequent analysis of red wine samples by comprehensive two-dimensional liquid chromatography (LC×LC) in order to compare their chromatographic profiles. Such studies are very scarcely found in literature. Ideally, it would be useful to optimize both dimensions simultaneously, but in practice such procedure is not attainable, mostly because the separation conditions in the second dimension (²D) depends on the experimental conditions of the first dimension (¹D), and varying both conditions simultaneously would threaten any conclusion on the best separation conditions in both dimensions.

For this work, red wine samples were chosen as the matrix for analysis since this beverage is well appreciated in the Mediterranean, and contains large amounts of antioxidants, which have beneficial effects on health. The majority of antioxidants present in red wine play an important role against oxidative damage, which is responsible for the process of aging and for many degenerative conditions like Alzheimer's, Parkinson's, and Huntington's (Gazova *et al.*, 2013), but also type 2 diabetes (Napoli *et al.*, 2005) and cancer (Kraft *et al.*, 2009). Phenolic compounds (polyphenols and flavonoids), which have antioxidant and anti-inflammatory activity, make up a large family of naturally occurring compounds in red wine (Verma and Pratap, 2010) and a very important polyphenol is the resveratrol (Das *et al.*, 2011), which prevents heart diseases.

1.2. Aim of the dissertation

As previously mentioned, this dissertation has as its main goal the optimization of the separation conditions in LC×LC for the untargeted separation of compounds contained in red wine samples. For performing this optimization process, it was prepared a composite sample containing 1 mL of each wine sample. Both chromatographic dimensions were optimized independently and with the same columns that were subsequently used in LC×LC. The separation system comprised, in the first dimension (¹D), a mixed-mode reversed-phase/anionic exchange column (Acclaim® Mixed-Mode WAX-1), and in the second dimension (²D), a classic C18 reversed phase (RP) column (Kromasil® RP-C18). The effluent of the ²D column was monitored using a diode array detector (DAD). The separation conditions were firstly optimized for the ¹D, using the one-dimensional liquid chromatography (1D-LC) approach. Afterwards, the chromatographic conditions for the ²D were optimized using the LC×LC approach. In this optimization process, two algorithms were applied for evaluating the quality of the separation of the red wine samples: the quality of separation in the ¹D was assessed using the chromatographic response function (CRF) developed by Duarte and Duarte (2010) for a 1D-LC approach, whereas the quality of separation in the ²D was assessed using the chromatographic response function (DCRF_{f,2D}) developed by Duarte *et al.* (2011) for a LC×LC approach.

1.3. Structure of the dissertation

This dissertation is divided into eight chapters. Chapter I describe the aims and the structure of this dissertation, providing an overview of the work as well as its organization.

Chapter II contains a brief introduction on the basic concepts of 2D-LC, as well as the structure and the processing of the data sets obtained with such technique. Lastly, some issues that may occur when using this technique are discussed together with the

chromatographic response functions that were used to evaluate the quality of separation in the chromatograms.

Chapter III includes details about the optimization process as a whole, as well as a brief discussion on the chemometric methods (D-Optimal and Simplex) used in this work for the optimization of the conditions in both ¹D and ²D.

Chapter IV describes the application of LC×LC to the analysis of complex samples, and it includes a literature review on the studies where this technique has been applied.

Chapter V contains all the chromatographic conditions, some of the preliminary results regarding the optimization processes, as well as a description of the instrumentation applied in this work.

Chapter VI introduces and discusses the results obtained from the optimization process applied to the 1D chromatography to the wine samples.

Chapter VII contains the results, discussion, and main conclusions of the optimization process of the ²D of the LC×LC system.

Chapter VIII contains the final conclusions and suggestions for further work. Finally, there is a list of references, followed by Annexes A and B containing additional experimental data obtained in this work.

II

Two-dimensional liquid chromatography: basic concepts

2.1. The emergence of comprehensive two-dimensional liquid chromatography (LC×LC)

Nowadays, there has been a growing interest in multidimensional techniques since they have far greater resolving power and allow analysing complex matrices when compared with 1D chromatography. One of multidimensional chromatographic techniques that are in an exponential growth, and consequently the subject of a large number of publications, is the 2D-LC. Liquid chromatography techniques are characterized by a variety of separation mechanisms with different selectivity, and the separation in 2D-LC is performed by means of two dimensions, having different or similar separation mechanisms. According to the review of François *et al.* (2009), the major advantage of using two dimensions is the high peak capacity that can be obtained, which means the reduction of overlapping peaks. The same authors reported that there are two possible schemes of operation in 2D-LC: a) off-line, where all fractions are collected and stored for an indefinitely period of time and, afterwards, the solvent is evaporated, and then each fraction is re-dissolved and re-injected into a second column (i.e., the ²D); and b) on-line, where the sample is transferred from the ¹D to the ²D. According to the work of Fairchild *et al.* (2009), the best peak capacity is obtained with the off-line scheme, but at the expense of a long time of analysis. In on-line 2D-LC systems, there are two modes of operation (van Mispelaar *et al.*, 2003, Gray *et al.*, 2004, Matos *et al.*, 2012): a) heart-cutting, where only the peaks of interest which are separated in the ¹D, are further separated in the ²D; and b) comprehensive (usually abbreviated as LC×LC (Marriott *et al.*, 2012)), where the effluent from the first column is constantly sampled and re-injected into the second column, by an interfacing valve. An advantage of the heart-cutting operation mode is that only the components of interest will be analysed through both dimensions, whereas in the comprehensive mode, the whole sample is analysed throughout both dimensions, allowing, therefore, a better separation of the sample components. Donato *et al.* (2011) also referred that the on-line method is the most convenient, because losses can be minimized when working with very small amounts of sample.

As referred in the review work of Tranchida *et al.* (2004), the concept of comprehensive chromatography emerged with thin-layer chromatography in 1944, and according to the reviews of Stoll *et al.* (2007) and Matos *et al.* (2012), LC×LC was the first type of multidimensional chromatographic technique, which was developed by Erni and Frei in 1978. This work was followed by that of Bushey and Jorgenson (1990), and was just only a decade later that the comprehensive 2D gas chromatography (GC×GC) took the first steps. Phillips and Beens (1999) highlighted in their work that was only after the development of GC×GC that the multidimensional chromatography has become more relevant as a separation science, and the GC×GC analysis attracted more attention than the LC×LC technique.

A literature survey also shows that the application of the LC×LC technique has been mostly focused in the analysis of foodstuffs and beverages (Kivilompolo *et al.*, 2008, Dugo *et al.*, 2009, Montero *et al.*, 2013, Larson *et al.*, 2013, Bailey and Rutan, 2013), macromolecules (such as polymers and copolymers) (Greiderer *et al.*, 2011, Lee *et al.*, 2011, Sinha *et al.*, 2012, Malik *et al.*, 2012), biological tissues (Jeong *et al.*, 2010, Scoparo *et al.*, 2012, Cai *et al.*, 2012, Halquist *et al.*, 2012), and natural organic matter (NOM) (Duarte *et al.*, 2012).

2.2. Structure of data in LC×LC

A LC×LC system produces a huge amount of information, which can be in the order of millions of data points, in a short period of time (Stoll *et al.*, 2007, François *et al.*, 2009). When the LC×LC is coupled with a spectrophotometer detector (e.g., a DAD) or a mass spectrometry (MS) detector, the acquired chromatograms comprise an enormous number of data points and, thus, the real-time acquisition of data produces huge files. These data sets need specific processing software for a quick and adequate chemical identification, and classification of complex peaks and, consequently, extract the maximum amount of information. For better understanding the structure of LC×LC data, it is

important to start at looking at an example of a simulated chromatogram, as shown in Figure 1, obtained from a hypothetical detector positioned at the end of the ^2D .

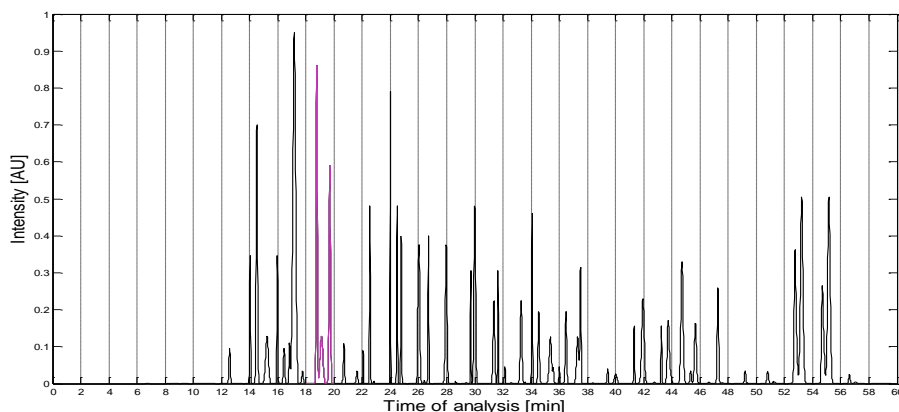


Figure 1: Simulated output at the end of the ^2D of a $\text{LC}\times\text{LC}$ system.

In Figure 1, each modulation period of 2 minutes contains the chromatographic profile of each fraction of the sample exiting from the ^1D column. Each fraction is collected during 2 minutes in one of the 2 identical loops of an interfacing valve, being then transferred to the ^2D column where it is separated. The data shown in Figure 1 contains information that has to be assembled in order to show the individual 1D chromatograms that are stacked in each modulation period of 2 minutes. For example, the chromatogram in violet color in Figure 1, from minute 18 to minute 20, is placed in Figure 2 in time 18 (also in violet). Figure 2 shows the whole dataset of Figure 1, but now plotted in the two chromatographic dimensions of an $\text{LC}\times\text{LC}$ system

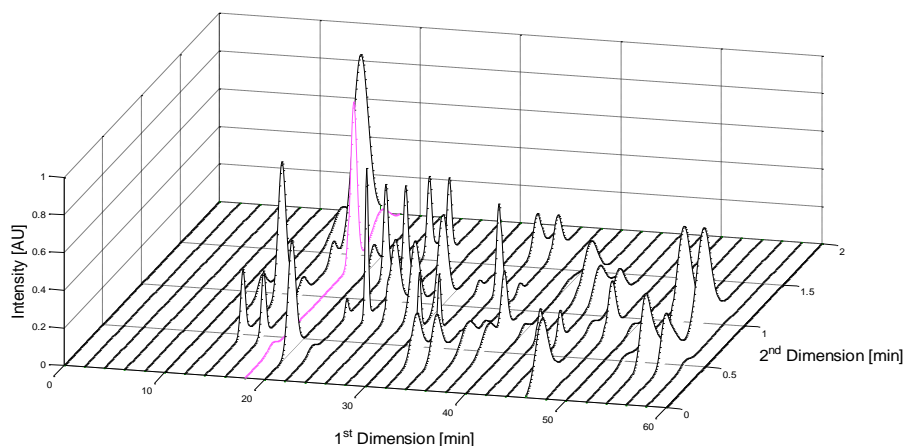


Figure 2: Assembling the individual chromatograms in the ^2D defined by a modulation time of 2 minutes.

The interpolation and smoothing of the data assembled in Figure 2, for a given grid size (2 min \times 0.01 min, in this case) allow obtaining a three dimensional (3D) representation of the 2D chromatographic data, as shown in Figure 3, where a color code must be used for highlighting the values of intensity of the analytical signal.

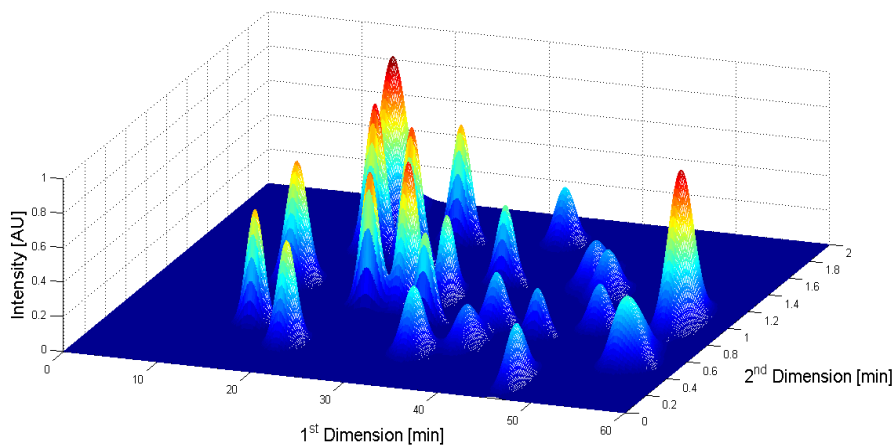


Figure 3: Three-dimensional (3D) representation of an interpolated and smoothed LC \times LC chromatogram.

An alternative to the 3D representation of a 2D chromatogram is shown in Figure 4, under the form of a contour plot, which can be considered an excellent tool for the visualization of 3D representations. The use of a color code associated with the peak intensity allows an easy assessment of the distribution and resolution of the chromatographic peaks.

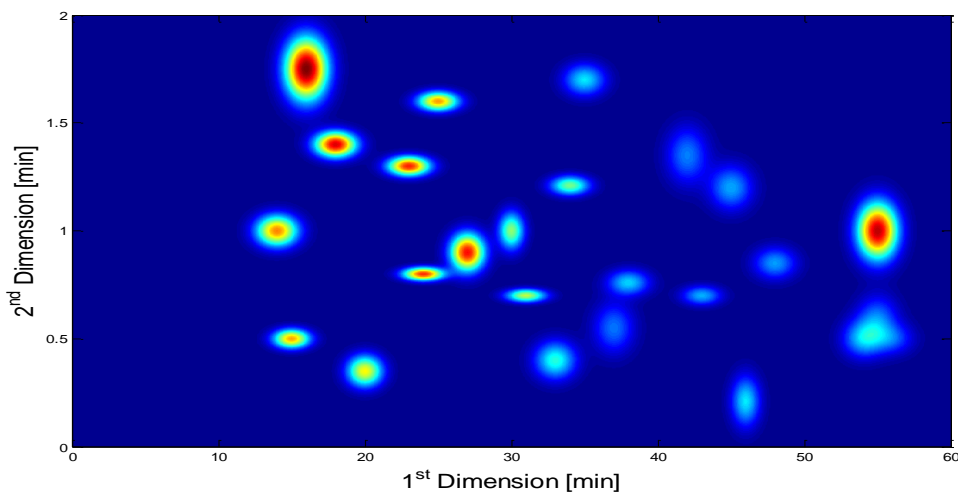


Figure 4: Contour plot of a LC \times LC chromatogram.

In ideal 2D chromatography, the above mentioned representations may not be as clear as one would like. There are artifacts, such as background fluctuations and noise (Reichenbach *et al.*, 2003, Zhang *et al.*, 2007, Zeng *et al.*, 2011, Amigo *et al.*, 2010, Matos *et al.*, 2012, Paraster and Tauler, 2013), overlapped peaks (Stoll *et al.*, 2007, Amigo *et al.*, 2010, Allan and Rutan, 2011), and shifts in retention time (Fraga *et al.*, 2001, van Mispelaar *et al.*, 2003, Johnson *et al.*, 2004, Pierce *et al.*, 2005, Zhang *et al.*, 2008, Alen and Rutan, 2011, Matos *et al.*, 2012, Yu *et al.*, 2013, Bailey and Rutan, 2013) that should be removed or avoided in order to glean chemical information from the 2D chromatograms. These types of artifacts are common to other 2D separation methods (e.g. GC×GC) and the way to remove them is the same as in any of these systems.

2.2.1 Removal of background and noise

The raw data provided by 2D chromatograms are not always ready for their immediate interpretation because it may contain artifacts, such as background and noise that hinder the extraction of chemical information. Background can be understood as any kind of signal not related to the analyte that causes a systematic interference, as shown in Figure 5, and according to Pierce *et al.* (2012) its removal is the first step most usually performed in chromatographic data analysis.

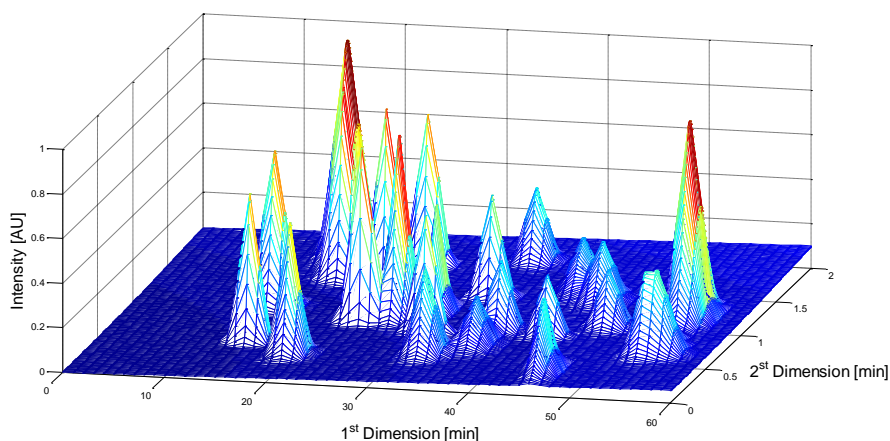


Figure 5: Representation of the background signal on a simulated LC×LC chromatogram.

Reichenbach *et al.* (2003) suggested an algorithm based on image processing software for background estimation and removal, taking into consideration the statistical and structural properties of different regions of pixels observed on the images obtained in their work with GC×GC. Amigo *et al.* (2010) proposed another two methods to solve the problem of background removal: a) fit a certain curve (e.g. polynomial) to be able to subtract this curve from the overall signal; and b) model the baseline as part of an overall factor model. The first method is the most easily to be used but it does not provide always the best data quality, while the second approach is an added benefit of the factor model and cannot be taken as a separate component. Zhang *et al.* (2007) also developed a chemometric method to be used in trilinear data from 2D separation instruments coupled to multichannel detectors. The main idea of this method is to model the background variations on the raw datasets by subtracting the individual signal of background drift from the original raw chromatographic data, thus removing the three dimensional drift. This technique can be applied for all 2D separations coupled to multichannel detectors. Another methodology was developed by Zeng *et al.* (2011) for dealing with the background consisting in the application to each 2D chromatographic peak, a baseline correction as well as a “moving windows average” method for data smoothing.

As pointed out by Matos *et al.* (2012), one strategy to elude the background problem is to avoid changes in the composition of the mobile phase, as well as reduce to a minimum the variations in columns temperature, pressure, and fluctuations caused by the interfacing valve.

Noise is another interference generally observed in analytical signals (Matos *et al.*, 2012), which is usually related to the sensitivity of the detector. An example of simulated chromatogram with noise interference is given in Figure 6. The noise refers to any random variation occurring in the signal. These non-systematic variations can cause quantification problems associated with changes in both the shape and the elution time of the peaks (Matos *et al.*, 2012). This interference may be reduced by applying smoothing algorithms, but it is particularly difficult in practice to separate the noise of the signal from the background, particularly when the signal-to-noise ratio (S/N) is low (Parastar and Tauler, 2013).

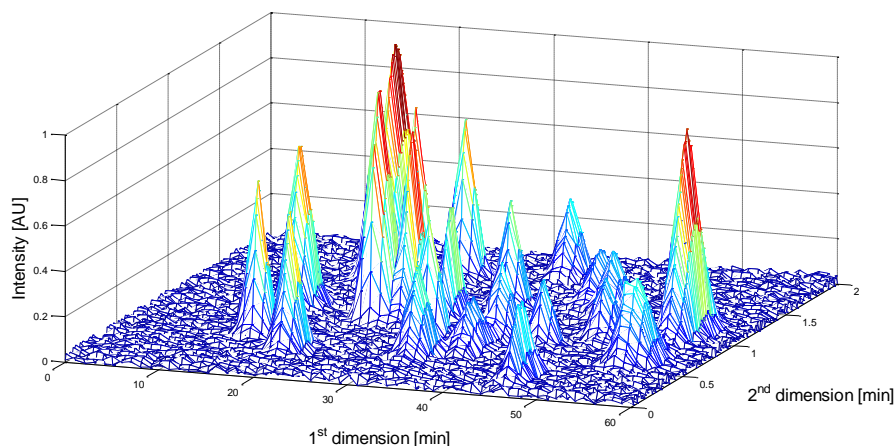


Figure 6: Representation of the noise on a simulated LC×LC chromatogram.

Most of time, it is not easy to separate background from noise and some authors use the same method to separate these two artifacts. Therefore, a completely different and alternative method based on the application of algorithms of image processing has been suggested by Reichenbach *et al.* (2003) for dealing with the background and noise in 2D chromatography. The authors claim that this method takes advantage of the following specific structural and statistical properties of the background from the images of 2D chromatograms, namely: a) dead-bands, which are the regions without analytical signal; b) the constant value of the average of background level, which does not change much in comparison with the characteristic peak widths; and c) the random nature of noise has the same statistical properties of the random noise.

On the other hand, according to Zhang *et al.* (2007), there are two methods to overcome the interferences caused by the background and noise: the first is to use the “mean centering”, and for its implementation the background must be stable; the second is to remove the background by subtraction of a blank chromatographic run. However, the subtraction of the response of the eluent does not always provide acceptable results due to two main sorts of variations: a) the variations in the response intensity of the spectrum of the eluent during a chromatographic run; and b) the occurrence of small shape changes in the spectrum of the eluent.

2.2.2. Dealing with overlapping

In their work, Stoll *et al.* (2007) refer that another problem usually detected is the occurrence of overlapped peaks, thus becoming difficult, if not impossible, to quantify the individual peaks. Figure 7 shows a simulated occurrence of overlapped peaks in the LC×LC data structure and its corresponding 1D chromatogram.

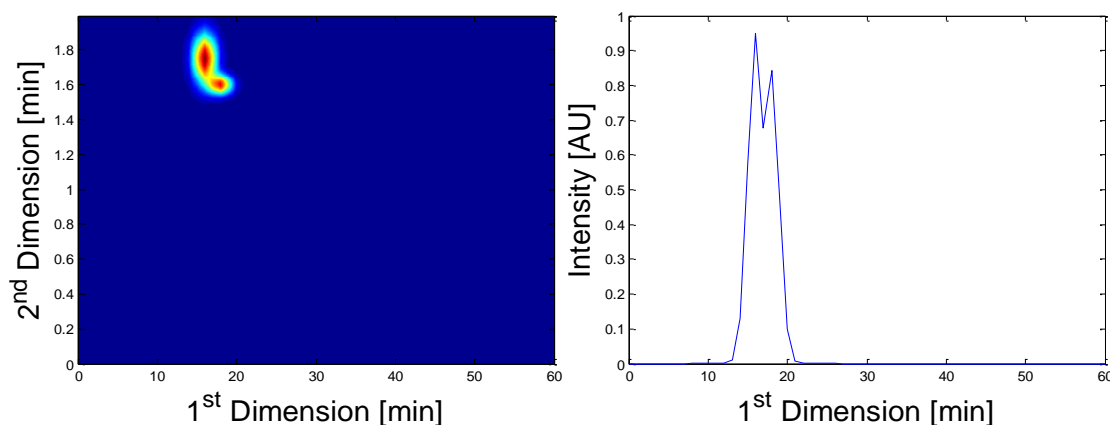


Figure 7: Representation of overlapped peaks on a simulated LC×LC chromatogram and its corresponding one-dimensional chromatogram.

As noted by Allen and Rutan (2012), two methods can be applied for the quantification of overlapped peaks: integration and multi-way analysis. The integration method consists on the summation of the areas of consecutive 2D peaks that contain a single 2D peak. This method has already been discussed by van Mispelaar *et al.* (2003) and they referred that it is only applied when there is a complete separation at the baseline level between adjacent 2D peaks. So, Bailey and Rutan (2011) developed an integration method to address the concern of van Mispelaar *et al.* (2003) when working with LC×LC systems. The multi-way algorithms proposed for resolving overlapped peaks encompass the multivariate curve resolution-alternating least squares (MCR-ALS), the generalized rank annihilation method (GRAM), and the parallel factor analysis- alternating least squares (PARAFAC-ALS).

2.2.2.1. Multivariate curve resolution- alternating least squares (MCR-ALS)

Hantao *et al.* (2012) reported that “the main goal of any MCR method is to transform the raw experimental data into a simple composition-weighted linear additive model of pure responses, with a single term per component contribution”. This method is widely used to resolve the issues caused by overlapping peaks in the analytical response, and it is especially used in 2D separations. As a non-iterative method, MCR searches for a single solution in which the pure variables are uniquely defined according to the mathematical principles involved, and the final objective is to analyze each individual constituent in its pure chromatograms (Stoll *et al.*, 2007). One widely used technique encompasses the connection of the MCR method with the ALS algorithm (MCR-ALS), which consists of a multivariate curve fitting technique that also allows to separate dataset components by least squares optimization of chemical data structure using mathematical constraints, such as non-negativity, unimodality, and multilinearity (Bailey and Rutan, 2011). The advantage of using the MCR-ALS method can be seen in the work of Jalali-Heravi *et al.* (2011), who applied GC-MS for the analysis of rosemary oil, resulting in the detection of 68 compounds. With the application of MCR-ALS, the number of compounds that were able to be identified increased to 99. Bailey and Rutan (2011) applied LC×LC-DAD for the analysis of human urine samples and for quantification purposes. The authors used MCR-ALS with only two constraints (non-negativity and selectivity) and did not apply the multilinearity constraint because the degree of retention time shifting from sample to sample, which occurs in both 1D and 2D chromatograms, is significant enough to prevent the validity of either the trilinearity or quadrilinearity assumptions. According to the same authors, the major disadvantage of this method is the lack of complete automation since it requires intervention of the analyst, but this intervention can be easily handled and it becomes very fast from the point of view of implementation. As reviewed by Arancibia *et al.* (2012), a significant advantage of the MCR-ALS is that this algorithm does not require time synchronization of the chromatograms, which in practical terms is very useful.

2.2.2.2. Generalized rank annihilation method (GRAM)

The GRAM is a non-iterative algorithm used for qualitative and quantitative analysis (Ferré and Comas, 2011) and it is particularly useful in chromatography, for the quantification of analytes that usually co-elute with interferences existing in complex samples. This method requires a previous calibration step for comparison with the obtained chromatograms and they should be perfectly matched. The start-up of the GRAM requires an input of an estimate of the number of different components existing in the samples under study (Fraga and Corley, 2005). The key requirement for GRAM application is that the two data matrices corresponding to the sample and the standard must be trilinear, thus becoming necessary to ensure that the peaks associated with the components of interest have the same retention time and the same profile in both the sample and the standard chromatograms (Matos *et al.*, 2012). Although GRAM is a non-iterative method, this technique tends to be computationally faster, but it has the limitation of dealing with up to three-way data sets, since only two samples can be analysed at a time, while other algorithms, such as PARAFAC-ALS, can deal with datasets of higher dimensions (Stoll *et al.*, 2007). The GRAM has been successfully applied in various studies using data obtained by GC×GC, such as in the analysis of fuels (Bruckner *et al.*, 1998, Prazen *et al.*, 1999), ethylbenzene and m-xylene in modified white gasoline (Bruckner *et al.*, 1998), methyl tert-butyl ether (Prazen *et al.*, 1999), and aromatic isomers (Fraga *et al.*, 2000).

2.2.2.3. Parallel factor analysis – alternating least squares (PARAFAC-ALS)

The PARAFAC is one of the most widely applied multi-way method, especially for resolving overlapping peaks occurring in 2D chromatograms (Fraga and Corley, 2005, Amigo *et al.*, 2010, Allen and Rutan, 2012), identifying spectral signals (Sinha *et al.*, 2004), removing background signals, and improving S/N (Porter *et al.*, 2006, Parastar and Tauler, 2013). Additionally, the PARAFAC is a mathematical model well suited to deal with 4-way data sets (Allen and Rutan, 2011).

The main requirements for the use of the PARAFAC model is that the component solutions produced must be unique and true if the correct number of components is selected and, thus, the data must obey the multilinearity rule (Allen and Rutan, 2011). It is of paramount importance to select the correct number of components, because if the components are not well selected then the obtained results may not be correct. The first algorithm used to adjust the parameters of the PARAFAC model was the ALS, since it is able to handle unresolved chemical components in three-way or even higher-order data array (Bro, 1997). The estimation of the number of appropriate factors in the PARAFAC model is a very difficult task. Typically, this value is estimated by the sum of interferences and analytes present in the 2D chromatogram, but it is extremely hard to know in advance that number, especially in the presence of a low S/N and overlapping peaks. In order to overcome this problem, Hoggard and Synovec (2007) proposed an algorithm that it is able to select automatically the number of factors to be used by PARAFAC. The models of PARAFAC are automatically generated having an incrementally higher number of factors until mass spectral matching of the corresponding loadings in the model against a target analyte mass spectrum indicates that over fitting has occurred. Then, the model selected simply has one less factor than the over fitted model. So, this model selection approach is viable across the detection range of the instrument from overloaded analyte signal down to low S/N analyte signal. As reported by Bro (1997), in each interaction, the ALS algorithm improves the estimates of the constants of the PARAFAC model, in order to find the solution using the method of least squares. The greatest advantage of the PARAFAC-ALS method when compared to GRAM is its ability to quantify and solve the components of interest taking into account only the sample information, without the need for a standard chromatogram or countless replicates (Porter *et al.*, 2006). A drawback was found by van Mispelaar *et al.* (2003) when comparing the performance of PARAFAC with that of a conventional integration method using data derived from GC×GC-FID. This integration method integrated 2D slices, followed by a summation along the 1D. The program worked well on baseline-separated peaks, but it lacked sophisticated integration algorithms to cope with a GC × GC chromatogram of a typical synthetic perfume sample with less than ideal situations. Therefore, van Mispelaar *et al.* (2003) developed a multi-way method to resolve the problem and concluded that the conventional method exhibits a better precision, while the PARAFAC works faster.

2.2.2 Synchronization and shifts of retention time

An artifact that can also appear in the chromatograms is the desynchronization of the retention time. The synchronization is important to ensure the precision of the retention time of each peak in the chromatographic analysis. The 2D chromatograms always show fluctuations in the retention time of the peaks, which may arise from variations in the temperature and pressure, but also from the degradation of the stationary phase or even due to matrix effects (François *et al.*, 2009). These deviations can be easily identified by the comparison with patterns, i.e., a standard sample containing all analytes that constitute each individual sample that would be analyzed. According to Matos *et al.* (2012), it is necessary to ensure that the retention times between replicates are repeatable and reproducible, that the time axes are synchronized and the peaks are aligned, because only then one can achieve a proper and successful data processing. In case of either complex or complicated data matrices, peak alignment can be attained by using different algorithms, such as MCR-ALS, GRAM, and PARAFAC. Fraga *et al.* (2001) proposed a technique using the GRAM method. In this technique, the alignment can be done in the ¹D or ²D, and the ²D alignment method corrects run-to-run shifts in the sample data matrix relative to a standard data matrix, on both separation time axes, and in an independent fashion. van Mispelaar *et al.* (2003) suggested a correlation/optimization method based on the inner product associated with selected regions of GC×GC data. The suggested algorithm uses as reference a 2D chromatogram to align all sections and to identify the site of the best fit position. Johnson *et al.* (2004), when quantifying naphthalenes in jet fuel by GC×GC, developed another method based on windowed rank minimization alignment with interpolative stretching between the windows. Pierce *et al.* (2005) proposed the use of an algorithm of alignment that allows deformation in both dimensions using a new chromatographic indexing scheme. Although this algorithm has been developed for GC data, it can be applied to any 2D separation problem. Zhang *et al.* (2008) developed the 2D Correlation Optimized Warping Algorithm (2D COWA) through the data obtained from GC×GC. This algorithm allows stretching and compressing a segment of the 2D chromatograms in order to maximize the correlation of the sample with a chromatographic reference. Hollingsworth *et al.* (2006) developed a different method for automatic

alignment of the chromatograms using software based on algorithms of image processing. As noted by Matos *et al.* (2012), a limitation of the described methods is their inability to deal with orders higher than three-way data sets. For example, multichannel detectors produce a 4-way data structure, which requires the development of more sophisticated techniques to align the retention time of the peaks. Allen and Rutan (2011) recently developed an algorithm especially suited to LC×LC-DAD that allows dealing with four-way data with satisfactory results. A new study was also recently developed by Yu *et al.* (2013) for alignment of chromatographic signals with multiple detection channels. This method uses a new strategy based on the rank minimization method (GRAM), which aligns the chromatographic peak shifts among samples and then uses trilinear decomposition methodology to interpret the overlapped chromatographic peaks in order to quantify the analytes of interest. The method corrects the displacements and can be used accurately, even in the presence of interferences. The results indicate that this method is more automatic than GRAM, and it could be suitable for the alignment of the retention time shifts of analytes that are completely overlapped by co-eluted interferences.

Recently, Bailey and Rutan (2013) suggested a new alignment algorithm for synchronizing the retention times in the 2D between sample injections, which consists in determining the position of the maximum of the peaks that appear in all samples injections. Then, the earliest eluting 2D retention time is used as a reference point for all the peaks, and the change in retention time of the sample compared to the reference is determined for all the peaks and for all sample injections. The average of the retention time deviations is calculated for all the peaks and for each sample injection and the maximum and minimum value of the shift parameter across all samples is determined. Finally, each sample chromatogram is then essentially shifted in the second retention time dimension by removing the same total number of data points from the beginning.

2.3. Chromatographic responses functions (CRF)

In order to assess the best chromatographic separation conditions in LC×LC, there are several parameters that can be used to evaluate the quality of the chromatograms

(Matos *et al.* 2012), such as the resolution, elution time, and number of peaks (Duarte and Duarte, 2010). These parameters can be combined into a single global index of quality referred to as chromatographic response function (CRF). Duarte and Duarte (2010) suggested the following CRF for 1D chromatography:

$$CRF = \sum_{i=1}^{N-1} \theta_{s,i} + N - \left(\frac{t_{R,L} - t_0}{t_{R,L}} \right) \quad (1)$$

Where θ corresponds to the resolution, N is the number of peaks, $t_{R,L}$ is the retention time of the last eluted peak, and t_0 is the elution time corresponding to the column void volume. This function was designed to reach a maximum as the optimum is approached. This equation is quite affected by the overlapped peaks, because the value of N is lower, which results also in a decrease of the CRF value, being also affected by the window time, where all the peaks appear in the chromatogram (Duarte and Duarte, 2010).

López-Grío *et al.* (2001) developed a mathematical equation to estimate the resolution between unresolved peaks. This mathematical formulation was derived using the Kaiser's definition, which is a function of overlapping peak. With this concept, Duarte and Duarte (2010) reformulated the previous equation for adjacent peaks, and the final equation can be observed below:

$$\theta_{s,l} = 1 - \left[\frac{(H_v \times |t_{R,l} - t_{R,s}|)}{(|t_{R,v} - t_{R,s}| \times (H_l - H_s) + H_s \times |t_{R,l} - t_{R,s}|)} \right] \quad (2)$$

where H_v , H_l , H_s , $t_{R,l}$, $t_{R,s}$ and $t_{R,v}$ are the heights of the large and small peaks, the valley between those peaks and their respective elution times, as can be seen in Figure 8 below.

Duarte and Duarte (2010) developed a new CRF (also called Duarte's Chromatographic Response Function, DCRF), whose form can be seen in equation 3, for analyzing complex samples by size exclusion chromatography (SEC). Nevertheless, as described by Matos *et al.* (2012), the DCRF function cannot be used to optimize separations when the time of analysis plays a major role, such as in the development of analytical procedures (e.g. RP separation methods) to be used in routine analysis.

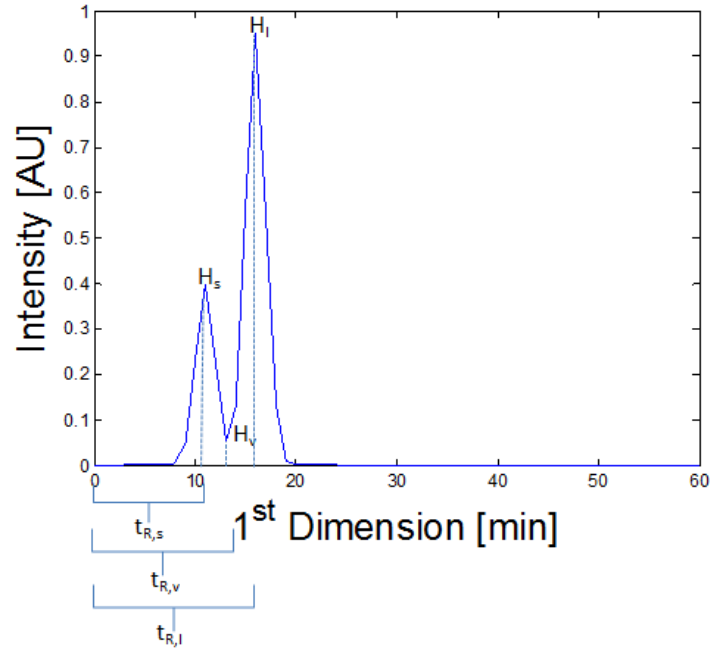


Figure 8: Schematic representation of a 1D chromatogram illustrating the parameters for the estimative of resolution between unresolved peaks using equation 2.

This equation also should not be used in cases where one only wants to identify the maximum number of chromatographic peaks present in a chromatogram, mostly because the degree of separation criterion and the number of peaks have the same weight: the function can choose as optimum a chromatogram with a low number of very well resolved peaks instead of a chromatogram with a higher number of poor resolved peaks (Matos *et al.*, 2012).

$$\text{DCRF} = N + \sum_{i=1}^{N-1} \theta_{s,i} - f(t) \quad (3)$$

and $f(t)$ is defined according Matos *et al.* (2012) as:

$$f(t) = \frac{t_{R,L} - t_0}{t_{R,L}} \quad (4)$$

where $t_{R,L}$ is the retention time of the last eluted peak and t_0 is the elution time corresponding to the column void volume, as mentioned above.

According to Matos *et al.* (2012), the $f(t)$ parameter, in equation 4, is defined as a ratio between the available time of analysis and total time of analysis. This parameter has a constrain: when the retention time of the last eluted peak ($t_{R,L}$) is 10 times more higher than

the retention time corresponding to the column void volume (t_0) (e.g., when dealing with a reversed phase separation process), the subtraction is very close to $t_{R,L}$, which implies that $f(t)$ is approximately 1, making it impossible to distinguish and differentiate the chromatograms obtained under such operational conditions (Matos *et al.*, 2012). Another limitation of this parameter has been mentioned by Duarte and Duarte (2010): the criterion $f(t)$ is only important for distinguish between chromatograms with the same number of peaks and the degree of separation, but with different analysis times. Indeed, the total time of analysis is an important criterion in chromatography but it does produce a relevant impact in the value of the DCRF (equation 3), especially in the case of chromatograms with a large number of peaks. Incorporating the criteria $t_{R,L}$, t_0 , and N , Matos *et al.* (2012) developed the following equation for a new time-saving term ($f(t)_w$):

$$f(t)_w = N \times \frac{\log[(1-f(t)) \times 100]}{2} \quad (5)$$

where N is the total number of resolvable and overlapped chromatographic peaks detected in a chromatogram, and the other parameters have been already described. The value of $f(t)_w$ is then maximum when $t_{R,L}$ is very close to t_0 . For example, for a chromatogram with five detected peaks and a t_0 value of 500 (100 times higher), the value of $f(t)_w$ is close to five. The logarithm effect incorporated in equation 5 becomes notable because small times of analysis provide a better differentiation between chromatograms, but large times of analysis still allows achieving some degree of differentiation (Matos *et al.*, 2012).

The DCRF equation developed by Duarte and Duarte (2010) only works well when the number of peaks and degree of separation has the same impact on the result. In such cases, the $f(t)$ criterion becomes important for differentiating chromatograms with the same number of peaks and degree of separation. However, according to Matos *et al.* (2012), in practice, there are a plethora of different possible scenarios in the optimization of a chromatographic process that are not taken into account if applying the same weight to each one of these three criteria. In order to overcome this constrain, Matos *et al.* (2012) improved the model of equation (3) in order to include weights in each of the criteria, thus yielding the following equation 6:

$$DCRF_f = \alpha \times (N) + \beta \times \left(\sum_{i=1}^{N-1} \Theta_{S,L} \right) + \gamma \times (f(t)_w) \quad (6)$$

where α is the weigh associated to the number of peaks, β is the weigh associated to the degree of separation and the γ is the weigh associated to the new time-saving criterion. The condition of these three parameters for different weights is that their sum must be equal to the unity, i.e.: $\alpha + \beta + \gamma = 1$. There are several possible combinations (almost unlimited) of values of α , β , and γ , in order to verify this condition, and their values depend on the identification of the relevance of each criterion in the analytical work under consideration (Matos *et al.*, 2012). Table 1 describes the four major types of scenarios that usually translate the main needs of an analyst interested in applying the $DCRF_f$.

Table 1: Different weights for the parameters of $DCRF_f$ equation, used for different analytical scenarios.

Scenario	α	β	γ
1	0.80	0.10	0.10
2	0.50	0.25	0.25
3	0.60	0.10	0.30
4	0.10	0.80	0.10

The first scenario implies that the most important criterion is the number of peaks with an α value of 0.8, while degree of separation and time-saving have the same weigh. In the second scenario, the number of peaks is still the most important criterion, although the weigh given to this criterion is lower than in the first scenario. As in the previous case, the degree of separation and time-saving have the same weigh, however, the sum of β and γ has the same impact as the most important criterion (α). In the third scenario, the most important criterion still is the number of peaks, followed by the time-saving and finally the degree of separation of peaks. In the fourth scenario, the most important criterion is the degree of separation (β). The number of peaks and time saving criteria has the same relevance to the value of $DCRF_f$. As pointed out by Matos *et al.* (2012), “*the choice of either of these scenarios should be done carefully, since the result of the $DCRF_f$ will have a great impact on the choice of the best chromatogram, and consequently in the chromatographic optimization process*”.

The use of 2D-LC implies the use of different mathematical functions compared to 1D-LC. Duarte *et al.* (2012) introduced the following chromatographic function ($DCRF_{2D}$)

for 2D-LC systems, based on peak purity (P_{i2D}), number of peaks (N_{2D}), and time-saving $f(t)_{2D}$ criterion.

$$DCRF_{2D} = \sum_{i=1}^{N_{2D}} P_{i,2D} + N_{2D} - f(t)_{2D} \quad (7)$$

The term that measures the ration between the volume of the overlapped region of the 2D peak and the total volume of this same 2D peak is the peak purity (P_{i2D}). The $f(t)_{2D}$ is considered as a penalty for the $DCRF_{2D}$, and Duarte *et al.* (2012) suggested the following 2D time-saving equation, associated with the time spent in the analysis:

$$f(t)_{2D} = \frac{(t_{R,L,1D} \times t_{R,L,2D}) - (t_{0,1D} \times t_{R,L,2D}) - (t_{0,2D} \times t_{R,L,1D}) + (t_{0,1D} \times t_{0,2D})}{t_{R,L,1D} \times t_{R,L,2D}} \quad (8)$$

where $t_{R,L,1D}$ and $t_{R,L,2D}$ are the elution times of the last 2D peaks in the first and second chromatographic dimensions, respectively, and $t_{0,1D}$ and $t_{0,2D}$ are the elution times corresponding to the extra column volumes of the columns of the first and second dimensions, respectively. An improvement to this time-saving criterion has been further suggested by Matos *et al.* (2012), being this translated in Equation 9. As discussed by Matos *et al.* (2012), Equation 8 shows an important drawback. In this latter equation there is a direct relationship for the calculation of the chromatographic areas, especially between the time spent in the 1D and 2D , as this criterion gives similar values for a chromatogram with a short elution time in the 1D but with a large retention time in the 2D and another chromatogram with a large retention time in the 1D but with a short retention time in the 2D . According to Matos *et al.* (2012), and despite the fact these chromatograms exhibit the same geometric area, they are not equal in terms of time spent on the analysis and, therefore, they should not have the same result in terms of time-saving criterion.

$$f(t)_{2D} = \left(\frac{\sqrt{t_{R,L,1D}^2 + t_{R,L,2D}^2} - \sqrt{t_{0,1D}^2 + t_{0,2D}^2}}{\sqrt{t_{R,L,1D}^2 + t_{R,L,2D}^2}} \right) \times \frac{\emptyset - \arctan\left(\frac{t_{R,L,2D}}{t_{R,L,1D}}\right)}{\emptyset} \quad (9)$$

where the parameter \emptyset is $\pi/2$ and the arctan is calculated in radians, respectively. This parameter will penalize the least, the chromatogram with the lowest time spent in both chromatographic dimensions, but it gives more importance to the time spent in the 2D than in the 1D , which can benefit those chromatograms where the time spent in the 1D is

extremely long. Furthermore, when the time of the ²D is very close to zero, then the angle of the vector will also be zero and the result of Equation 9 will be the same as that given by the corresponding 1D equation, i.e., by Equation 4.

Matos *et al.* (2012) also mentioned some additional problems that the criterion in Equation (9) could impose in evaluating chromatograms with high elution time of the last chromatographic peak obtained in the ²D, and also the difference in its weight from the other criteria of the DCRF_{2D}. According to Matos *et al.* (2012), these problems can be avoided by the application of the logarithm operator (Equation 10) and a proper weight to the criterion in the same way as applied to 1D version:

$$f(t)_{w,2D} = N_{2D} \times \frac{\log[(1-f(t)_{2D}) \times 100]}{2} \quad (10)$$

The application of a logarithm operator benefits most the chromatograms with the lowest time spent in the analysis. The benefit varies between a minimum value of 0 for chromatograms with a time of analysis 100 times higher than the elution time corresponding to the column void-volume, and a maximum value equal to the number of 2D peaks for a theoretical chromatogram where the elution time of the last peak is the elution time corresponding to the column void-volume in both chromatographic dimensions (Matos *et al.*, 2012).

Taking into account the new time-saving criterion, Matos *et al.* (2012) suggested a new weighted and more flexible DCRF equation for LC×LC analysis, which is illustrated in Equation (11). All the parameters of this mathematical formula were presented above, and this can be considered the simplest way to estimate and rank the quality index of separation in non-targeted chromatographic analysis of complex samples.

$$DCRF_{f,2D} = \alpha \times N_{2D} + \beta \times \left(\sum_{i=1}^{N_{2D}} P_{i,2D} \right) + \gamma \times (f(t)_{w,2D}) \quad (11)$$

III

**Optimization in analytical chemistry –
basic concepts**

3.1. Introduction

For the optimization of an analytical chemistry methodology there are several designs available in order to obtain the best information with the lowest possible number of experiments. Experimental design or design of experiments (DOE) is the most popular approach, reported in the literature, for screening and optimization of the factors that play a significant role in any experiment. This method, improves the efficiency of scientific studies, in particular minimizing waste and costs. Schoenmakers and Mulholland (1988) and Deming *et al.* (1989) were the first to use DOE in their experiences. The first authors used a computer-assisted optimization in high performance liquid chromatography (HPLC) and the later authors applied the optimization process also in liquid chromatography.

According to D.L. Massart (1997) the experimental conditions, such as column temperature, characteristics of the column's stationary phase, mobile phase composition (including, the nature of organic modifier and its concentration, pH, and ionic strength), and the flow rate, are analytical variables that usually contribute to the success of any chromatographic separation to. The choice of the most appropriate non-adjustable variables (e.g. type of stationary phase, solvent and/or buffer nature) is usually performed on the basis of prior knowledge. On the other hand, the assessment of the best conditions of the readily adjustable variables (e.g. temperature, the concentration of organic modifier, pH, ionic strength, and flow rate) can be notably expedited by applying computer-assisted optimization strategies.

3.2. Design of experiments

When attempting an experimental design, it becomes important to find about any of the previous experiments that have already been studied. To perform an experimental design, there are some important steps that must be considered, like for example: the goal of the experiments, the number of significant factors, the ranges of the factors, and the

significant interactions between factors, and the model to fit to the data obtained in the experiments (Leardi, 2009). The experimental design is not only applied to obtain optimal responses but also optimal models, for example a regression model or an ANOVA model. The order of experiments is carried out randomly, not following any criteria. The real values of the experiments can be coded in two levels (+1 and -1), where -1 indicates the lower value, +1 indicates the highest value. The variables can be quantitative (e.g. temperature, pressure, concentrations) or qualitative (e.g. type of catalyst, type of apparatus, sequence of operations).

According to D.L. Massart (1997), there are several main steps of an experimental design, which can be systematized according to the flowchart shown in Figure 9.

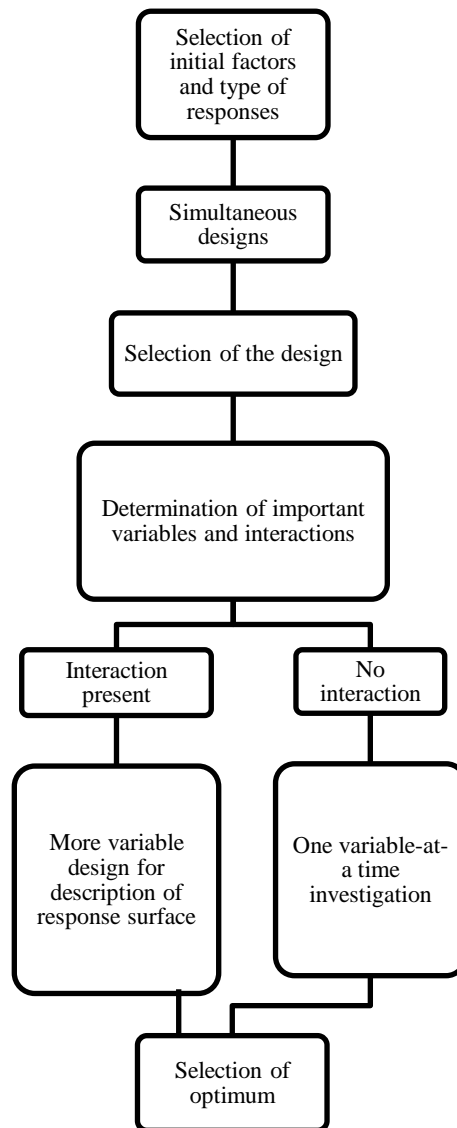


Figure 9: Several steps of an experimental design (Inspired by D.L. Massart, 1997)

The first step entails the selection of the factors that are going to be optimized, followed by the choice of the adequate experimental design that can be employed. The fourth step consists on the determination of the important variables and also the relevant interactions between the variables which most influence the type of the response previous selected. Next, if there is an interaction between the main factors, quadratic terms are added to the second degree polynomial, in order to check the curvature of the model and construct a response surface. The purpose of fitting a model is to try, in one equation, to represent all the results and hence all the information, from the experiments. In the absence of an interaction, a one variable-at-a-time procedure must be undertaken. Finally, with the previous results, the optimum value for each studied variable can be estimated.

Several designs can be applied for the optimization process based on the criterions that should be optimized. Those that are commonly found in literature include the two-level factorial, Plackett-Burman, central composite, Box-Behnken, and D-Optimal. The latter design is one of the methods most used in DOE, and it is applied when the experimental region is irregular (which is the case of chromatography) the qualitative factors have more than two levels, the number of design runs has to be reduced, special regression models must be fitted, or process and mixture factors are used in the same design. In the case that the designs are irregular in shape the common designs, such as: factorial designs, central composite design are not applied (Aguiar *et al.*, 1997), and all areas of the irregular experimental design may be restricted due to one corner of the region that may not be accessible for experimentation. Aguilar *et al.* (1997) have described an irregular experimental domain in HPLC, when optimizing, at the same time, the pH and the percentage of methanol in the mobile phase. A common reason for irregularly shaped experimental regions is that one of the combinations of the extreme levels of the variables is practically not possible. The possible experimental domain (i.e. the extreme levels at which the factors will be studied) is first delimited by a retention boundary map, i.e., one determines with a few experiments the area in which it is possible to have suitable retention. The D-optimal is a sequential design and they are one form of design provided by a computer algorithm. These types of computer-aided designs are particularly useful when classical designs do not apply. D-optimal designs are straight optimizations based on a chosen optimality criterion and the model that will be fit. This optimality criterion results in minimizing the generalized variance of the parameter estimates for a pre-specified

model. As a result, the 'optimality' of a given D-optimal design is model dependent. That is, the experimenter must specify a model for the design before a computer can generate the specific treatment combinations. Given the total number of treatment runs for an experiment and a specified model, the computer algorithm chooses the optimal set of design runs from a candidate set of possible design treatment runs. This candidate set of treatment runs usually consists of all possible combinations of various factor levels that one wishes to use in the experiment.

One advantage of the D-optimal design is its flexibility: not only does it allow to work in an experimental domain that is not cubical or spherical, but also one can impose that certain experiments must be included and then compute which additional points are needed to complete a design.

3.3. Simplex algorithm

An optimization process which has not been commonly used is the Simplex, although this method allows to obtain an immediate response. For a three-component mixture, a Simplex is a triangle, for a four-component mixture, it is a tetrahedron, and so on. For example, a typical mixture design equation, with three components, is given below:

$$Y_{123} = b_1x_1 + b_2x_2 + b_3x_3 + b_{12}x_1x_2 + b_{13}x_1x_3 + b_{23}x_2x_3 + b_{123}x_1x_2x_3 \quad (12)$$

where, the response y_{123} means that components x_1 , x_2 , and x_3 are present in equal proportions.

This type of design is based on an initial design of $k+1$ trials, where k is the number of variables. The geometric figure with a k -dimensional space is called a simplex. For example, if the number of factors is two, the design uses three points and thus forms one triangle. The optimization starts with the three first experiments, as shown in Figure 10. The points representing the experiments form an equilateral triangle and point 2, in Figure 10, shows the worst response of the three. It is logical to conclude that the response will probably be higher in the direction opposite to this point, as also shown in Figure 10.

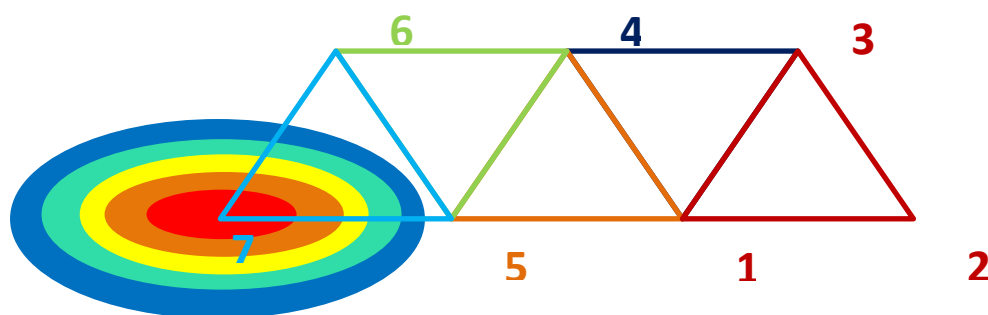


Figure 10: Example of Simplex optimization.

Therefore, the triangle is reflected so that point 4, opposite to point 2, is obtained. Points 1, 3 and 4 form together a new simplex. This procedure is repeated and the optimization process ends when the optimization objective is reached or when the response cannot be improved further, as it is shown by point 7 in Figure 10.

One advantage of Simplex algorithm is that allows to obtain the response after each chromatographic run, and It does not require blocks, which is a drawback when using non-sequential algorithms

IV

**Application of LC×LC applied to the
analysis of complex mixtures**

LC×LC has been increasingly used for the separation of complex mixtures, such as biological samples, macromolecules, foodstuffs, beverages and natural organic matter. Table 2 summarizes the studies published after 2008, inclusive, using LC×LC for the analysis of such complex mixtures. Before 2008, several authors (e.g. Stroink *et al.* (2005) and Stoll *et al.* (2007)) reviewed such fields of application and readers should consult those reviews for a deeper insight into the achievements of LC×LC. Overall, Table 2 shows that a large variety of LC×LC combinations can be used to resolve a specific separation problem, depending on the differences of the size, polarity, and shape of the compounds or groups of compounds.

In the field of foodstuffs and beverages, Kivilompolo *et al.* (2008) tested several columns in an RP×RP arrangement for the quantification of antioxidant polyphenols in red grape wine, red grape juice, and black currant wine. A C18 column was used in the ¹D whereas a C18 with an ion-pair reagent was used in ²D. Kivilompolo *et al.* (2008) also tested two additional columns in the ²D, a cyano and an amino column, nonetheless, the best results were obtained with the C18 with an ion-pair reagent which promotes a better separation of the analytes. These ion-pair reagents, as in the case of tetrapentylammonium bromide, can improve the shape of the peaks when a typical approach for achieving the best separation fails, such as changing the stationary phase or the eluent. The cyano columns are the most polar and the least retentive of all RP packings. Extremely hydrophobic compounds (e.g. polyphenols), which do not elute on a standard C18 packing with typical RP eluents, can be separated using a cyano stationary phase. In case of the amino column, the elution order is always based on the hydrophobicity of the analytes rather than on polar interactions with the base stationary phase.

Dugo *et al.* (2009) also evaluated the potential of RP×SEC for the separation and quantification of phenolic antioxidants in red wines, and compared the prediction capability of both ²D (RP and SEC) and the most commonly used ¹D approach (RP). Using 1D-LC with a C18 column, in a gradient mode, Dugo *et al.* (2009) were able to separate 13 phenolic compounds, although they observed a hump in the chromatogram, likely caused by unresolved interferences from the sample matrix. The authors concluded that the quantification using the 1D-LC methodology is difficult and highly inaccurate.

Table 2: Survey of the studies published after 2008, inclusive, using LC×LC for the analysis of complex samples.

Sample	Application		Separation Mechanism		Mobile phase		Elution mode	Detectors	References
	Matrix	Analyte	¹ D	² D	¹ D	² D			
Food stuffs and beverages	Red grape wines, red grape juice and black currant wine	Polyphenols	RP	RP with ion pair reagent	CH ₃ CN and 0.5% CH ₃ COOH	Tetrapentylammonium in CH ₃ CN and 0.05% CH ₃ COOH	¹ D: Gradient ² D: Isocratic	ESI-TOF-MS	Kivilompolo <i>et al.</i> (2008)
	Red wine	Polyphenols	RP	SEC	CH ₃ CN and H ₂ O	CH ₃ CN and H ₂ O	Gradient	DAD	Dugo <i>et al.</i> (2009)
Macro-molecules	Polymers	Polystyrene and polyethylene oxide	RP or NP	SEC	18% DMF 82% THF 96% DMF 4% THF	DMF and THF	¹ D: Isocratic ² D: Gradient	¹ D: ELSD ² D: FTIR	Malik <i>et al.</i> (2012)
	Polymers	Polystyrene	RP or NP	SEC	THF and C ₆ H ₁₂	THF and CH ₃ CN	Isocratic	ELSD	Sinha <i>et al.</i> (2012)
	Copolymers	Polyolefin	RP or NP	SEC	100% decane 100% TCB	TCB with ionol	¹ D: Isocratic ² D: Gradient	IR, LS, and RI	Lee <i>et al.</i> (2011)
	Polymers	Hydroxypropyl-methylcellulose	RP	SEC	0.05% C ₂ HF ₃ O ₂ and 0.05% C ₂ HF ₃ O ₂ in C ₃ H ₈ O	0.05% C ₂ HF ₃ O ₂	Gradient	CAD	Greiderer <i>et al.</i> (2011)
	Polymers	Polysorbates and fatty esters of polyethylene glycol	RP	HILIC	93% water	97% CH ₃ CN	¹ D: Isocratic ² D: Gradient	ELSD	Abrar and Trathnigg (2010)

Table 2: (Continued)

Sample	Application		Separation Mechanism		Mobile phase		Elution mode	Detectors	References
	Matrix	Analyte	¹ D	² D	¹ D	² D			
Herbs and Plants	<i>Camellia Sinensis</i>	Extracts	SEC	RP	H ₂ O and CH ₃ CN	0.1 FA and CH ₃ OH	Gradient	UV and MS	Scoparo <i>et al.</i> (2012)
	<i>Platycodi Radix</i>	Platycosides	RP	HILIC and NP (cyano and amino columns)	5% CH ₃ CN and 95% CH ₃ CN containing 0.1% CH ₂ O ₂	5% CH ₃ CN and 95% CH ₃ CN containing 0.1% CH ₂ O ₂ for HILIC column and 20% and 70% CH ₃ CN containing 0.1% CH ₂ O ₂ for cyano and amino column	Gradient	ESI-MS	Jeong <i>et al.</i> (2010)
Biological Tissues	Rat brain	Peptides	RP or WCX	RP	H ₂ O, CH ₃ CN, NH ₄ FA in H ₂ O and 2% CH ₂ O ₂	0.1% FA and 0.1% FA in CH ₃ CN	Gradient	Q-TOF-MS	Cai <i>et al.</i> (2012)
	Rat plasma	Polypeptide	RP	RP	0.1% 3-NBA ⁵	0.1% 3-NBA in CH ₃ CN	Isocratic	MS	Halquist <i>et al.</i> (2012)
	Bovine serum	Proteins	SCX	RP	0.1% FA and 0.1% FA in CH ₃ CN	0.1% FA and 0.1% FA in CH ₃ CN	¹ D: Gradient ² D: Isocratic	MS	Kajdan <i>et al.</i> (2008)
Natural Organic matter	Atmospheric particles	Aerosols	RP or HILIC	SEC	20% CH ₃ CN 20 mM CH ₃ COONH ₄ , 10% CH ₃ CN (in HILIC)	20 mM NH ₄ HCO ₃ , 11% CH ₃ CN	Isocratic	DAD FLD ELSD	Duarte <i>et al.</i> (2012)

The RP×SEC method was then used in order to improve the sample separation and to reduce the interferences from the sample matrix. The authors concluded that the compounds were well separated, but with a low degree of orthogonality. Nevertheless, a higher number of compounds could be correctly identified and quantified.

Malik *et al.* (2012) used critical conditions of polystyrene and polyethylene oxide (PEO) as the basis for LC×LC separation of PS-*b*-PEO polymers. The liquid chromatography at critical conditions (LCCC) technique is often used to achieve a separation based only on a portion of interest of the polymers. In this work, the critical conditions were established for both polymers, using a mixture of DMF-THF at several percentages, whereas the separation mechanisms in ¹D was either RP or NP depending on the hydrophilic or hydrophobic blocks of these amphiphilic copolymers. In the LC×LC approach, the authors used SEC as the separation mechanism in ²D in order to determine the molar mass distribution of the copolymers.

Sinha *et al.* (2012) also investigated the feasibility of using critical conditions and LC×LC to separate protonated (H-PS) and deuterated polystyrene (D-PS) of similar molar masses and chemical composition. The critical conditions for separating blends of H-PS and D-PS were established using a mixture of THF-CH₃CN and a C18 column for H-PS, and a mixture of THF-C₆H₁₂ and a Si column for D-PS. LC×LC analysis of the blend components, where LCCC was used in the ¹D and SEC in the ²D, showed that the separation was solely based on isotopic effects and not influenced by the molar mass of the blended components.

Lee *et al.* (2011) applied high temperature (150°C) in a RP×SEC and NP×SEC methods for the quantitative determination and characterization of molecular weight heterogeneities of polyolefins. Being less sensitive to temperature variation than refractive index (RI) detector, the coupling of an infrared (IR) detector to the RP ×SEC and NP×SEC allowed determining the distribution and the chemical composition of polymers with adequate sensitivity and linearity. The use of a light sensor (LS) detector in addition to an IR resulted in the determination of the absolute mass weight of the separated fractions.

Greidere *et al.* (2011) characterized samples of hydroxypropylmethylcellulose (HPMC) polymers by RP×SEC, exploring both the size distribution and chemical composition (percentage of methoxyl and hydroxyl-propoxyl substitutes) of the samples. The authors concluded that RP×SEC was able to separate different HPMC polymers in

terms of their molecular weight, molecular composition (degree of methoxyl substitution and molar hydroxypropyl substitution), and polydispersity. Since temperature has a significant effect on hydrophobicity, it can change the solubility of HPMC. Taking advantage of this feature, Greidere *et al.* (2011) performed their studies at low (18°C) and high (38°C) temperatures, and found a significant retention of HPMC in both separation mechanisms (RP and SEC) at the lower temperature.

Abrar and Trathnigg (2010) tested the separation of amphiphilic polymers, such as fatty esters of polyethylene glycol (PEG) and polysorbates (higher esters), by LC×LC. In the ¹D it was used a RP column (because retention of higher esters is very strong), whereas in the ²D an HILIC column and an organic-rich mobile phase were employed, where acetone was used instead of acetonitrile due to the higher price and toxicity of the second. Abrar and Trathnigg (2010) concluded that fatty ester ethoxylates, which are synthesized from ethoxylation of fatty alcohols, were separated on the HILIC column, while higher esters were separated in the RP column.

Scoparo *et al.* (2012) tried to identify the composition of green and black tea of the *Camellia sinensis* with 1D-LC and LC×LC systems. In 1D-LC, several classes of compounds were identified (e.g., quinic acid, 3- and 5-p-coumaroylquinic acid, 3- and 5-galloylquinic acid and 3-, 4- and 5-caffeoylquinic acid) using a C18 column and a detection system composed of a DAD and an evaporative light scattering detector (ELSD). Regarding the LC×LC analyses, the ¹D encompassed a SEC column, which proved to have hydrophobic interactions with the sample, whereas a C18 column was used in the ²D. The authors concluded that several compounds from the plant extracts, namely flavonoids and their glycosides, were well separated by the SEC column.

Jeong *et al.* (2010) developed a LC×LC method for the separation of platycosides extracted from *Platycodi Radix*, and subsequent quantification by MS. The researchers tested two different separation mechanisms, cyano NP and HILIC amino columns, in the ²D. The cyano NP column did not provide any increase in peak capacity, while the HILIC amino column provided a good separation and a better peak resolution. Indeed, the HILIC column shows a high orthogonality when combined with RP, but the use of that column for the separation of platycosides is limited to non-aqueous mobile phases.

Cai *et al.* (2012) applied a RP and WCX column in the ¹D and a RP column in the ²D for proteome analysis. The mixed-mode column was synthesized in the authors'

laboratory and showed adjustable selectivity under different pH conditions. Under acidic conditions, the column mainly provided hydrophobic interactions and showed selectivity similar to that of the common classic RP column. Under neutral and weak basic conditions, it offered multiple retention mechanisms, including RP and cation-exchange mechanisms, and differed in selectivity from the classic RP column.

Halquist *et al.* (2012) showed that the LC×LC technique provide a robustness and an efficient separation when attempting the determination of an anorectic polypeptide (oxyntomodulin) in rat plasma. The authors applied a C8 column in the ¹D, and a C18 in the ²D and a mobile phase was 3-nitrobenzyl alcohol in both dimensions, but in ²D also was used CH₃CN because it shows adequate results for the ionization of peptides.

Kajdan *et al.* (2008) described an LC×LC-ESI-TOF-MS method for the separation of several bovine serum albumin (BSA) variants, one of which was characterized as oxidized BSA and the other as unoxidized BSA. The two chromatographic dimensions involved the use of a cation-exchange (SCX) column in the ¹D (that allows a better recovery of peptides) and a RP column in the ²D. This combination of separation mechanisms (LC×LC-ESI-TOF-MS) offered the advantages of the unique selectivity and high efficiency of the separation methods combined with the mass specificity and sensitivity of MS.

Duarte *et al.* (2012) analysed natural organic matter (NOM), namely standard Suwannee River Fulvic Acids (SR-FA) and reference Pony Lake Fulvic Acids (PL-FA) samples, in a LC×LC system using either a conventional C18 column or a mixed-mode hydrophilic column (operating in per aqueous liquid chromatography (PALC) mode) in the ¹D and a size-exclusion column in the ²D. The detection system comprised a DAD operating at 254 nm, a fluorescence detector operating at excitation/emission wavelengths ($\lambda_{Exc}/\lambda_{Em}$) of 240/450 nm, and an ELSD, with all the three detectors coupled in series. Firstly, the authors searched for the most appropriate chromatographic conditions in both dimensions, especially in terms of mobile phase composition, flow rate, modulation period, and total analysis time. The authors concluded that both C18×SEC and PALC×SEC assemblages seem to be promising in resolving the chemical heterogeneity of complex unknown organic mixtures. Using the data from the UV detector, the authors also concluded that the molecular weight distribution of the NOM samples estimated through both LC×LC systems was lower than those reported in the literature.

V

Experimental conditions for chromatographic analysis of wine samples

5.1. Chemicals

All chemicals used in this work were of analytical reagent grade and obtained from commercial suppliers without further purification. All solutions were prepared with ultra-pure water (18 M Ω cm).

Mobile phases for the LC \times LC experiments were prepared with HPLC grade methanol (MeOH), potassium phosphate buffer (KH₂PO₄ and K₂HPO₄). The compositions of the mobile phases for the first and second dimensions were adjusted according to the experimental conditions described in sections 5.4.1. and 5.4.2., respectively. Prior to use, the mobile phases were filtered through membrane filters (PVDF, Gelman Sciences) of 0.22 μ m pore size.

The wine samples, used for each chromatographic analysis, were filtered through HPLC Certified Syringe Filters (SPARTAN, Whatman GmbH, Germany) of 0.20 μ m pore size and diluted in 20% of the mobile phase (v/v).

5.2. Description and preparation of wine samples

All samples of wine were obtained from red wine purchased at local supermarkets. After purchasing, a 12 mL aliquot of each sample was stored in a refrigerator at 4 °C. For preparing a composite red wine sample, which will be representative of all wine samples, 1 mL of each individual sample was pipetted and batched together. This composite sample was used through all the entire optimization process in order to estimate the best LC \times LC conditions and to predict the localization of the peaks in the individual red wine samples. Before the injection, an aliquot of 3 mL of each sample (composite or individual) was withdrawn into a 4 mL vial, where it was filtered through an HPLC Certified Syringe Filter (hydrophilic regenerated cellulose of 0.20 μ m pore size, SPARTAN, Whatman). Afterwards, the sample was diluted in 20 % (v/v) of the mobile phase and left to stand for

about 30 minutes to stabilize its temperature before analysis. All solutions of phosphate buffer were acidified to a value close to the pH of the wine samples (pH=3).

5.3. Instrumentation

In Figure 11 it is shown a schematic representation of the instrumentation set-up used in this work. The LC×LC assemblage is equipped with two columns that have different separation mechanisms, three pumps (two to control the elution in the ¹D and one to control the elution in the ²D), a chamber mixture for the ¹D, a DAD at the end of the ²D column, and an eight-port interfacing valve equipped with two identical sampling loops and two positions

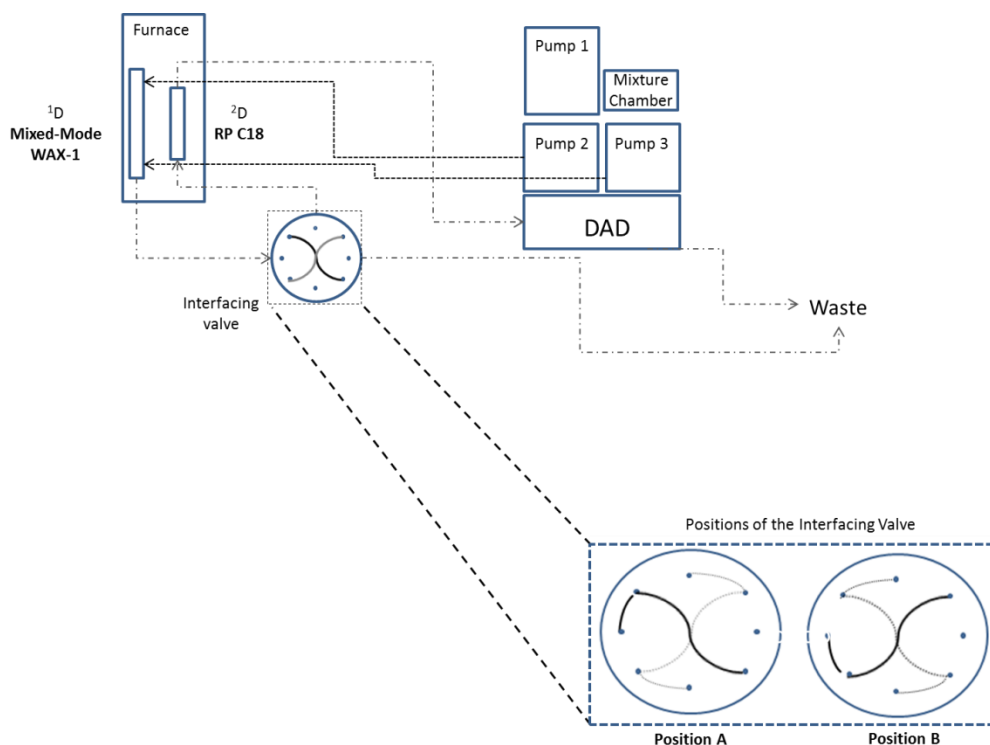


Figure 11: Schematic arrangement of the LC×LC assemblage used in this work (inset: operation positions A and B of the eight-port interfacing valve).

The ¹D consisted of two JASCO semi-micro HPLC pumps (model PU-2085 Plus), a Rheodyne injection valve (model 7725i) equipped with a 20 μ L loop, and an Acclaim Mixed-Mode WAX-1 column (Dionex, Sunnyvale, CA, USA; diameter 4.6 mm, length

150 mm, comprised of 5 μm high-purity, porous, spherical silica particles with 120 \AA diameter pores, bonded with alkyl diol functional groups), and a mixture chamber (model MX 2080-32 Dynamic Mixer). The ^1D was operated in gradient mode, and the temperature of the analytical column was maintained at 40 $^\circ\text{C}$ in a JASCO column oven (model CO-2065 Plus).

The column used in the ^1D optimization was an Acclaim Mixed-Mode WAX-1 column, already used in a wide range of separation challenges, including applications in pharmaceutical (Jaworska *et al.*, 2012), food stuffs and beverage (Chen *et al.*, 2013), and chemicals (Ordóñez *et al.*, 2012). As referred in the work of Ordóñez *et al.* (2012), the Mixed-Mode WAX-1 column packing features a silica-based stationary phase that incorporates both RP and weak anion-exchange properties. Unlike the traditional RP stationary phases, the new packing material features a hydrophobic alkyl chain with an ionizable terminus that gives the chromatographer total control of selectivity in the simultaneous separation of acids, bases, and neutral molecules.

The ^2D consisted of a JASCO quaternary low pressure gradient pump (model PU-2089 Plus) and a RP Kromasil[®] 100-5-C18 column (Eka Chemicals AB - Separation Products, Bohus, Sweden; diameter 4.6 mm; length 50 mm). The elution was also operated in the gradient mode. The temperature of the analytical column was also maintained at 40 $^\circ\text{C}$ in a JASCO column oven. The effluent of the ^2D column was connected to a DAD. The ^1D and ^2D were interfaced with an eight-port high pressure two-position interfacing valve (VICI[®] AG International, Schenkon, Switzerland) equipped with two identical 50 μL sampling loops.

The column used in the ^2D optimization was a RP-C18, which exhibits a high performance and it is manufactured using monofunctional silanes. The column is fully end-capped, which gives high reproducibility, chemical stability, and allows obtaining successful separations. The mobile phases commonly used in this type of columns consist in mixtures of water or aqueous buffer and organic solvents. In this work, the mobile phases comprised MeOH and phosphate buffer, whose proportions were adjusted according to the results of the Simplex algorithm as described in section 7.1.

5.4. Chromatographic conditions for experimental design

Ideally, the optimization for the ¹D and for ²D should be done at the same time, but there are limitations in terms of equipment and software, which makes it impossible to pursue. Thus, the first part of the work consisted in the optimization of different operational conditions, namely the mobile phase composition (including the concentrations of MeOH and phosphate buffer) and the time of analysis for the first chromatographic dimension. Table 3 shows the experimental variables and the corresponding ranges of variation used for attempting to find the optimum separation conditions by gradient elution in the ¹D. The gradient mode of elution was applied during the entire optimization procedure and it consists in changing the concentration of both organic solvent (i.e., MeOH) and phosphate buffer between the time of analysis 30 and 31 minutes. The flow rate applied in this optimization process was 0.5 mL min⁻¹.

Table 3: Experimental variables and their ranges of variation used in the optimization procedure for the ¹D.

Parameters	Units	Values
MeOH_i	%	5-10
[Buffer]_i	mM	40-50
t_i	min	2-3
MeOH_f	%	40-50
[Buffer]_f	mM	5-10
t_f	min	4-6

The ranges of concentration of MeOH were chosen according to some preliminary studies. There was a prior knowledge that MeOH concentration in RP columns (which will be used in the ²D) should not be less than 5 % (v/v) (diluted samples are required in order to increase the lifetime of the column), and can be not greater than 50 % (v/v) (higher % of MeOH favors the retention of compounds thus causing problems in the ²D column, such as fluctuations on the baseline and too long time of analysis). The ranges variation of buffer concentration were chosen based on the work of Dufrechou *et al.* (2012), where it is reported that the ionic strength in wine samples must be maintained between 0.02 and

0.15 M in order to avoid protein unfolding and aggregation. The ranges of the values of time of analysis were chosen by comparison with preliminary experiments performed in advance on the same samples used for this work.

5.4.1 Optimization of one-dimensional liquid chromatography (1D-LC)

D-Optimal was chosen as experimental design because it is the most economical design, it allows the spread of experiments by blocks and the number of experiments is smaller when compared to other designs, like Box-Benhken or factorial composite design. The optimization procedure was performed using the composite wine sample and by testing several possibilities of concentration of MeOH and phosphate buffer that are given by the design in order to find the optimal conditions for the chromatographic separation, whose proportions were adjusted according to the results of the D-Optimal as described in section 6.1. The ¹D was operated in gradient mode, where between minute 30 to 31, as can be seen in Figure 12 in purple colour, it occurred the change of the % of the organic solvent. The used solvent organic was methanol and the salt was phosphate buffer. The flow rate was 0.5 mL min⁻¹.

5.4.2. Optimization of the second dimension (²D) in LC×LC

The D-Optimal was also the first choice for an experimental design for the optimization of the ²D separation conditions due to the possibility of performing the experiments in blocks. The results obtained through the optimization of the ¹D allowed concluding that only two factors are determining for the optimization of the ²D using the gradient mode of elution, i.e., the initial and final concentration of MeOH (in %, v/v). D-Optimal led to more issues that are carefully discussed in section 7 and this design does not

work for the optimization of the 2D with only two experimental variables. Therefore, one of the solutions was to follow a new optimization procedure, namely a design which could produce an immediate response after each analysis. The Simplex was found to be the most suitable for the new optimization for the 2D , since the response after each analysis can be used to direct the path to the optimal conditions. Also, the number of the runs of Simplex compared with that of the D-Optimal is lower, which allows saving time of analysis and amount of solvent. For the Simplex algorithm, the range between the initial and final concentration of MeOH was narrower than that of the 1D , due to problems that have been detected with a more ample range of MeOH concentration. Thus, the range of MeOH concentration in this new optimization is from 25% to 50% (v/v).

After determining the optimal conditions, either in the 1D and the 2D , some individually wine samples were further analyzed by means of the LC \times LC technique.

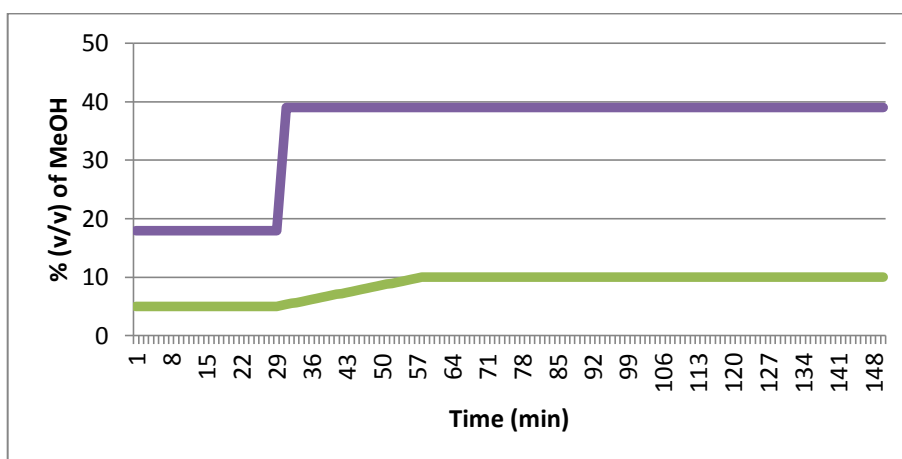


Figure 12: Elution program applied into 1D (purple) and 2D (green).

The 2D also operated in gradient mode where between minute 30 to 60 occurred the change of the % of methanol, as demonstrated in Figure 12. The mobile phase composition consisting of 40 mM phosphate, and the flow rate was $3.0 \text{ mL}\cdot\text{min}^{-1}$.

5.5. Software for control and data acquisition

For the 1D-LC analysis, the instrumentation was controlled and data set acquired with ChromNav Chromatography Data System software (JASCO Corporation, Tokyo, Japan). In the LC×LC analyses, all data set was acquired with the PSS WinGPC Unity (Polymer Standards Service GmbH, Mainz, German) software.

In 1D-LC, the optimization was performed by using Design Expert 7.0.0 trial software and the results were represented using MATLAB R2011a program (The Mathworks Inc., Natick, MA, USA). The chosen method was the D-Optimal design, which allowed the experiences to be distributed in blocks. For the LC×LC optimization, a D-Optimal design was firstly employed, but since it was intended to optimize only two parameters, the D-Optimal design cannot respond to long analysis times and cannot make the needed blocks. Therefore, it was decided to apply a Simplex, which allows obtaining an immediate response and then verify the tendency of the optimum value. For LC×LC optimization, two different softwares were employed: the first one was the Design Expert 7.0.0 trial; and the second was the MultiSimplex[®] 98. The representation of all chromatograms obtained in 1D-LC and LC×LC analyses were performed by MATLAB software (Mathworks Inc., Natick, MA, USA R2011a). The algorithms developed in this study and data treatment were coded also in MATLAB environment.

This algorithm is based in the work of Matos *et al.* (2013) and consists in calculating the backgrounds associated with the initial data due to some baseline instability. Then, the background was subtracted from the original data. The next step entailed the estimative of the blank, which was then incorporated in the corrected data matrix.

VI

**Search of optimum conditions for
1D-LC of wine samples**

6.1. Choice of operational details and starting conditions

The first step of any analytical procedure consists in the optimization of the conditions for producing the best results. This section describes the results of the optimization procedure in the ¹D in order to find the most adequate LC×LC chromatographic conditions.

For ¹D optimization, in the gradient mode, the D-Optimal design was used because it is the most economical design, i.e., it requires a smaller number of experiments and, on the other hand, it allows the spread of experiments into blocks. As described in section 5.4, Table 3, the experimental variables that were subject to optimization are: initial and final concentration (% v/v) of MeOH, initial and final concentration of phosphate buffer, and the start time and end time of the gradient elution. All analyses were conducted at a flow rate of 0.5 mL min⁻¹ for a total time of analysis of 40 minutes. The experimental conditions proposed by the design are shown in Table 4, wherein a total of 45 experiments and 8 blocks were involved in the D-Optimal design.

This array of experimental conditions were generated by the D-Optimal design randomly and, after the 45th analysis, the obtained ¹D chromatographic profiles were translated into a numerical value considering only the number of peaks appearing in the chromatogram and the f(t)w criterion (Equation 4). The CRF used in this part of the work is a “sub-function” of the DCRF_f in Equation (6), where only the number of peaks and the time-saving criteria are considered to discriminate between chromatograms with different separation quality. The weight applied to each of these criteria was 20% to the number of peaks and 80% for the total time of analysis. It was decided to attribute a huge weight to the total time of analysis because it is intended to minimize the time of analysis in the ²D. These calculation methods were performed using the algorithm described in section 5.5, where it was calculated the backgrounds associated with the initial data due to some baseline instability. Then, the background was subtracted from the original data. The next step entailed the estimative of the blank, which was then incorporated in the corrected data matrix. The chromatograms obtained in the optimization of the ¹D are shown in the Annex A from Figure 29 to Figure 73, which contains all 45 runs with the composite sample.

Table 4: Experimental design table produced by D-Optimal design for the 1D, using the Design-Expert software version 7.00.

Experimentes	Blocks	MeOH _i	[Buffer] _i	t _i	MeOH _f	[Buffer] _f	t _f	CFR
		% (v/v)	(mM)	(min)	% (v/v)	(nM)	(min)	
1	1	10.00	40.00	2.61	42.83	5.00	4.93	16.236
2		10.00	50.00	3.00	40.00	10.00	6.00	12.910
3		5.00	40.00	3.00	50.00	5.00	4.00	18.892
4		10.00	46.43	2.00	50.00	7.44	4.00	16.447
5		10.00	50.00	3.00	40.00	10.00	6.00	19.119
6		7.46	40.00	2.46	40.00	10.00	4.00	17.356
7	2	9.39	40.00	2.00	40.00	5.00	4.00	13.249
8		10.00	50.00	3.00	50.00	5.00	4.00	15.666
9		7.75	45.93	2.48	50.00	10.00	5.03	20.410
10		5.00	50.00	2.00	46.55	5.00	6.00	15.298
11		10.00	50.00	3.00	50.00	5.00	4.00	15.777
12		10.00	40.00	2.55	40.00	7.88	6.00	18.664
13	3	5.00	50.00	2.00	50.00	5.00	4.00	18.121
14		10.00	50.00	2.36	44.49	10.00	4.00	17.193
15		10.00	40.00	2.00	50.00	5.00	6.00	16.970
16		10.00	50.00	2.36	44.49	10.00	4.00	16.537
17		5.00	50.00	2.00	40.00	8.34	6.00	19.0487
18		5.00	40.00	3.00	50.00	1000	6.00	19.946
19	4	5.00	40.00	3.00	40.00	10.00	4.00	18.401
20		5.00	40.00	2.00	50.00	10.00	4.00	18.647
21		5.00	43.21	2.00	40.00	5.00	6.00	18.872
22		9.69	50.00	2.08	41.23	5.41	4.00	13.619
23		5.00	40.00	2.00	50.00	10.00	4.00	20.146
24		8.09	40.00	3.00	50.00	7.05	5.66	18.722
25	5	10.00	45.49	3.00	47.47	5.00	6.00	18.810
26		10.00	50.00	2.00	50.00	10.00	6.00	17.067
27		5.70	40.00	2.89	40.00	10.00	6.00	22.288
28		5.00	50.00	3.00	40.00	5.00	4.97	21.658
29		10.00	50.00	2.00	50.00	10.00	6.00	18.228
30		5.00	40.00	2.00	50.00	5.00	6.00	18.042
31	6	5.00	50.00	2.44	40.00	5.00	4.00	14.792
32		6.63	40.00	2.00	49.22	5.00	4.00	18.501
33		5.00	50.00	3.00	50.00	10.00	4.00	16.712
34		10.00	43.29	2.00	40.00	10.00	4.97	20.340
35		6.63	40.00	3.00	40.00	5.00	6.00	18.484
36		10.00	40.00	3.00	50.00	10.00	4.00	15.987
37	7	5.00	50.00	3.00	48.91	5.00	4.00	17.988
38		5.00	50.00	2.76	40.00	10.00	6.00	17.509
39		5.00	40.00	2.00	40.00	6.91	4.42	18.258
40		10.00	44.29	3.00	40.00	5.00	4.00	15.840
41	8	8.72	40.00	2.00	44.72	10.00	6.00	15.535
42		5.00	50.00	3.00	50.00	5.00	6.00	17.959
43		5.39	40.31	2.91	40.00	5.00	4.03	18.789
44		5.00	50.00	2.00	40.00	10.00	4.00	18.467
45		10.00	50.00	2.00	40.00	5.00	6.00	15.343

These analyses were performed according the array shown in Table 4 and by that order. Before estimating the value of the $DCRF_f$, the algorithm previously described in section 5.5 for removing the background signal was applied to each chromatogram.

The response values for all 45 experiments were introduced into the Design-Expert software and after a careful evaluation given by statistical tests, including ANOVA, and it was possible to assign an optimum value for each design variable. The ANOVA test proved that all statistical parameters are consistent, which means that the results are trustworthy. Thus, the chromatographic separation quality in 1D was found to be optimal (the maximal response obtained for the $DCRF_f$ was 20.214) when the gradient conditions consists of: 0-3 min 5% (v/v) MeOH and 40 mM phosphate buffer, 6-40 min 40% (v/v) MeOH and 10 mM phosphate buffer (Table 5), with a flow rate of 0.5 mL min^{-1} . ANOVA also allowed to know which variables are significant, i.e., those that should be optimized in the 2D . The D-Optimal design suggests that the initial and final concentrations of MeOH have a significant effect on the $DCRF_f$ values, which means that these experimental variables will be the object of optimization in the 2D (i.e., in LC \times LC).

Table 5: Optimum values of each experimental variable achieved by D-optimal design for 1D .

Experimental variables	Units	Values
$MeOH_i$	% (v/v)	5
$[Buffer]_i$	mM	40
t_i	min	3
$MeOH_f$	% (v/v)	40.01
$[Buffer]_f$	mM	10
t_f	min	6

The D-Optimal design also allowed obtaining a response surface, such as that shown in the Figure 13, which shows the effect of the experimental variables $MeOH_i$ and $[Buffer]_i$ on the values of the $DCRF_f$. The values of % (v/v) of $MeOH_f$ and $[Buffer]_f$ were held constant at 40.01 and 10, respectively. The remaining interactions between the other experimental variables are also possible to represent by means of a response surface. As it can be observed, the highest values for the $DCRF_f$ are verified when the values of $MeOH_i$ and $[Buffer]_i$ are close to 5% (v/v) and 40 mM, respectively.

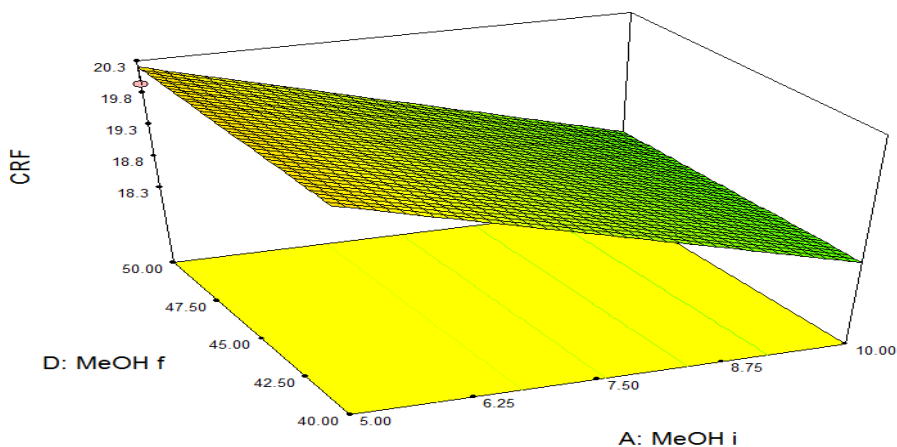


Figure 13: Response surface showing the effect of the experimental variables MeOH_i and $[\text{Buffer}]_i$ on the values of the DCRF_f given by the D-optimal design for ${}^1\text{D}$.

Figure 14 shows the 1D chromatogram obtained under the optimal conditions previously indicated by the D-Optimal design for the composite wine sample. With a pH of 3 of the mobile phase, the acidic compounds of the wine samples are less retained due to their lower affinity to the anion part of the Mixed-Mode WAX-1 and, consequently, the compounds elute earlier. The amount of organic solvent present in the mobile phase also influence the separation and, therefore, it is advisable to use low percentages of MeOH to avoid a strong interaction of the compounds with the column's stationary phase.

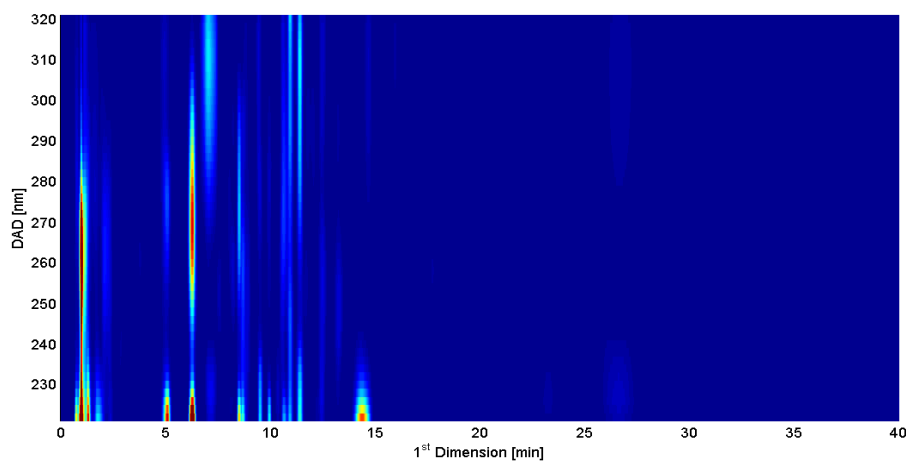


Figure 14: Optimum conditions chromatogram obtained by D-Optimal design.

As shown in Figure 14, the 1D chromatogram, which was recorded between $\lambda=221$ nm and $\lambda=320$ nm exhibits a high degree of peak overlapping. This effect is even more pronounced in the first 5 minutes of the chromatographic run, as shown in the inset of Figure 15. Nevertheless, a maximum of 50 peaks were identified in this 1D chromatogram, yielding a value of 20.214 for the DCRF_r.

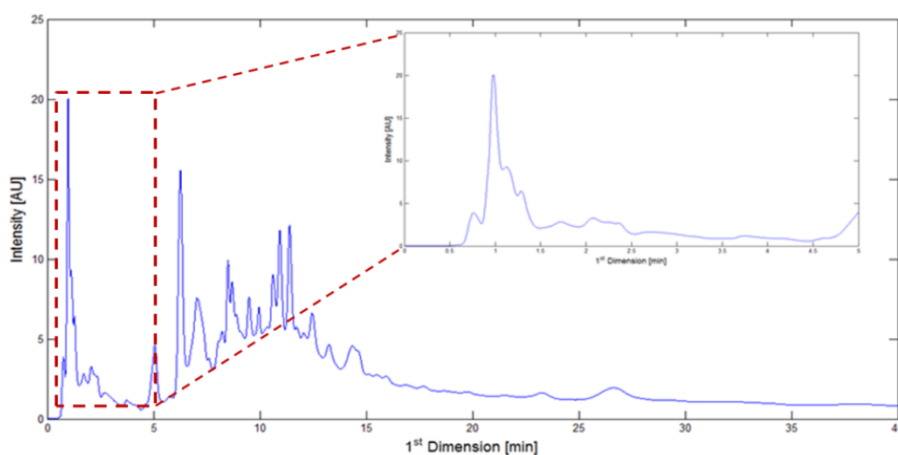


Figure 15: Chromatogram with overlapped peaks obtained by optimization in ¹D.

As shown in Figures 14 and 15, the total time of analysis found under the optimal conditions is about 15 minutes using a flow rate of 0.5 mL min^{-1} , which is a great disadvantage in terms of analysis time in LC \times LC, mostly because 15 minutes at 0.5 mL min^{-1} implies a total time of analysis of 150 minutes when performing LC \times LC at flow rate of 0.05 mL min^{-1} in the ¹D. As it can be seen in Figure 15, there is a small peak around minute 27, but the highest number of peaks appear in the first 15 minutes. Furthermore, the intensity of this peak is very low compared to the other peaks, which means that when performing LC \times LC this peak is likely to be diluted in the mobile phase of the ²D, thus becoming negligible. Therefore, it was decided to consider only the initial 15 minutes of the chromatographic run for the subsequent optimization of the ²D under the LC \times LC approach.

6.2. Conclusions and planning of following work

The D-Optimal design allowed obtaining the following conditions to attain the best analytical window for performing the 1D chromatography of wine samples: 0-3 min 5% (v/v) MeOH and 40 mM phosphate buffer, 6-40 min 40.01% (v/v) MeOH and 10 mM phosphate buffer, with a flow rate of 0.5 mL min⁻¹. Under the optimal conditions, the 1D chromatographic profile of the composite wine sample exhibit 50 peaks in a total time of analysis of 15 minutes. The major disadvantage found in this test was the time of analysis: a run of 15 minutes in the ¹D, implies about 100 times more in LC×LC, i.e., about 150 minutes. After a careful analysis of the results obtained by the D-Optimal design, the experimental variables that are needed to optimize the chromatographic separation in the ²D are the initial and final concentration of MeOH. Therefore, the next step of the optimization process is to proceed to the optimization of the ²D.

VII

**Search of optimum conditions of the
²D in LC×LC of wine samples**

7.1. Choice of operational conditions details and starting conditions

The following step on the optimization of the whole LC×LC of wine samples was the search of optimal chromatographic conditions in the ²D. A flow rate of 3 mL min⁻¹ was applied on the ²D, and in an attempt to improve the chromatographic resolution of the samples, higher volume loops (50 µL) were used in interfacing valve. The flow rate along the ¹D was also reduced, to 0.05 mL min⁻¹, in order to accommodate the use of such volume loops. The chromatograms were recorded using a RP-C18 column and a DAD at the end of the ²D, and all chromatograms were based on a total analysis time of 150 minutes and modulation time of 1 minute.

In first instance the, D-Optimal design was also applied at this stage for the LC×LC taking into consideration the parameters found as relevant in the optimization of 1D-LC, such as: the initial and the final % of MeOH. In this case, and because there are only two parameters to be optimized, the D-Optimal design produced 18 runs divided in 6 blocks, as shown in Table 6. The range of % of MeOH subject to the optimization varied between 5% and 50%. A phosphate buffer, in concentration of 10 mM, was also used as in the optimization of 1D-LC. Guiochon *et al.* (2008) referred in their work, that the compatibility of the two mobile phases is an important issue in LC×LC, so this part of the optimization has special relevance, since the results depend on the composition of the mobile phase. There are also other aspects such as viscous fingering due to the different viscosity of the mobile phases, and the low retention of the samples solvent, which must be taken into account.

As shown in Figure 16 there are two optimal values at two extreme values of MeOH: one at 5% of initial MeOH and 50% of final MeOH, and the other at 50% of initial MeOH and 5% of final MeOH. However the highest response value occurs at the first combination of MeOH concentration and those values were considered the best conditions for the optimization is the ²D operated as LC×LC. The DCRF formulation described in section 2.3 was used for evaluating the response of the ²D optimization, and for those conditions produced a value of 78.293. The same weights of 20% for the number of peaks and 80% for the total analysis time were applied as in the previous case.

Table 6: Experimental design generated by Design-Expert software version 7.0.0, for the ²D.

Number of the exp.	Block	% (v/v) MeOH _i	% (v/v) MeOH _f	DCRF
1	1	5.00	50.00	75.935
2		38.75	38.53	43.011
3		5.00	5.00	56.425
4	2	50.00	24.24	92.157
5		22.29	5.00	66.860
6		7.11	35.58	86.477
7	3	38.75	17.95	54.655
8		5.00	21.00	55.609
9		28.43	50.00	72.601
10	4	50.00	5.00	60.932
11		22.07	31.57	36.557
12		50.00	5.00	90.946
13	5	50.00	38.58	93.621
14		50.00	38.58	99.860
15		35.02	5.00	59.739
16	6	50.00	50.00	67.104
17		50.00	50.00	107.89
18		24.19	25.60	97.324

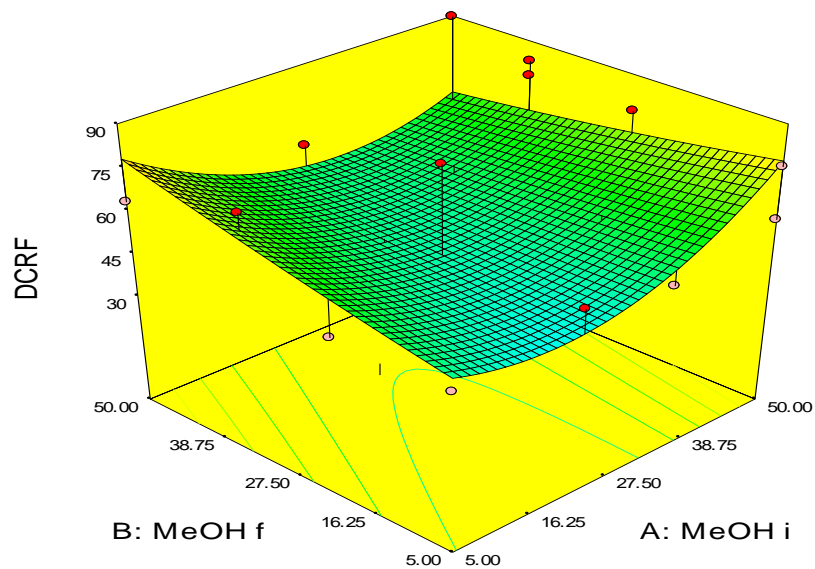
**Figure 16:** Response function expressed in terms of DCFR values for the initial and the final % of methanol given by D-Optimal design for the ²D.

Figure 17 shows the ANOVA of the various models fitted to the results obtained by following the D-Optimal design, and Figure 18 shows the ANOVA of the parameters of the quadratic model suggested in Figure 17 as the most appropriate for fitting the results. Both the model and the lack of fit are not significant and the predicted R² is negative value.

Model Summary Statistics						
Source	Std. Dev.	R-Squared	Adjusted R-Squared	Predicted R-Squared	PRESS	
Linear	16.77	0.0770	-0.1076	-2.1609	9630.29	
2FI	16.59	0.1867	-0.0844	-3.1160	12540.18	
<u>Quadratic</u>	<u>15.63</u>	<u>0.4388</u>	<u>0.0379</u>	<u>-4.3432</u>	<u>16279.30</u>	<u>Suggested</u>
Cubic	15.53	0.7626	0.0502		+	

+ Case(s) with leverage of 1.0000: PRESS statistic not defined

"Model Summary Statistics": Focus on the model maximizing the "Adjusted R-Squared" and the "Predicted R-Squared".

Figure 17: ANOVA of various models fitted to the results obtained following the D-Optimal design.

As commented in Figure 18 the “model F-value” of 1.09 means the model is not significant relative to the noise and the “lack of fit F-value” of 1.02 also means that the lack of fit is not significant to the pure experimental error.

The somewhat inconclusive ANOVA and the unusual behaviour of the response function showing the existence of two local best operating conditions at extreme values for the initial and the final % of MeOH (Figure 16) suggested there might be an expected chromatographic artifact which was not taken into account in the previous experiments. Figure 19 shows the chromatogram of the local optimum corresponding to the initial % of MeOH of 50% and the final % of MeOH of 5% and it becomes obvious that the CRF is high due to the extreme low value of the time of analysis although it produces a low value of number of peaks. However this optimum is obtained at conditions where the components of the wine sample are too diluted and they cannot be detected by the DAD due to the abrupt change in % of MeOH. Furthermore, the column appears to be adversely dewetting due to low percentages of MeOH.

Analysis of variance table [Partial sum of squares - Type III]						
Source	Sum of Squares	df	Mean Square	F Value	p-value Prob > F	
Block	1878.59	5	375.72			
Model	1336.87	5	267.37	1.09	0.4397	not significant
<i>A-MeOH i</i>	37.09	1	37.09	0.15	0.7084	
<i>B-MeOH f</i>	51.54	1	51.54	0.21	0.6599	
AB	418.33	1	418.33	1.71	0.2320	
A ²	746.79	1	746.79	3.06	0.1239	
B ²	3.52	1	3.52	0.014	0.9078	
Residual	1709.85	7	244.26			
Lack of Fit	986.42	4	246.60	1.02	0.5134	not significant
Pure Error	723.43	3	241.14			
Cor Total	4925.31	17				

The "Model F-value" of 1.09 implies the model is not significant relative to the noise. There is a 43.97 % chance that a "Model F-value" this large could occur due to noise.

Values of "Prob > F" less than 0.0500 indicate model terms are significant.

In this case there are no significant model terms.

Values greater than 0.1000 indicate the model terms are not significant.

If there are many insignificant model terms (not counting those required to support hierarchy), model reduction may improve your model.

The "Lack of Fit F-value" of 1.02 implies the Lack of Fit is not significant relative to the pure error. There is a 51.34% chance that a "Lack of Fit F-value" this large could occur due to noise. Non-significant lack of fit is good – we want the model to fit.

Figure 18: ANOVA of the quadratic model suggested as the most appropriate for fitting the results obtained by the D-Optimal design.

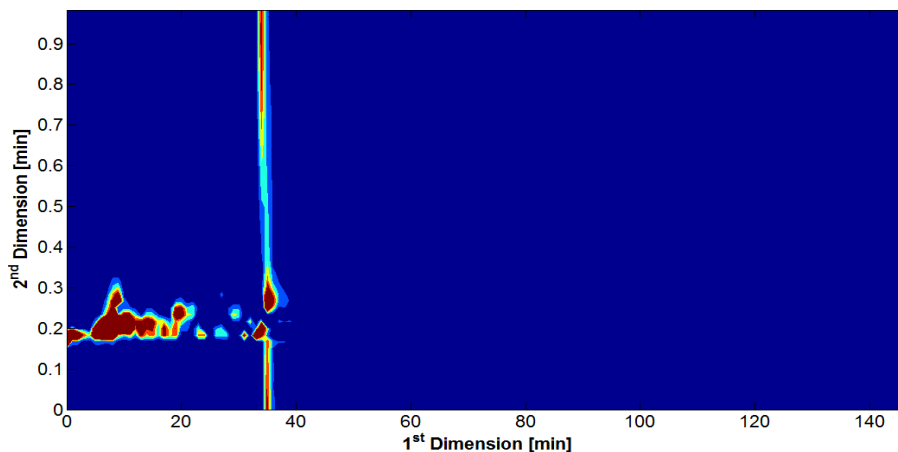


Figure 19: Chromatogram obtained by D-Optimal design for 50% of initial methanol and 5% of final methanol.

The gathering of all the above mentioned experimental evidence led to the suggestion of a more sequential type of experimental design, where the evolution of the chromatograms associated with the search of optimum could be followed continuously rather than after performing the whole set of experiments suggested by the D-Optimal design. Furthermore, the minimum concentration of MeOH had to be increased and controlled in order to avoid very low concentrations and consequently the dewetting of the silica C18. Consequently, Simplex seemed to be the right choice for optimization of the ²D when operating the LC×LC system.

7.2. Change from D-Optimal design to Simplex

7.2.1. Choice of operational details and starting conditions

The choice of the Simplex algorithm was based primarily on the fact that this sequential design allows envisaging the direction the method is taking in the search of the optimum after each experiment, contrary to the D-optimal design where data analysis is performed at the end of the randomized set of experiments. Furthermore, as shown in

Table 7, a new range of % of MeOH was set with minimum values higher than used in earlier experiments.

Table 7: Range of percentages of methanol for the Simplex algorithm.

Parameters	Units	Initial Values	Final Values
MeOH_i	% (v/v)	25	50
MeOH_f	% (v/v)	25	50

The chromatograms obtained by Simplex for the ²D are shown in Annex B containing Figures 74 to 87, and the separation of the components is well distributed in the whole chromatographic space with different operational conditions of initial and final % of MeOH. The results of the Simplex are shown in Figure 20 and the new optimal conditions are 18 % (v/v) (for initial MeOH and 39% (v/v) for final MeOH, which can be seen in pink colour (number 12). With these optimal conditions a chromatogram of the composite sample was obtained as shown in Figure 21. The LC×LC analysis produced a total of 59 peaks in 150 minutes corresponding to a maximum response of 33.68 for the DCRF. The weights applied for the estimation of the DCRF were the same as before, that is, 20% for the number of peaks and 80% for the total analysis time.

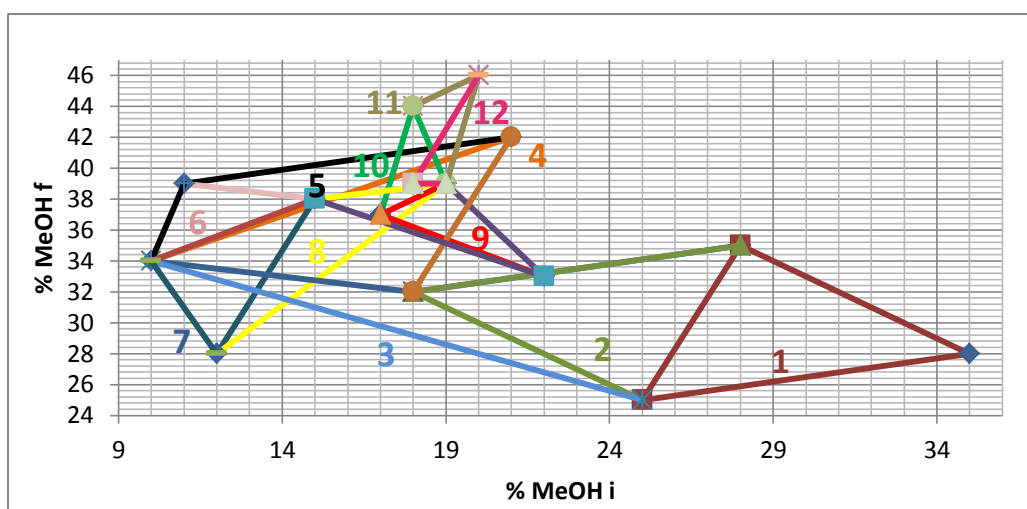


Figure 20: Simplex scheme to find optimal conditions for ²D.

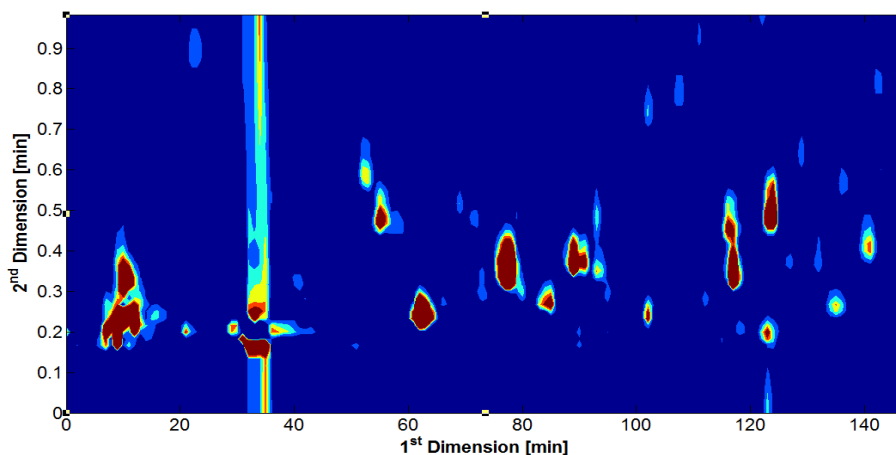


Figure 21: Two-dimensional liquid chromatography of the composite sample obtained at optimal conditions.

The LC \times LC chromatogram in Figure 21 shows the adequate separation of the composite sample in optimal conditions using as 2D a RP-C18 column, that is, with hydrophobic characteristics in the stationary phase, and employing a polar (aqueous) mobile phase. As a result of this chromatographic arrangement, the hydrophobic molecules in the polar mobile phase tend to adsorb to the hydrophobic stationary phase, and hydrophilic molecules in the mobile phase will pass through the column and are eluted first. Hydrophobic molecules can be eluted from the column by decreasing the polarity of the mobile phase using an organic (non-polar) solvent, which reduces hydrophobic interactions.

Chromatograms such as those obtained in this work and shown in Figure 21 contain 4-way data matrices which are not very amenable to available chemometric methods for providing valuable chemical information for the samples under study. In order to overcome this problem Matos *et al.* (2013) suggested an algorithm for calculating the number of peaks based on regional maximum of each peak, thus decreasing the dimensionality of data and making it more amenable to data treatment without loss of a great deal of information. The algorithm was applied to Figure 21 and the resulting peaks are displayed with the original in Figure 22. Finally, Figure 23 shows the 3D representation of the regional maxima allowing the original 4-way data matrix to be used by chemometric methods and to define preliminary patterns for fingerprinting.

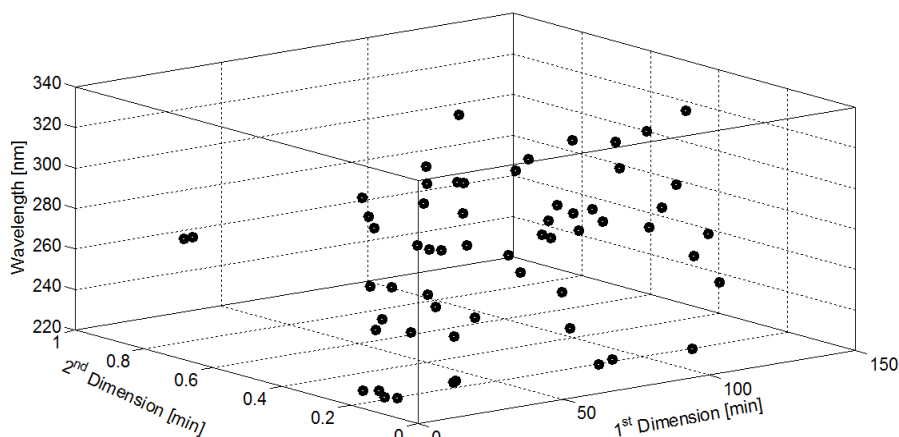


Figure 22: Representation of peaks for optimum condition of composite sample.

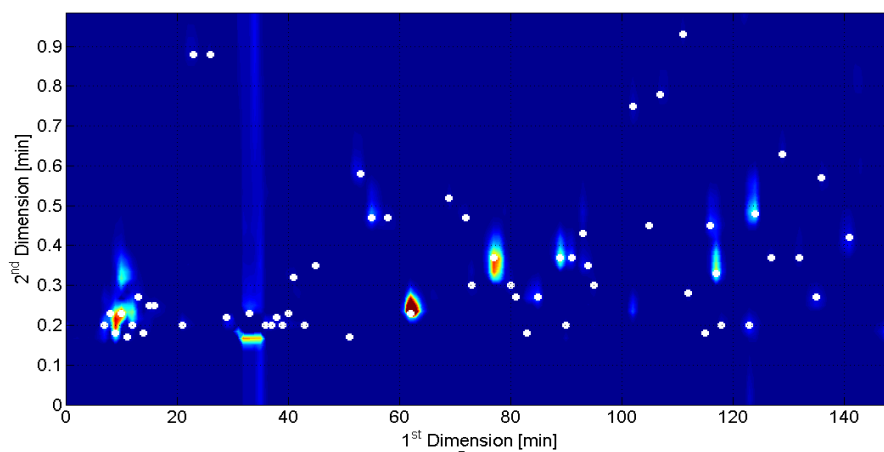


Figure 23: Representation of the peaks in 2D chromatogram.

7.2.2. LC×LC applied to the analysis of wine samples

Samples of the following Portuguese red wines were used for testing the optimal conditions of the LC×LC: EA – Vinho Regional Alentejano (2010), CICONIA - Vinho Regional Alentejano (2010), Príncipe do Dão (2009), and Torre de Estremoz – Vinho Regional Alentejano (2010). Some operational issues were detected due to variations of temperature, and a lack of reproducibility in the chromatograms was observed when the oven, where the columns were maintained, was turned off overnight. The period of

temperature stabilization produced peaks with several degrees of dragging as shown in Figure 24 (without any dragging) and Figure 25 (with dragging). Therefore, it becomes of paramount importance that the temperature remains stable throughout all the analytical work. Another problem that occurred, and also related to temperature, is the operation of the mixing chamber in medium mode causes overheating and the samples reach the column after passing through the mixing chamber at a higher temperature than that of the column. The solution was then to change the operating mode of the mixing chamber from medium to slow. Figures 26, 27, and 28 shows the obtained chromatograms for CICONIA - Vinho Regional Alentejano (2010), Príncipe do Dão (2009), and Torre de Estremoz – Vinho Regional Alentejano (2010) samples.

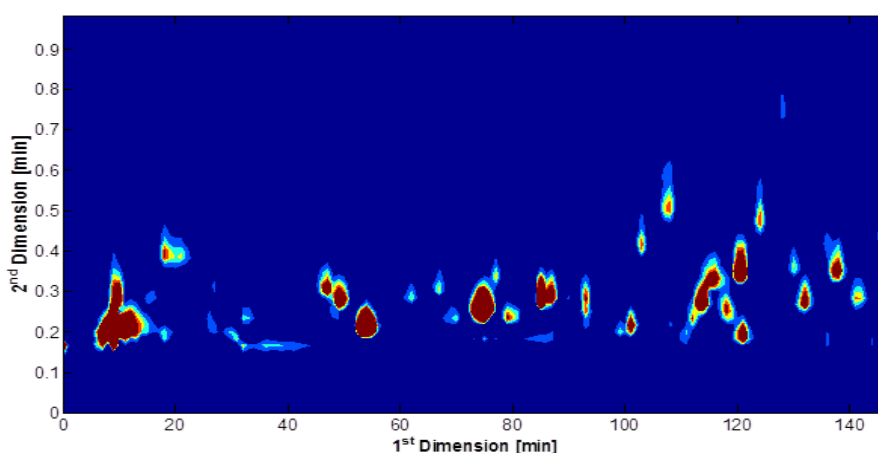


Figure 24: Chromatogram of red wine sample (EA – Vinho Regional Alentejano (2010)) without any problem of dragging.

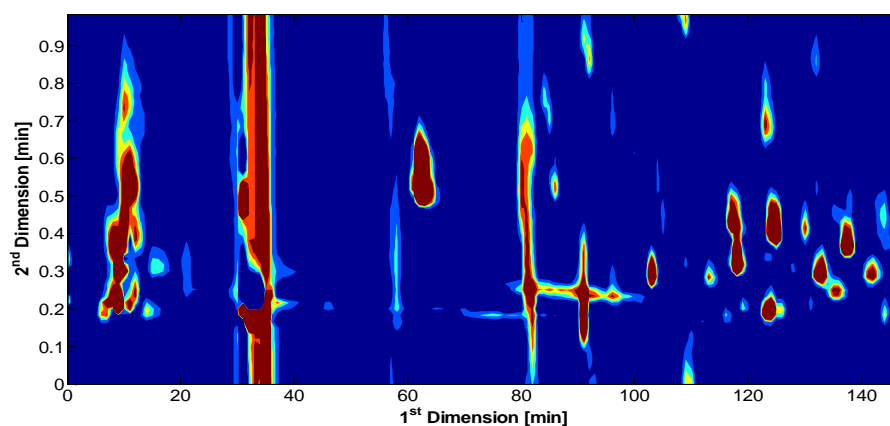


Figure 25: Chromatogram of red wine sample (EA – Vinho Regional Alentejano (2010)) with dragging.

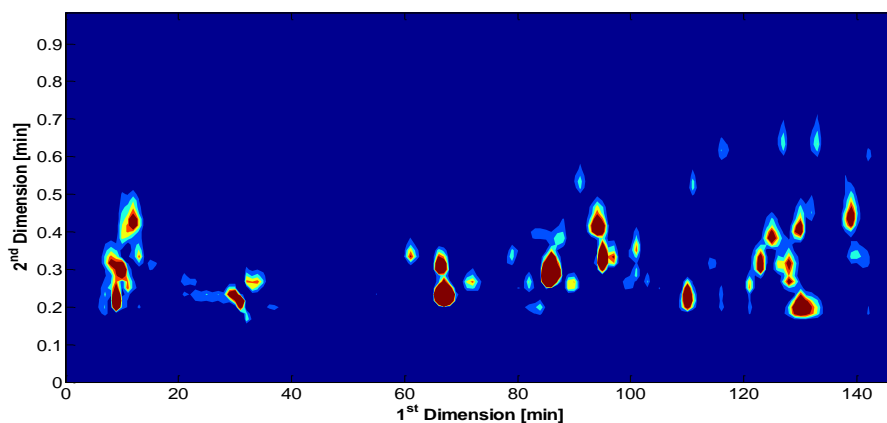


Figure 26: Chromatogram of red wine sample (CICONIA – Vinho Regional Alentejano (2010)).

In qualitative terms the chromatograms of the four individually red wine samples shows an adequate separation of the compounds which is only possible with the optimization process of the parameters through the DOE and Simplex algorithm. The localization of the peaks of every sample is different, which was expected because the samples are of different regions of Portugal.

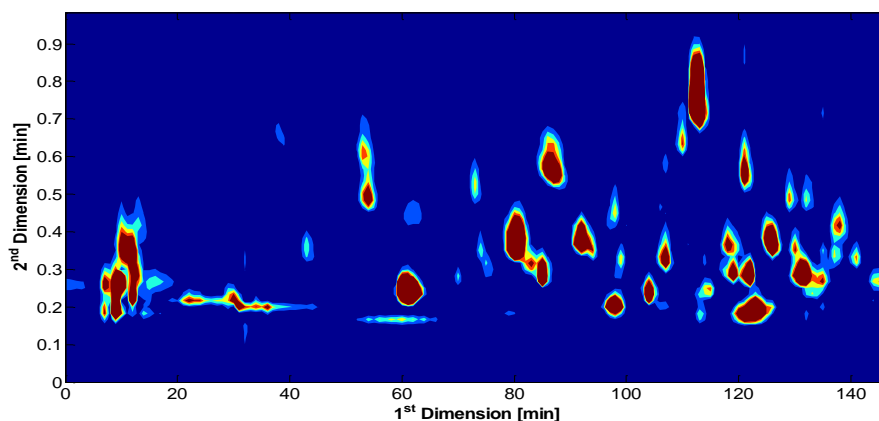


Figure 27: Chromatogram of red wine sample (Príncipe do Dão (2009)).

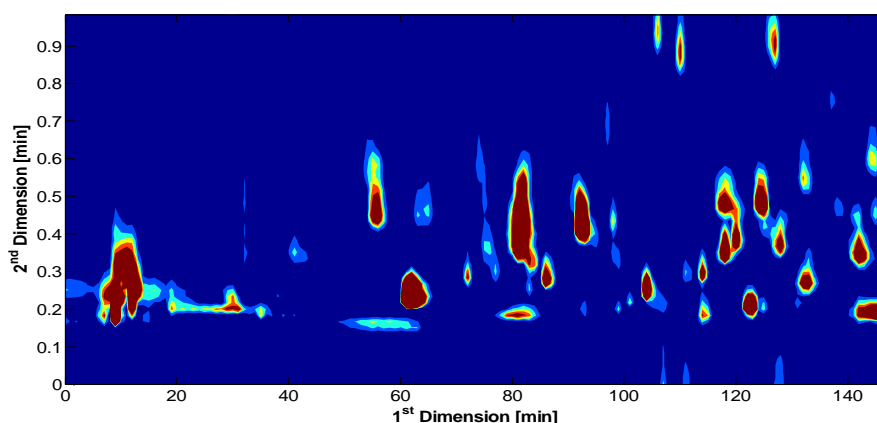


Figure 28: Chromatogram of red wine sample (Torre de Estremoz – Vinho Regional Alentejano (2010)).

In terms of number of peaks, the chromatogram shown in Figure 26, has the highest value (107), followed by Figure 27 with 86 number of peaks, and finally Figure 24 e 28 have the same number of peaks (74). Therefore the sample of CICONIA – Vinho Regional Alentejano (2010) produces the highest number of peaks, although the distribution of peaks does not occupy the entire space of 2D chromatographic space.

Relatively of to the values of DCRF, it was used the same percentage of weights than were always used to calculate de CFR, i.e., 20% for the number of peaks and 80% to the total time of analysis. The sample that shows the higher value of DCRF was CICONIA – Vinho Regional Alentejano (2010) (Figure 26), followed by Príncipe do Dão (2009) (Figure 27) with 48.70, the next one was EA – Vinho Regional Alentejano (2010) (Figure 24) with a value of DCRF of 41.95, and finally Torre de Estremoz – Vinho Regional Alentejano (2010) (Figure 28) has a DCRF of 41.92. The last two samples (Figure 24 e 28) present produced the same number of peaks and the value of the DCRF is very close, which was expected, since they are of the same region of Portugal. These results may indicate that there is a similarity between varieties of the same region.

7.3. Conclusions

For the optimization of 2D using the D-Optimal, it was possible to test several percentages (initial and final) of methanol but in this first attempt, the optimization did not work, due to very low % (v/v) of MeOH, which caused dewetting of the stationary phase. Also the ANOVA showed that the model and the lack of fit are not significant, which means that there are no significant optimization parameters. The Simplex algorithm was then used for smaller range of % (v/v) of MeOH and the optimal conditions obtained through this new sequential design were: 18% (v/v) for initial MeOH, and 39% (v/v) for final MeOH. The composite sample was tested with the optimal conditions producing a total of 59 peaks in 150 minutes and a DCRF of 33.68. Four individual red wine samples were analyzed and CICONIA - Vinho Regional Alentejano (2010) produced the best response (60.74) with the largest number of peaks (107). Although the chromatographic separation of the peaks was found adequate, overall the 2D chromatographic space cannot be considered totally fulfilled. At this stage of the work, some operational problems have to be overcome in order to produce acceptable chromatograms without dragging and peaks turnover.

VIII

Final conclusions and further work

LC×LC has emerged as a powerful technique for the separation of complex organic mixtures. This separation technique when associated with multichannel detectors in series can be the basis for obtaining n-way data matrices providing valuable insights into the characterization of some challenging analytical problems, such as the characterization of foodstuffs, beverages, and natural organic matter. Apart from the difficulties of extracting information from such large data files due to the use of software that is only a loose part of the analytical information there is an additional limitation due to the lack of strategies for optimization of the conditions for proper operation of LC×LC systems.

The concepts of 2D chromatography were developed mainly from the concepts of 1D chromatography, where there are much more software packages to deal with the separation problems. There have been some recent developments in order to overcome this lack of appropriate software for 2D chromatography, and new algorithms and proposals have been put forward to improve the handling from n-way data provided by LC×LC. However, on the optimization side there has been no attempt to formulate any strategy on how to deal with the two chromatographic dimensions in order to help establishing the optimal conditions of operation based on the principles of experimental design.

This work was the first known attempt to apply optimization methods to the first and second dimensions of a LC×LC system in the analysis of red wine samples. A two-part optimization strategy was followed in this work: firstly, a D-Optimal design was applied in the 1D optimization, and secondly a Simplex was used for the 2D, for overcoming some issues with the D-Optimal design. A composite sample was made of various samples of wines and used for test of both optimizations. This composite sample allowed obtaining a general overview of the distribution of all peaks of each individual red wine sample.

The following parameters were subjected in the 1D optimization: initial and final % of MeOH, initial and final concentration of Buffer, the initial and final time of gradient elution. The optimal conditions were found after 45 runs, distributed by 8 blocks, and randomly generated by the D-Optimal design: 5% (v/v) for initial MeOH, 40 mM for initial concentration of phosphate buffer, 3 minutes for initial time of gradient elution, 40.01% (v/v) for final MeOH, 10% (v/v) for final concentration of buffer, and 6 minutes for final time of gradient mode. These optimal conditions were tested with the composite sample and the following results were obtained: 50 peaks in the first 15 minutes, and a CRF value of 20.214.

The following step was the optimization of the ²D, where only two-parameters were found relevant: the initial and the final % (v/v) of MeOH. The D-Optimal design was also the first choice for the ²D optimization. The ranges of initial and final % (v/v) of MeOH were chosen based on the previous 1D optimization, but soon it was observed that the low % (v/v) of MeOH in the RP column promotes dewatering, which means that probably the samples are too diluted and no analytical signal was observed. Besides, the ANOVA test highlighted the lack of fit and the non-significance of the model, which means the parameters are not significant. A decision was taken to change the range of initial % (v/v) of MeOH as well as the design. The new design adopted, the Simplex algorithm, allowed to obtain the response immediately after each experiment, and it normally requires a lower number of runs when compared to other designs. Thus, the optimal conditions for the composite sample were 18% (v/v) for initial MeOH and 30% (v/v) of final MeOH. With these values the following 4 commercial red wine samples were analyzed: EA – Vinho Regional Alentejano (2010), CICONIA – Vinho Regional Alentejano, Príncipe do Dão (2009), and Torre de Estremoz – Vinho Regional Alentejano (2010). The sample that showed the highest number of peaks (107) was CICONIA – Vinho Regional Alentejano, and the highest value (60.74) of DCR also belonged to this same sample. The 4 chromatograms corresponding to the wines above mentioned showed a good separation of the peaks which may be only possible due to the optimal conditions achieved by the experimental used designs for optimization of the particular LC×LC system. Thus, the results show that it becomes possible to separate by LC×LC several sample components which were not shown as individual components in 1D-LC due to their similar hydrophobicity. The resolving power due to the different mechanisms of separation in the two columns (Mixed-Mode WAX-1×RP-C18) was greatly enhanced by the application of LC×LC.

In the near future, the trend will be to develop an even faster separation, because a lower time of analysis also implies lower running costs associated with the price of the mobile phases. A procedure that may bring another advantage for this LC×LC system is the replacement of the column in the ¹D for a core-shell, because this type of stationary phases produces much a faster separation at reasonable pressures. This work may also represent a basis for developing strategies for characterization of samples due to the possibility of using the chromatographic patterns for fingerprinting each wine sample.

References

-
- ABRAR, S. & TRATHNIGG, B. 2010. Separation of nonionic surfactants according to functionality by hydrophilic interaction chromatography and comprehensive two-dimensional liquid chromatography. *Journal of Chromatography A*, **1217**, 8222-8229.
- ALLEN, R. C. & RUTAN, S. C. 2012. Semi-automated alignment and quantification of peaks using parallel factor analysis for comprehensive two-dimensional liquid chromatography–diode array detector data sets. *Analytica Chimica Acta*, **723**, 7-17.
- ALLEN, R. C. & RUTAN, S. C. 2011. Investigation of interpolation techniques for the reconstruction of the first dimension of comprehensive two-dimensional liquid chromatography–diode array detector data. *Analytica Chimica Acta*, **705**, 253-260.
- AMIGO, J. M., SKOV, T. & BRO, R. 2010. ChroMATHography: Solving Chromatographic Issues with Mathematical Models and Intuitive Graphics. *Chemical Reviews*, **110**, 4582-4605.
- ARANCIBIA, J. A., DAMIANI, P. C., ESCANDAR, G. M., IBAÑEZ, G. A. & OLIVIERI, A. C. 2012. A review on second- and third-order multivariate calibration applied to chromatographic data. *Journal of Chromatography B*, **910**, 22-30.
- BAILEY, H. P. & RUTAN, S. C. 2013. Comparison of chemometric methods for the screening of comprehensive two-dimensional liquid chromatographic analysis of wine. *Analytica Chimica Acta*, **770**, 18-28.
- BAILEY, H. P. & RUTAN, S. C. 2011. Chemometric resolution and quantification of four-way data arising from comprehensive 2D-LC-DAD analysis of human urine. *Chemometrics and Intelligent Laboratory Systems*, **106**, 131-141.
- BRO, R. 1997. PARAFAC. Tutorial and applications. *Chemometrics and Intelligent Laboratory Systems*, **38**, 149-171.
- BUSHEY, M. M. & JORGENSON, J. W. 1990. Automated instrumentation for comprehensive two-dimensional high-performance liquid chromatography/capillary zone electrophoresis. *Analytical Chemistry*, **62**, 978-984.
- BRUCKNER, C. A., PRAZEN, B. J. & SYNOVEC, R. E. 1998. Comprehensive Two-Dimensional High-Speed Gas Chromatography with Chemometric Analysis. *Analytical Chemistry*, **70**, 2796-2804.
- CAI, X., GUO, Z., XUE, X., XU, J., ZHANG, X. & LIANG, X. 2012. Two-dimensional liquid chromatography separation of peptides using reversed-phase/weak cation-exchange mixed-mode column in first dimension. *Journal of Chromatography A*, **1228**, 242-249.
- CHEN, M.-X., CAO, Z.-Y., JIANG, Y. & ZHU, Z.-W. 2013. Direct determination of glyphosate and its major metabolite, aminomethylphosphonic acid, in fruits and vegetables by mixed-mode hydrophilic interaction/weak anion-exchange liquid chromatography coupled with electrospray tandem mass spectrometry. *Journal of Chromatography A*, **1272**, 90-99.
- D.L. MASSART, B. G. M. V., L.M.C. BUYDENS, S. DE JONG, P.J. LEWI AND J. SMEYERS-VERBEKE 1997. *Handbook of Chemometrics and Qualimetrics: Part A*, Elsevier.
- DAS, D., MUKHERJEE, S. & RAY, D. 2011. Erratum to: Resveratrol and red wine, healthy heart and longevity. *Heart Failure Reviews*, **16**, 425-435.
- DE AGUIAR, P. F., BOURGUIGNON, B. & MASSART, D. L. 1997. Comparison of models and designs for optimisation of the pH and solvent strength in HPLC. *Analytica Chimica Acta*, **356**, 7-17.
-

-
- DEMING, S. N., M. PALASOTA, J., LEE, J. & SUN, L. 1989. Computer-assisted optimization in high-performance liquid chromatographic method development. *Journal of Chromatography A*, **485**, 15-25.
- DONATO, P., CACCIOLA, F., SOMMELLA, E., FANALI, C., DUGO, L., DACHÀ, M., CAMPIGLIA, P., NOVELLINO, E., DUGO, P. & MONDELLO, L. 2011. Online Comprehensive RPLC × RPLC with Mass Spectrometry Detection for the Analysis of Proteome Samples. *Analytical Chemistry*, **83**, 2485-2491.
- DUARTE, R. M. B. O., MATOS, J. T. V. & DUARTE, A. C. 2012. A new chromatographic response function for assessing the separation quality in comprehensive two-dimensional liquid chromatography. *Journal of Chromatography A*, **1225**, 121-131.
- DUARTE, R. M. B. O., BARROS, A. C. & DUARTE, A. C. 2012. Resolving the chemical heterogeneity of natural organic matter: New insights from comprehensive two-dimensional liquid chromatography. *Journal of Chromatography A*, **1249**, 138-146.
- DUARTE, R. M. B. O. & DUARTE, A. C. 2011. Optimizing size-exclusion chromatographic conditions using a composite objective function and chemometric tools: Application to natural organic matter profiling. *Analytica Chimica Acta*, **688**, 90-98.
- DUARTE, R. M. B. O. & DUARTE, A. C. 2010. A new chromatographic response function for use in size-exclusion chromatography optimization strategies: Application to complex organic mixtures. *Journal of Chromatography A*, **1217**, 7556-7563.
- DUFRECHOU, M., PONCET-LEGRAND, C., SAUVAGE, F.-X. & VERNHET, A. 2011. Stability of White Wine Proteins: Combined Effect of pH, Ionic Strength, and Temperature on Their Aggregation. *Journal of Agricultural and Food Chemistry*, **60**, 1308-1319.
- DUGO, P., CACCIOLA, F., DONATO, P., AIRADO-RODRÍGUEZ, D., HERRERO, M. & MONDELLO, L. 2009. Comprehensive two-dimensional liquid chromatography to quantify polyphenols in red wines. *Journal of Chromatography A*, **1216**, 7483-7487.
- ERNI, F. & FREI, R. W. 1978. Two-dimensional column liquid chromatographic technique for resolution of complex mixtures. *Journal of Chromatography A*, **149**, 561-569.
- FAIRCHILD, J. N., HORVÁTH, K. & GUIOCHON, G. 2009. Approaches to comprehensive multidimensional liquid chromatography systems. *Journal of Chromatography A*, **1216**, 1363-1371.
- FERRÉ, J. & COMAS, E. 2011. Outlier detection for the Generalized Rank Annihilation Method in HPLC-DAD analysis. *Talanta*, **83**, 1147-1157.
- FRAGA, C. G. & CORLEY, C. A. 2005. The chemometric resolution and quantification of overlapped peaks from comprehensive two-dimensional liquid chromatography. *Journal of Chromatography A*, **1096**, 40-49.
- FRAGA, C. G., PRAZEN, B. J. & SYNOVEC, R. E. 2001. Objective Data Alignment and Chemometric Analysis of Comprehensive Two-Dimensional Separations with Run-to-Run Peak Shifting on Both Dimensions. *Analytical Chemistry*, **73**, 5833-5840.
- FRANÇOIS, I., SANDRA, K. & SANDRA, P. 2009. Comprehensive liquid chromatography: Fundamental aspects and practical considerations—A review. *Analytica Chimica Acta*, **641**, 14-31.
- FRANÇOIS, I., DE VILLIERS, A., TIENPONT, B., DAVID, F. & SANDRA, P. 2008. Comprehensive two-dimensional liquid chromatography applying two parallel columns in the second dimension. *Journal of Chromatography A*, **1178**, 33-42.
-

-
- GAZOVA, Z., SIPOSOVA, K., KURIN, E., MUČAJI, P. & NAGY, M. 2013. Amyloid aggregation of lysozyme: The synergy study of red wine polyphenols. *Proteins: Structure, Function, and Bioinformatics*, **81**, 994-1004.
- GRAY, M. J., DENNIS, G. R., SLONECKER, P. J. & SHALLIKER, R. A. 2004. Separation of oligostyrene isomers in a complex mixture using two-dimensional heart-cutting reversed-phased liquid chromatography. *Journal of Chromatography A*, **1028**, 247-257.
- GREIDERER, A., STEENEKEN, L., AALBERS, T., VIVÓ-TRUYOLS, G. & SCHOENMAKERS, P. 2011. Characterization of hydroxypropylmethylcellulose (HPMC) using comprehensive two-dimensional liquid chromatography. *Journal of Chromatography A*, **1218**, 5787-5793.
- GUIOCHON, G., MARCHETTI, N., MRIZIQ, K. & SHALLIKER, R. A. 2008. Implementations of two-dimensional liquid chromatography. *Journal of Chromatography A*, **1189**, 109-168.
- HANTAO, L. W., ALEME, H. G., PEDROSO, M. P., SABIN, G. P., POPPI, R. J. & AUGUSTO, F. 2012. Multivariate curve resolution combined with gas chromatography to enhance analytical separation in complex samples: A review. *Analytica Chimica Acta*, **731**, 11-23.
- HALQUIST, M. S., SAKAGAMI, M. & KARNES, H. T. 2012. Determination of oxyntomodulin, an anorectic polypeptide, in rat plasma using 2D-LC-MS/MS coupled with ion pair chromatography. *Journal of Chromatography B*, **903**, 102-111.
- HOGGARD, J. C. & SYNOVEC, R. E. 2007. Parallel Factor Analysis (PARAFAC) of Target Analytes in GC × GC-TOFMS Data: Automated Selection of a Model with an Appropriate Number of Factors. *Analytical Chemistry*, **79**, 1611-1619.
- HOLLINGSWORTH, B. V., REICHENBACH, S. E., TAO, Q. & VISVANATHAN, A. 2006. Comparative visualization for comprehensive two-dimensional gas chromatography. *Journal of Chromatography A*, **1105**, 51-58.
- JALALI-HERAVI, M., MOAZENI, R. S. & SERESHTI, H. 2011. Analysis of Iranian rosemary essential oil: Application of gas chromatography-mass spectrometry combined with chemometrics. *Journal of Chromatography A*, **1218**, 2569-2576.
- JAWORSKA, K., KRYNITSKY, A. J. & RADER, J. I. 2012. Simultaneous Analysis of Steviol and Steviol Glycosides by Liquid Chromatography with Ultraviolet Detection on a Mixed-Mode Column: Application to Stevia Plant Material and Stevia-Containing Dietary Supplements. *Journal of AOAC International*, **95**, 1588-1596.
- JEONG, E.-K., CHA, H.-J., HA, Y. W., KIM, Y. S., HA, I. J. & NA, Y.-C. 2010. Development and optimization of a method for the separation of platycosides in *Platycodi Radix* by comprehensive two-dimensional liquid chromatography with mass spectrometric detection. *Journal of Chromatography A*, **1217**, 4375-4382.
- JOHNSON, K. J., PRAZEN, B. J., YOUNG, D. C. & SYNOVEC, R. E. 2004. Quantification of naphthalenes in jet fuel with GC×GC/Tri-PLS and windowed rank minimization retention time alignment. *Journal of Separation Science*, **27**, 410-416.
- KAJDAN, T., CORTES, H., KUPPANNAN, K. & YOUNG, S. A. 2008. Development of a comprehensive multidimensional liquid chromatography system with tandem mass spectrometry detection for detailed characterization of recombinant proteins. *Journal of Chromatography A*, **1189**, 183-195.
- KIVILOMPOLO, M., OBŮRKA, V. & HYÖTYLÄINEN, T. 2008. Comprehensive two-dimensional liquid chromatography in the analysis of antioxidant phenolic compounds in wines and juices. *Analytical and Bioanalytical Chemistry*, **391**, 373-380. Copolymers. *Journal of Chromatography A*, **1218**, 7173-7179.
-

-
- KRAFT, T. E., PARISOTTO, D., SCHEMP, C. & EFFERTH, T. 2009. Fighting Cancer with Red Wine? Molecular Mechanisms of Resveratrol. *Critical Reviews in Food Science and Nutrition*, **49**, 782-799.
- LARSON, E., GROSKREUTZ, S., HARMES, D., GIBBS-HALL, I., TRUDO, S., ALLEN, R., RUTAN, S. & STOLL, D. 2013. Development of selective comprehensive two-dimensional liquid chromatography with parallel first-dimension sampling and second-dimension separation—application to the quantitative analysis of furanocoumarins in apiaceous vegetables. *Analytical and Bioanalytical Chemistry*, **405**, 4639-4653.
- LEARDI, R. 2009. Experimental design in chemistry: A tutorial. *Analytica Chimica Acta*, **652**, 161-172.
- LEE, D., MILLER, M. D., MEUNIER, D. M., LYONS, J. W., BONNER, J. M., PELL, R. J., SHAN, C. L. P. & HUANG, T. 2011. Development of high temperature comprehensive two-dimensional liquid chromatography hyphenated with infrared and light scattering detectors for characterization of chemical composition and molecular weight heterogeneities in polyolefin copolymers. *Journal of Chromatography A*, **1218**, 7173-7179.
- LÓPEZ-GRÍO, S. J., VIVÓ-TRUYOLS, G., TORRES-LAPASÍO, J. R. & GARCÍA-ALVAREZ-COQUE, M. C. 2001. Resolution assessment and performance of several organic modifiers in hybrid micellar liquid chromatography. *Analytica Chimica Acta*, **433**, 187-198.
- MALIK, M. I., HARDING, G. W., GRABOWSKY, M. E. & PASCH, H. 2012. Two-dimensional liquid chromatography of polystyrene–polyethylene oxide block copolymers. *Journal of Chromatography A*, **1244**, 77-87.
- MARRIOTT, P. J., SCHOENMAKERS, P. & ZE-YING, W. 2012. Nomenclature and Conventions in Comprehensive Multidimensional Chromatography — An Update. *LC-GC Europe*, **25**, 266-275.
- MATOS, J. T. V., DUARTE, R. M. B. O. & DUARTE, A. C. 2013. A simple approach to reduce dimensionality from comprehensive two-dimensional liquid chromatography coupled with a multichannel detector. *Analytica Chimica Acta*, **804**, 296-303.
- MATOS, J. T. V., DUARTE, R. M. B. O. & DUARTE, A. C. 2012. Trends in data processing of comprehensive two-dimensional chromatography: State of the art. *Journal of Chromatography B*, **910**, 31-45.
- MATOS, J. T. V., DUARTE, R. M. B. O. & DUARTE, A. C. 2012. A generalization of a chromatographic response function for application in non-target one- and two-dimensional chromatography of complex samples. *Journal of Chromatography A*, **1263**, 141-150.
- MONTERO, L., HERRERO, M., IBÁÑEZ, E. & CIFUENTES, A. 2013. Profiling of phenolic compounds from different apple varieties using comprehensive two-dimensional liquid chromatography. *Journal of Chromatography A*, **1313**, 275-283.
- MURPHY, R. E., SCHURE, M. R. & FOLEY, J. P. 1998. Effect of Sampling Rate on Resolution in Comprehensive Two-Dimensional Liquid Chromatography. *Analytical Chemistry*, **70**, 1585-1594.
- NAPOLI, R., COZZOLINO, D., GUARDASOLE, V., ANGELINI, V., ZARRA, E., MATARAZZO, M., CITTADINI, A., SACCÀ, L. & TORELLA, R. 2005. Red wine consumption improves insulin resistance but not endothelial function in type 2 diabetic patients. *Metabolism*, **54**, 306-313.
- ORDÓÑEZ, E. Y., QUINTANA, J. B., RODIL, R. & CELA, R. 2012. Determination of artificial sweeteners in water samples by solid-phase extraction and liquid chromatography–tandem mass spectrometry. *Journal of Chromatography A*, **1256**, 197-205.
-

-
- PARASTAR, H. & TAULER, R. 2013. Multivariate Curve Resolution of Hyphenated and Multidimensional Chromatographic Measurements: A New Insight to Address Current Chromatographic Challenges. *Analytical Chemistry*. (doi: 10.1021/ac402377d)
- PHILLIPS, J. B. & BEENS, J. 1999. Comprehensive two-dimensional gas chromatography: a hyphenated method with strong coupling between the two dimensions. *Journal of Chromatography A*, **856**, 331-347.
- PIERCE, K. M., KEHIMKAR, B., MARNEY, L. C., HOGGARD, J. C. & SYNOVEC, R. E. 2012. Review of chemometric analysis techniques for comprehensive two dimensional separations data. *Journal of Chromatography A*, **1255**, 3-11.
- PIERCE, K. M., WOOD, L. F., WRIGHT, B. W. & SYNOVEC, R. E. 2005. A Comprehensive Two-Dimensional Retention Time Alignment Algorithm To Enhance Chemometric Analysis of Comprehensive Two-Dimensional Separation Data. *Analytical Chemistry*, **77**, 7735-7743.
- PRAZEN, B. J., BRUCKNER, C. A., SYNOVEC, R. E. & KOWALSKI, B. R. 1999. Second-order chemometric standardization for high-speed hyphenated gas chromatography: Analysis of GC/MS and comprehensive GC×GC data. *Journal of Microcolumn Separations*, **11**, 97-107.
- PORTER, S. E. G., STOLL, D. R., RUTAN, S. C., CARR, P. W. & COHEN, J. D. 2006. Analysis of Four-Way Two-Dimensional Liquid Chromatography-Diode Array Data: Application to Metabolomics. *Analytical Chemistry*, **78**, 5559-5569.
- REICHENBACH, S. E., NI, M., KOTTAPALLI, V. & VISVANATHAN, A. 2004. Information technologies for comprehensive two-dimensional gas chromatography. *Chemometrics and Intelligent Laboratory Systems*, **71**, 107-120.
- REICHENBACH, S. E., NI, M., ZHANG, D. & LEDFORD JR, E. B. 2003. Image background removal in comprehensive two-dimensional gas chromatography. *Journal of Chromatography A*, **985**, 47-56.
- SCHOENMAKERS, P. J. & MULHOLLAND, M. 1988. An overview of contemporary method development in liquid chromatography. *Chromatographia*, **25**, 737-748.
- SCOPARO, C. T., DE SOUZA, L. M., DARTORA, N., SASSAKI, G. L., GORIN, P. A. J. & IACOMINI, M. 2012. Analysis of Camellia sinensis green and black teas via ultra high performance liquid chromatography assisted by liquid-liquid partition and two-dimensional liquid chromatography (size exclusion×reversed phase). *Journal of Chromatography A*, **1222**, 29-37.
- SINHA, P., HARDING, G. W., MAIKO, K., HILLER, W. & PASCH, H. 2012. Comprehensive two-dimensional liquid chromatography for the separation of protonated and deuterated polystyrene. *Journal of Chromatography A*, **1265**, 95-104.
- SINHA, A. E., FRAGA, C. G., PRAZEN, B. J. & SYNOVEC, R. E. 2004. Trilinear chemometric analysis of two-dimensional comprehensive gas chromatography–time-of-flight mass spectrometry data. *Journal of Chromatography A*, **1027**, 269-277. STOLL, D. R., LI, X., WANG, X., CARR, P. W., PORTER, S. E. G. & RUTAN, S. C. 2007. Fast, comprehensive two-dimensional liquid chromatography. *Journal of Chromatography A*, **1168**, 3-43.
- STROINK, T., ORTIZ, M. C., BULT, A., LINGEMAN, H., DE JONG, G. J. & UNDERBERG, W. J. M. 2005. On-line multidimensional liquid chromatography and capillary electrophoresis systems for peptides and proteins. *Journal of Chromatography B*, **817**, 49-66.
- STOLL, D. R., LI, X., WANG, X., CARR, P. W., PORTER, S. E. G. & RUTAN, S. C. 2007. Fast, comprehensive two-dimensional liquid chromatography. *Journal of Chromatography A*, **1168**, 3-43.
-

- TRANCHIDA, P. Q., DUGO, P., DUGO, G. & MONDELLO, L. 2004. Comprehensive two-dimensional chromatography in food analysis. *Journal of Chromatography A*, **1054**, 3-16.
- VAN MISPELAAR, V. G., TAS, A. C., SMILDE, A. K., SCHOENMAKERS, P. J. & VAN ASTEN, A. C. 2003. Quantitative analysis of target components by comprehensive two-dimensional gas chromatography. *Journal of Chromatography A*, **1019**, 15-29.
- VERMA, A. K. & PRATAP, R. 2010. The biological potential of flavones. *Natural Product Reports*, **27**, 1571-1593.
- YU, Y.-J., WU, H.-L., NIU, J.-F., ZHAO, J., LI, Y.-N., KANG, C. & YU, R.-Q. 2013. A novel chromatographic peak alignment method coupled with trilinear decomposition for three dimensional chromatographic data analysis to obtain the second-order advantage. *Analyst*, **138**, 627-634.
- ZENG, Z.-D., CHIN, S.-T., HUGEL, H. M. & MARRIOTT, P. J. 2011. Simultaneous deconvolution and reconstruction of primary and secondary overlapping peak clusters in comprehensive two-dimensional gas chromatography. *Journal of Chromatography A*, **1218**, 2301-2310.
- ZHANG, Y., WU, H.-L., XIA, A. L., HU, L.-H., ZOU, H.-F. & YU, R.-Q. 2007. Trilinear decomposition method applied to removal of three-dimensional background drift in comprehensive two-dimensional separation data. *Journal of Chromatography A*, **1167**, 178-183.
- ZHANG, D., HUANG, X., REGNIER, F. E. & ZHANG, M. 2008. Two-Dimensional Correlation Optimized Warping Algorithm for Aligning GC×GC-MS Data. *Analytical Chemistry*, **80**, 2664-2671.

Annex A: Optimization of 1D-LC

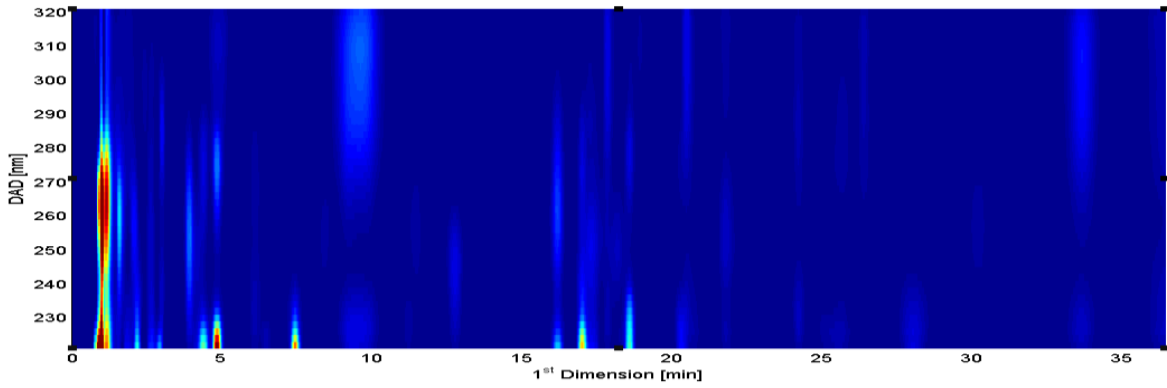


Figure 29: Chromatogram obtained by optimization in the ¹D (10% of MeOH_f; 40mM [PPB]_f; 2.61 t_f; 42.83% of MeOH_f; 5mM [PPB]_f; 4.93 t_f).

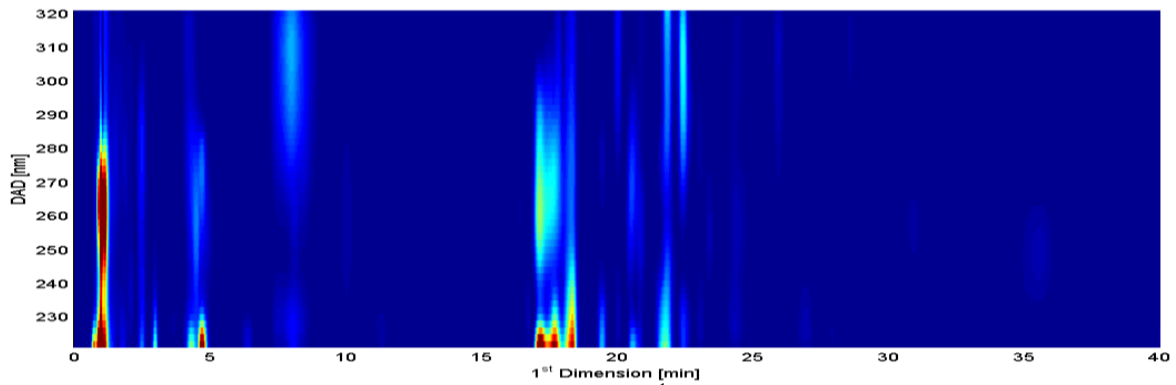


Figure 30: Chromatogram obtained by optimization in the ¹D (10% of MeOH_f; 50mM [PPB]_f; 3 t_f; 40.00% of MeOH_f; 10mM [PPB]_f; 6 t_f).

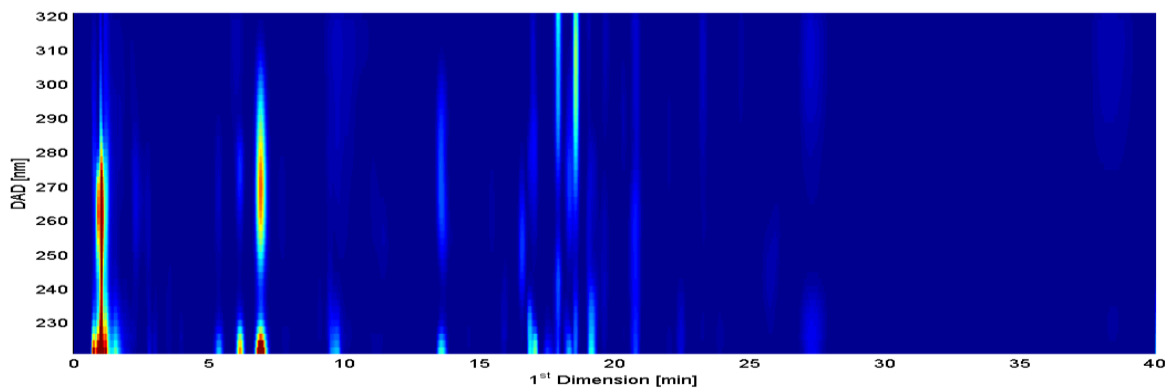


Figure 31: Chromatogram obtained by optimization in the ¹D (5% of MeOH_f; 40mM [PPB]_f; 3 t_f; 50.00% of MeOH_f; 5mM [PPB]_f; 4 t_f).

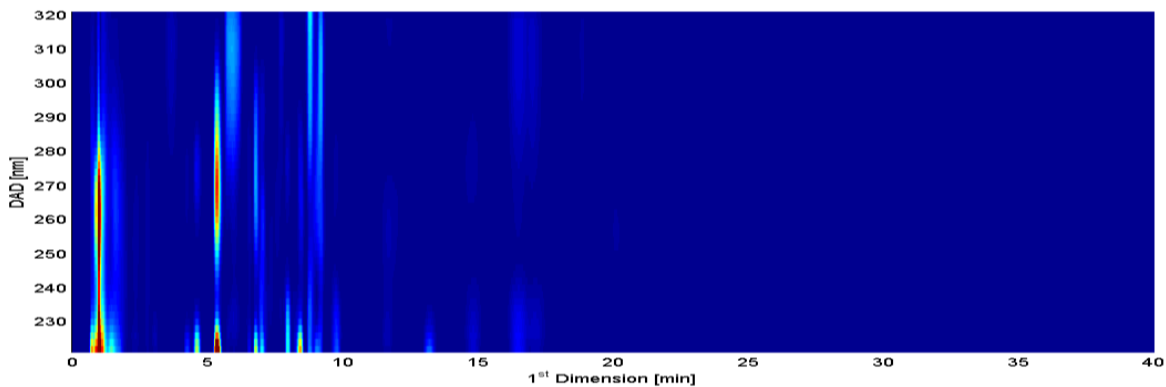


Figure 32: Chromatogram obtained by optimization in the 1D (10% of MeOH_i; 46.43mM [PPB]_i; 2 t_i; 50.00% of MeOH_f; 7.44mM [PPB]_f; 4 t_f).

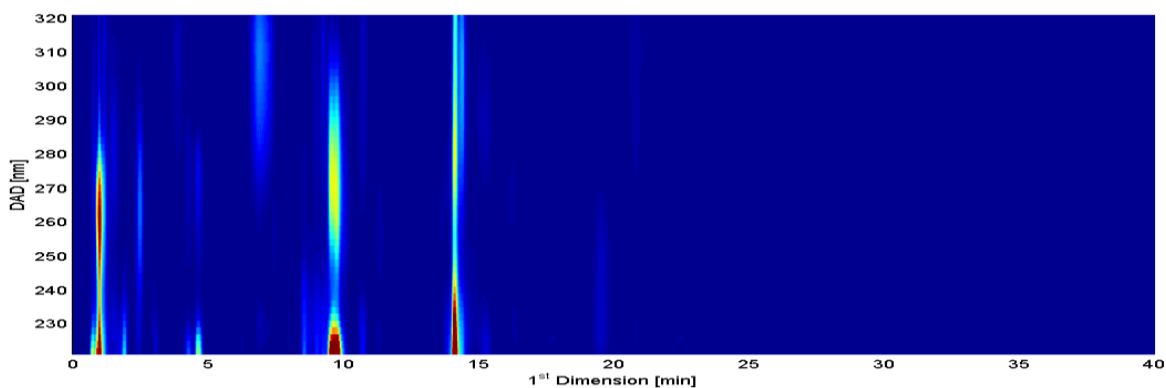


Figure 33: Chromatogram obtained by optimization in the 1D (10% of MeOH_i; 50mM [PPB]_i; 3 t_i; 40.00% of MeOH_f; 10mM [PPB]_f; 6 t_f).

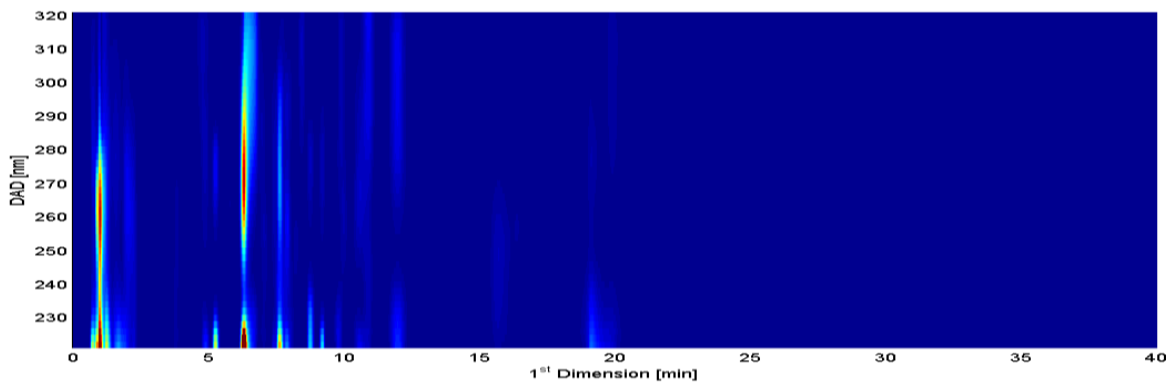


Figure 34: Chromatogram obtained by optimization in the 1D (7.46% of MeOH_i; 40mM [PPB]_i; 2.46 t_i; 40.00% of MeOH_f; 10mM [PPB]_f; 4 t_f).

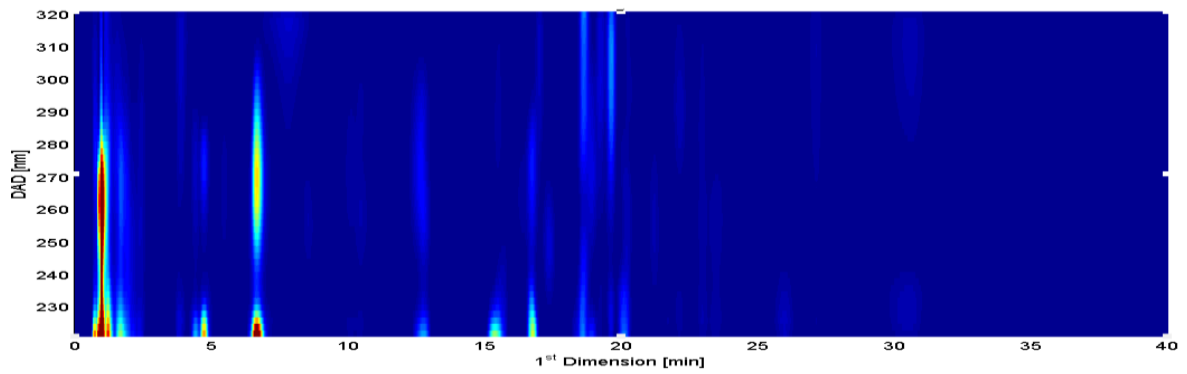


Figure 35: Chromatogram obtained by optimization in the 1D (9.39% of MeOH_i, 40mM [PPB]_i, 2 t_i, 40%MeOH_f, 5mM [PPB]_f, and 4 t_f).

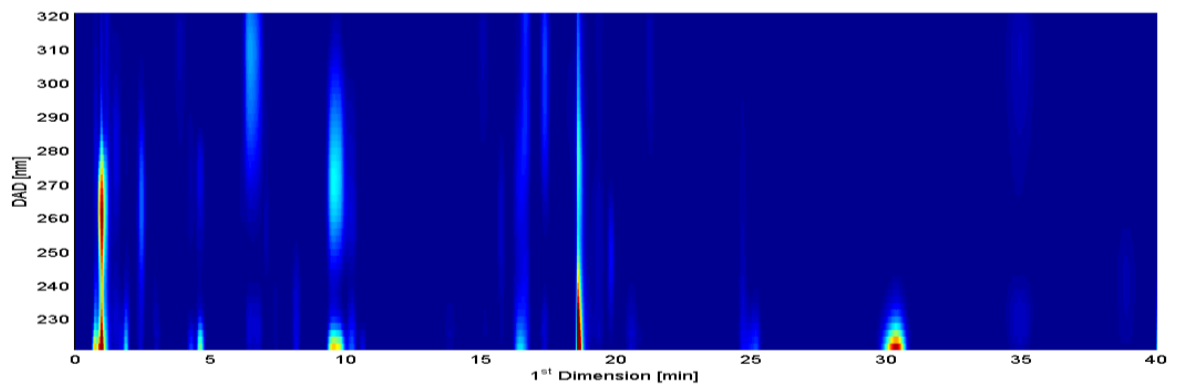


Figure 36: Chromatogram obtained by optimization in the 1D (10% of MeOH_i, 50mM [PPB]_i, 3 t_i, 50%MeOH_f, 5mM [PPB]_f, and 4 t_f).

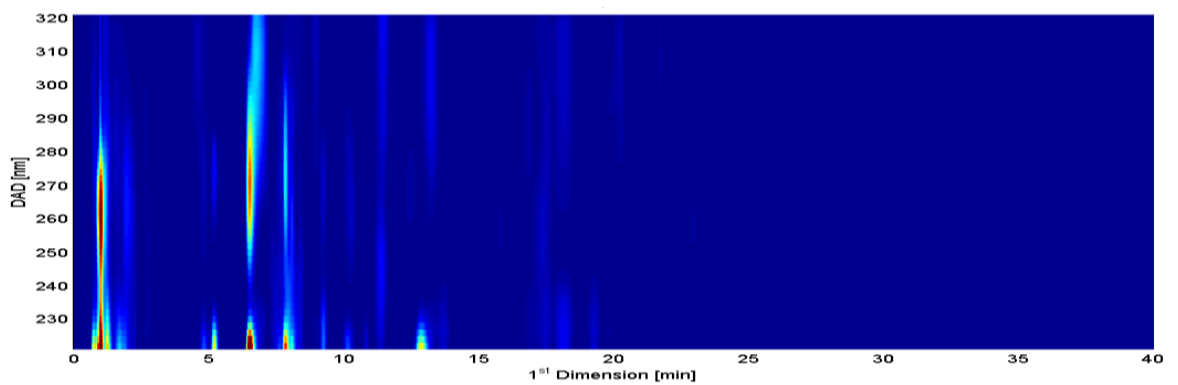


Figure 37: Chromatogram obtained by optimization in the 1D (7.75% of MeOH_i, 45.93mM [PPB]_i, 2.48 t_i, 50%MeOH_f, 10mM [PPB]_f, and 5.03 t_f).

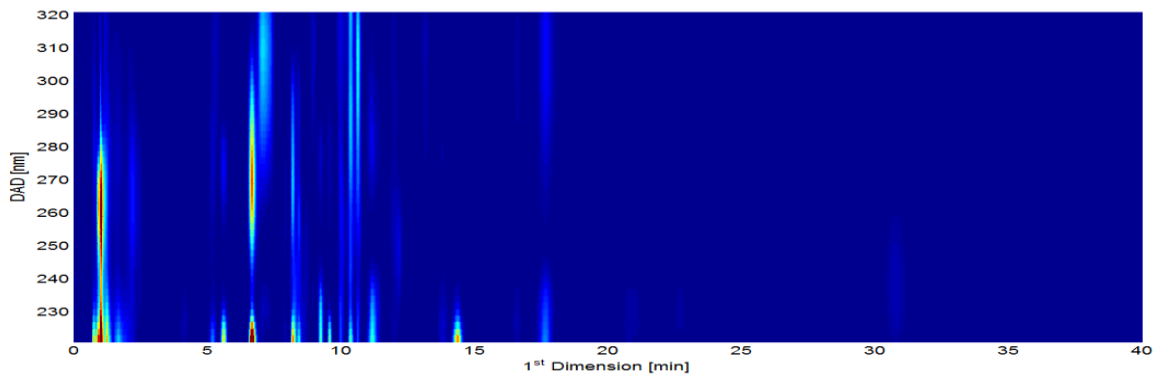


Figure 38: Chromatogram obtained by optimization in the ¹D (5% of MeOH_i, 50mM [PPB]_i, 2 t_i, 46.55% MeOH_f, 5mM [PPB]_f, and 6 t_f).

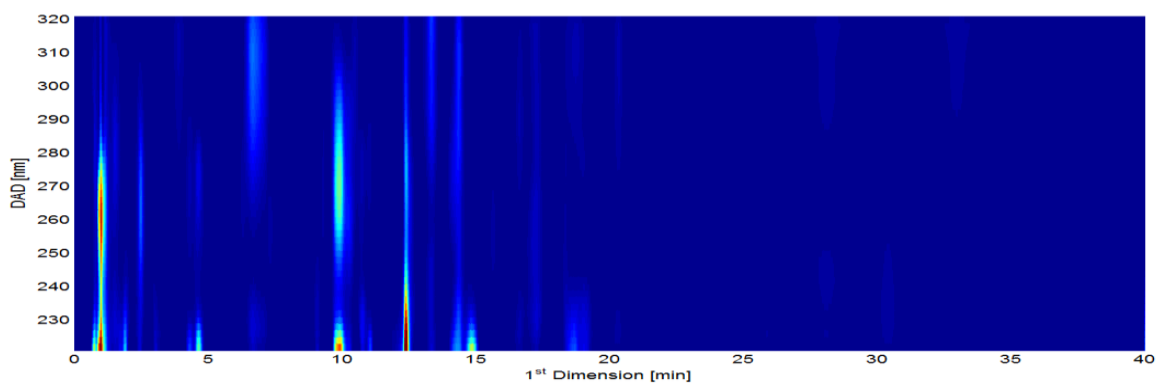


Figure 39: Chromatogram obtained by optimization in the ¹D (10% of MeOH_i, 50mM [PPB]_i, 3 t_i, 50% MeOH_f, 5mM [PPB]_f, and 4 t_f).

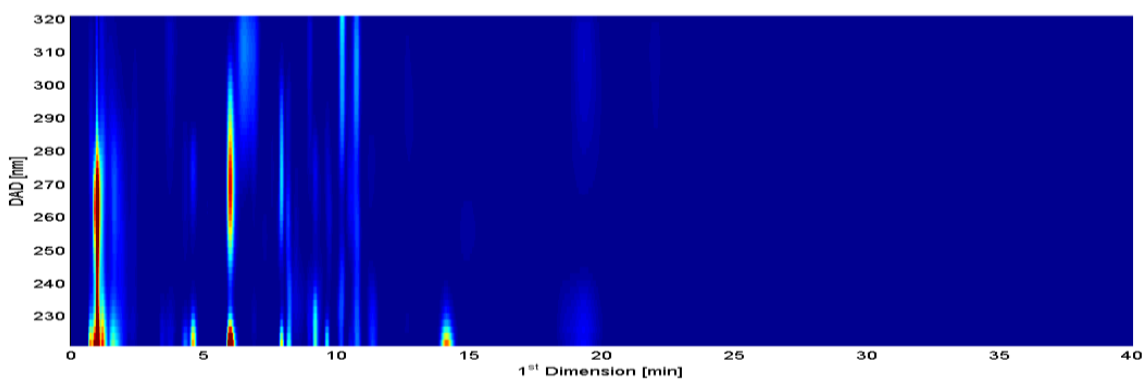


Figure 40: Chromatogram obtained by optimization in the ¹D (10% of MeOH_i, 40mM [PPB]_i, 2.55 t_i, 40% MeOH_f, 7.88mM [PPB]_f, and 6 t_f).

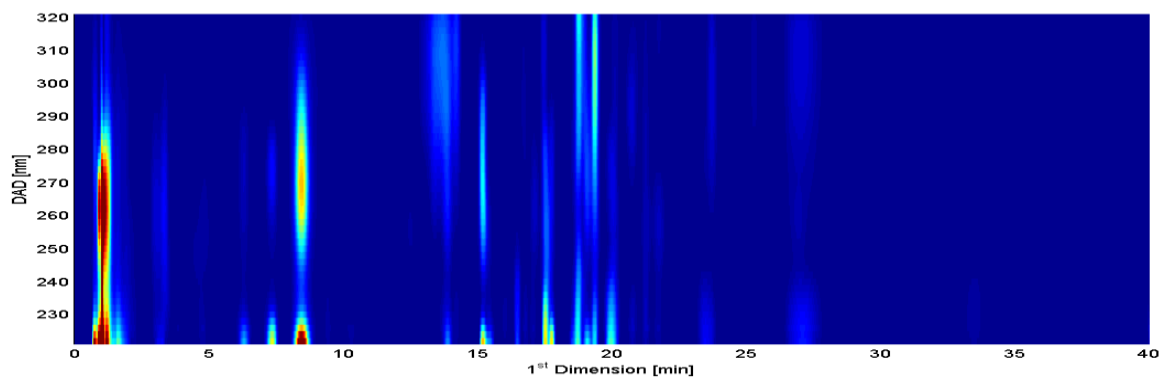


Figure 41: Chromatogram obtained by optimization in the ¹D (5% of MeOH_i, 50mM [PPB]_i, 2 t_i, 50%MeOH_f, 5mM [PPB]_f, and 4 t_f).

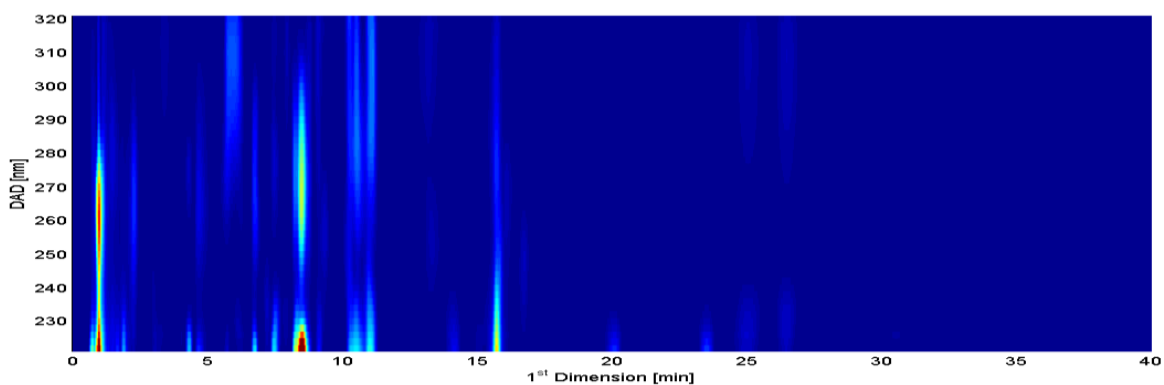


Figure 42: Chromatogram obtained by optimization in the ¹D (10% of MeOH_i, 50mM [PPB]_i, 2.36 t_i, 44.49%MeOH_f, 10mM [PPB]_f, and 4 t_f).

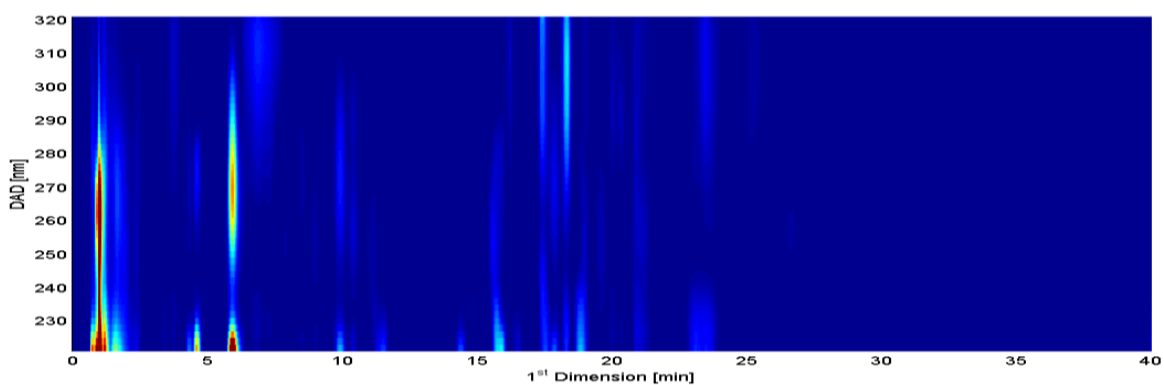


Figure 43: Chromatogram obtained by optimization in the ¹D (10% of MeOH_i, 40mM [PPB]_i, 2 t_i, 50%MeOH_f, 5mM [PPB]_f, and 6 t_f).

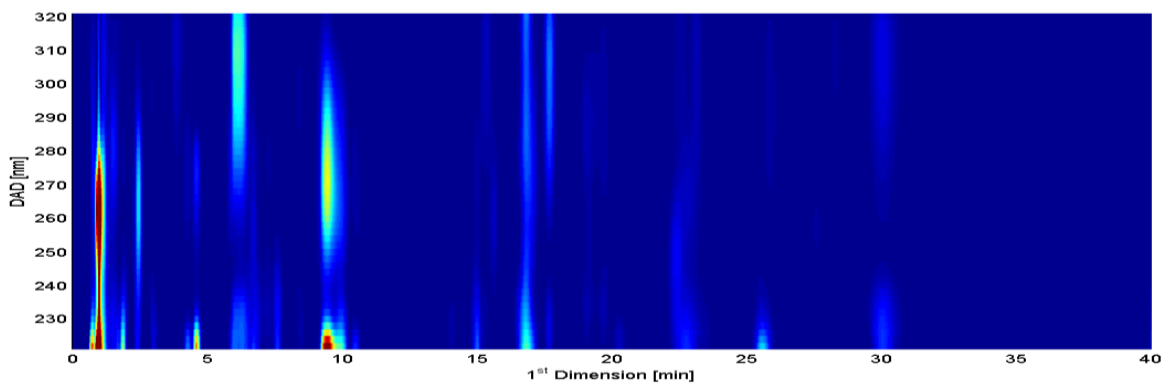


Figure 44: Chromatogram obtained by optimization in the ¹D (10% of MeOH_i, 50 mM [PPB]_i, 2.36 t_i, 44.49% MeOH_f, 10mM [PPB]_f, and 4 t_f).

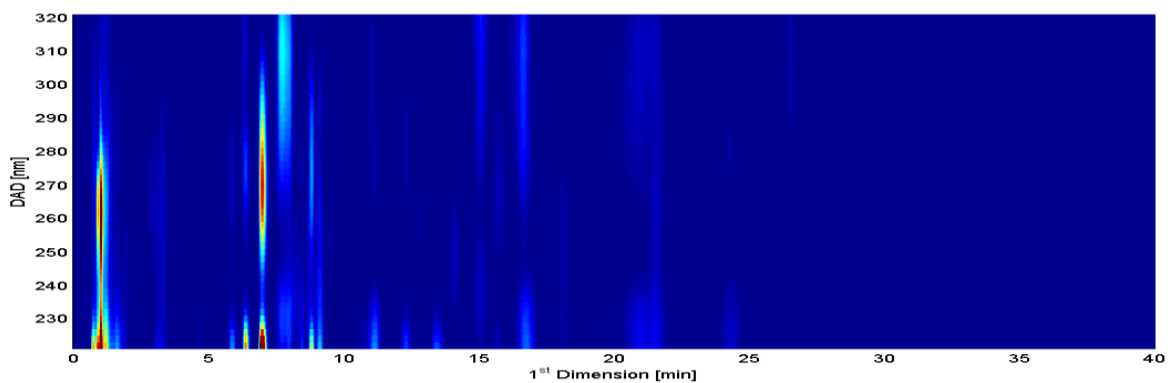


Figure 45: Chromatogram obtained by optimization in the ¹D (5% of MeOH_i, 50 mM [PPB]_i, 2 t_i, 40% MeOH_f, 8.34mM [PPB]_f, and 6 t_f).

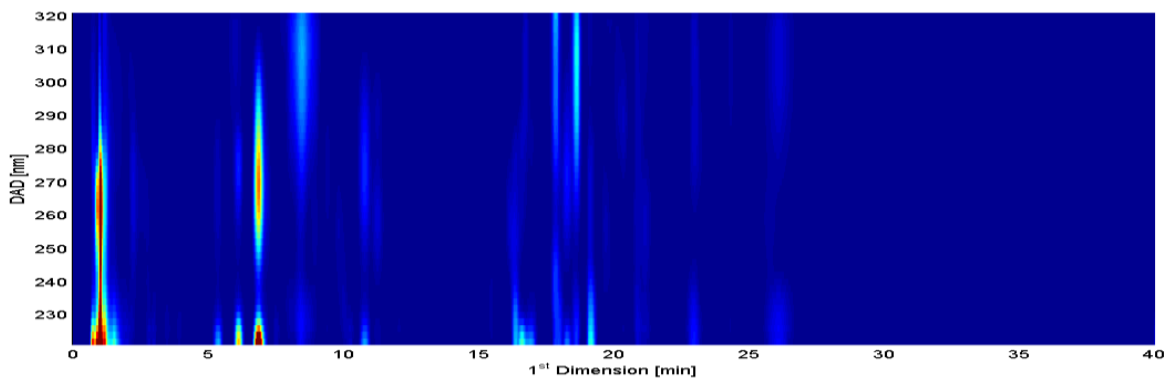


Figure 46: Chromatogram obtained by optimization in the ¹D (5% of MeOH_i, 40 mM [PPB]_i, 3 t_i, 50% MeOH_f, 10mM [PPB]_f, and 6 t_f).

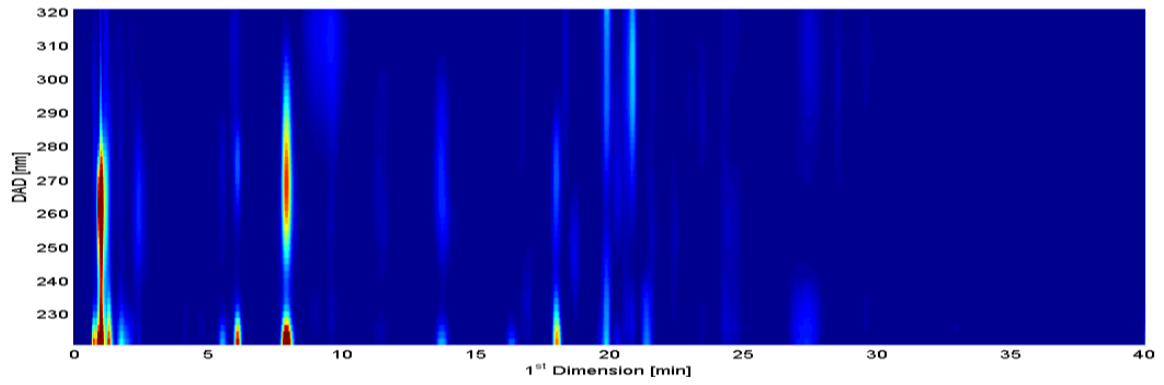


Figure 47: Chromatogram obtained by optimization in the ²D (5% of MeOH_i, 40mM [PPB]_i, 3 t_i, 40%MeOH_f, 10mM [PPB]_f, and 4 t_f).

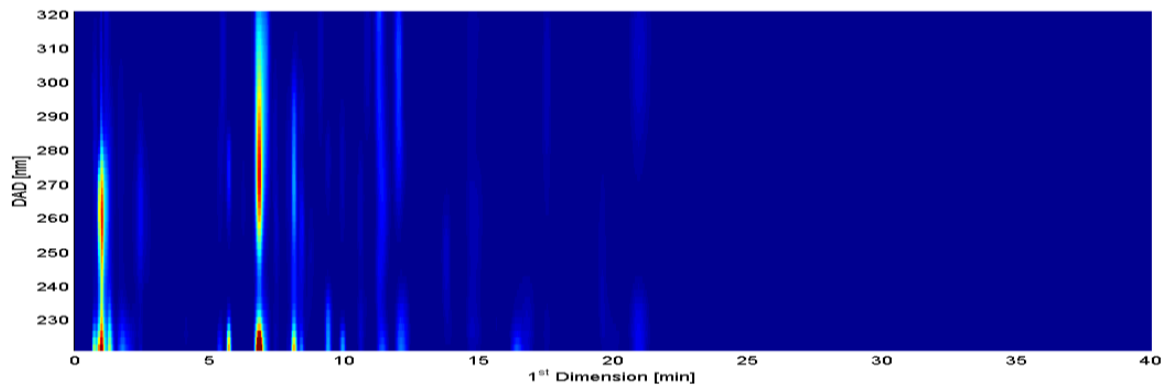


Figure 48: Chromatogram obtained by optimization in the ¹D (5% of MeOH_i, 40mM [PPB]_i, 2 t_i, 50%MeOH_f, 10mM [PPB]_f, and 4 t_f).

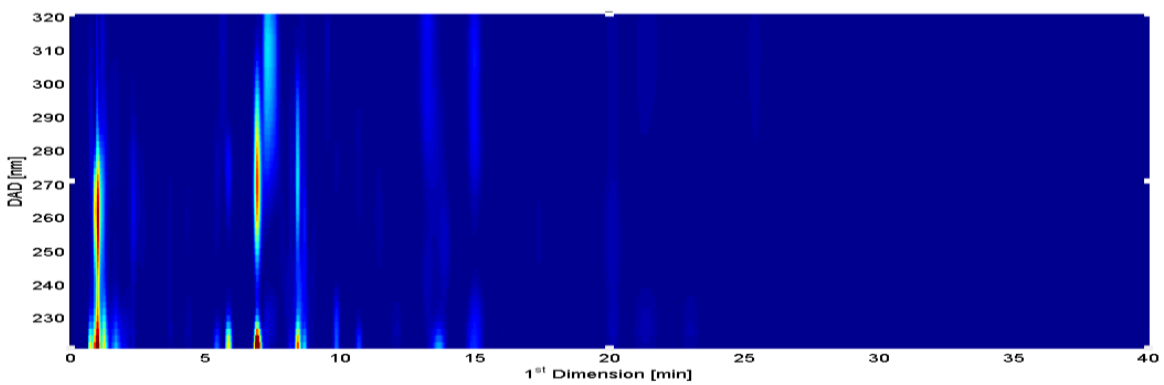


Figure 49: Chromatogram obtained by optimization in the ¹D (5% of MeOH_i, 43.21mM [PPB]_i, 2 t_i, 40%MeOH_f, 5mM [PPB]_f, and 6 t_f).

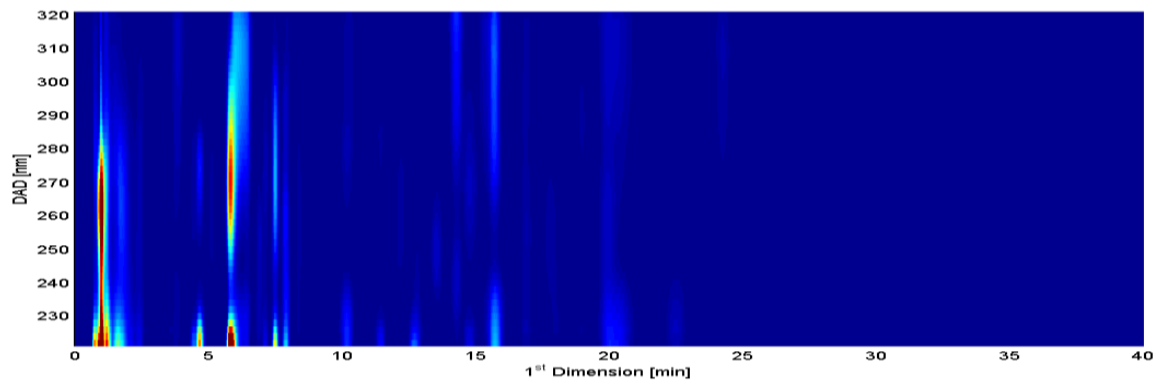


Figure 50: Chromatogram obtained by optimization in the ¹D (9.69% of MeOH_i, 50 mM [PPB]_i, 2.08 t_i, 41.23% MeOH_f, 5.41mM [PPB]_f, and 4 t_f).

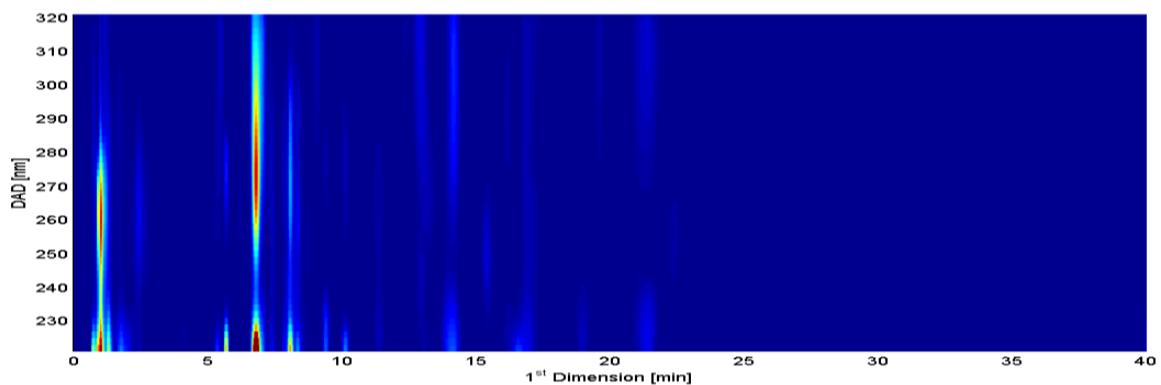


Figure 51: Chromatogram obtained by optimization in the ¹D (5% of MeOH_i, 40 mM [PPB]_i, 2 t_i, 50% MeOH_f, 10mM [PPB]_f, and 4 t_f).

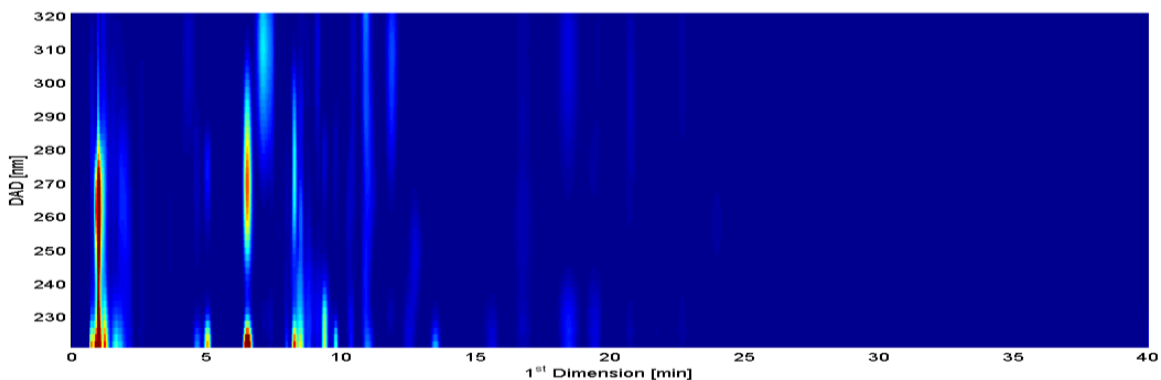


Figure 52: Chromatogram obtained by optimization in the ¹D (8.09% of MeOH_i, 40 mM [PPB]_i, 3 t_i, 50% MeOH_f, 7.05mM [PPB]_f, and 5.66 t_f).

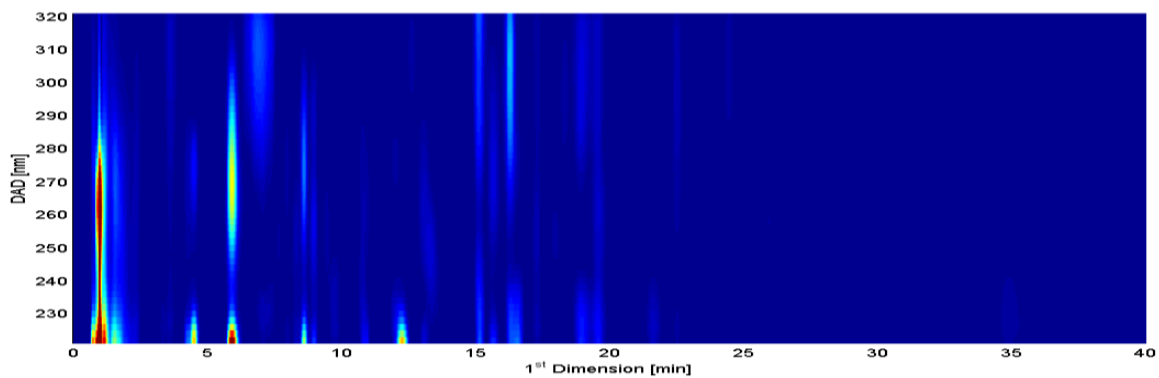


Figure 53: Chromatogram obtained by optimization in the ¹D (10% of MeOH_i, 45.49mM [PPB]_i, 3 t_i, 47.%MeOH_f, 5mM [PPB]_f, and 6 t_f).

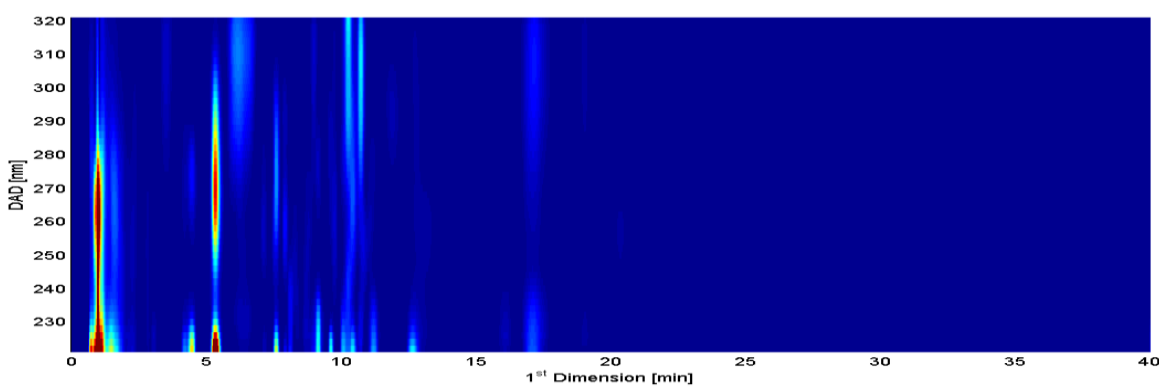


Figure 54: Chromatogram obtained by optimization in the ¹D (10% of MeOH_i, 50mM [PPB]_i, 2 t_i, 50%MeOH_f, 10mM [PPB]_f, and 6 t_f).

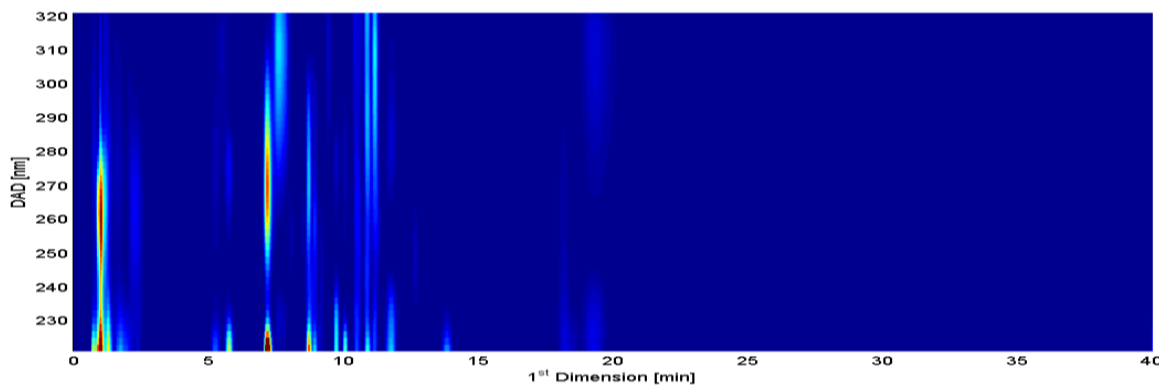


Figure 55: Chromatogram obtained by optimization in the ²D (5.70% of MeOH_i, 40mM [PPB]_i, 2.89 t_i, 40%MeOH_f, 10mM [PPB]_f, and 6 t_f).

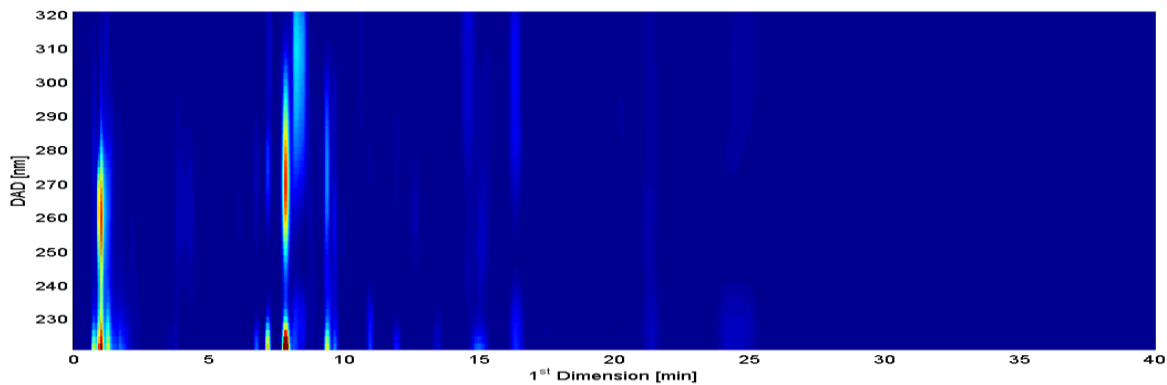


Figure 56: Chromatogram obtained by optimization in the 1D (5% of MeOH_i, 50 mM [PPB]_i, 3 t_i, 40% MeOH_f, 5mM [PPB]_f, and 4.97 t_f).

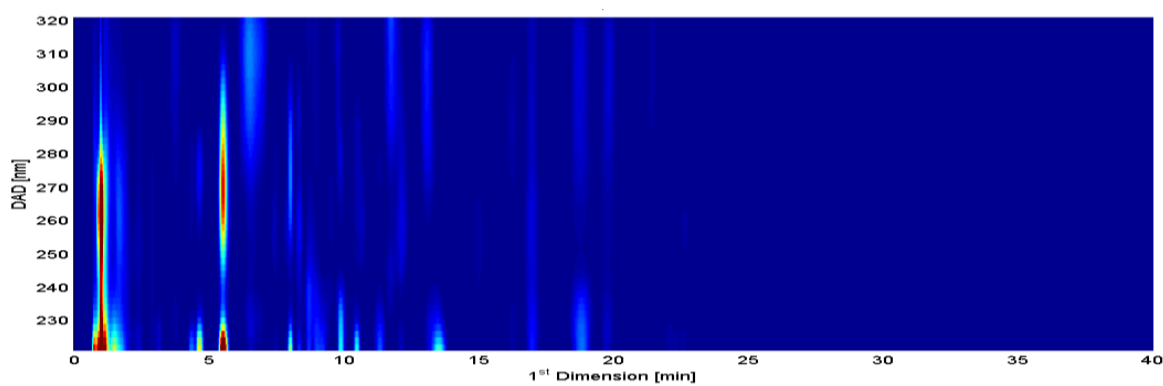


Figure 57: Chromatogram obtained by optimization in the 1D (10% of MeOH_i, 50 mM [PPB]_i, 2 t_i, 50% MeOH_f, 10mM [PPB]_f, and 6 t_f).

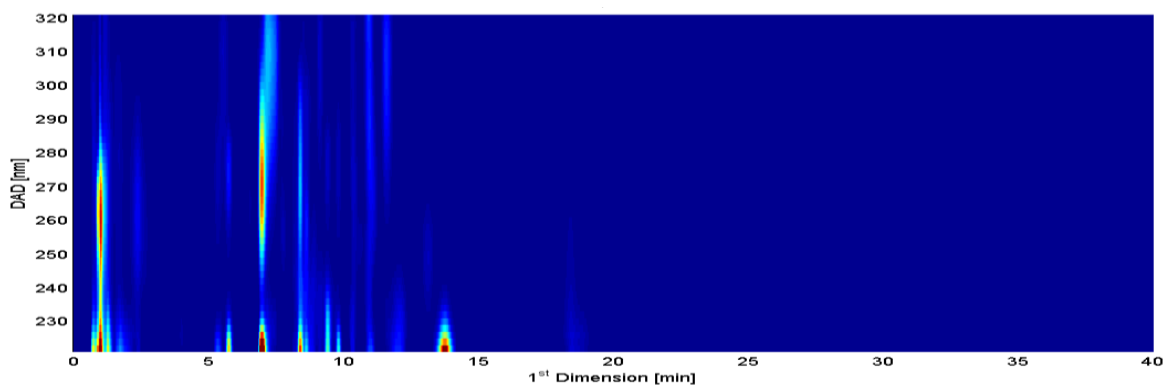


Figure 58: Chromatogram obtained by optimization in the 1D (5% of MeOH_i, 40 mM [PPB]_i, 2 t_i, 50% MeOH_f, 5mM [PPB]_f, and 6 t_f).

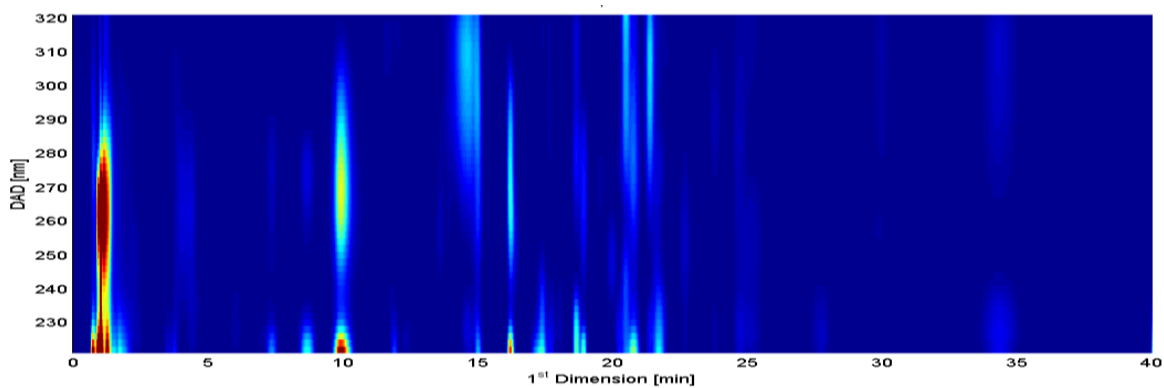


Figure 59: Chromatogram obtained by optimization in the 1D (5% of MeOH_i, 50mM [PPB]_i, 2.44 t_i, 40%MeOH_f, 5mM [PPB]_f, and 4 t_f).

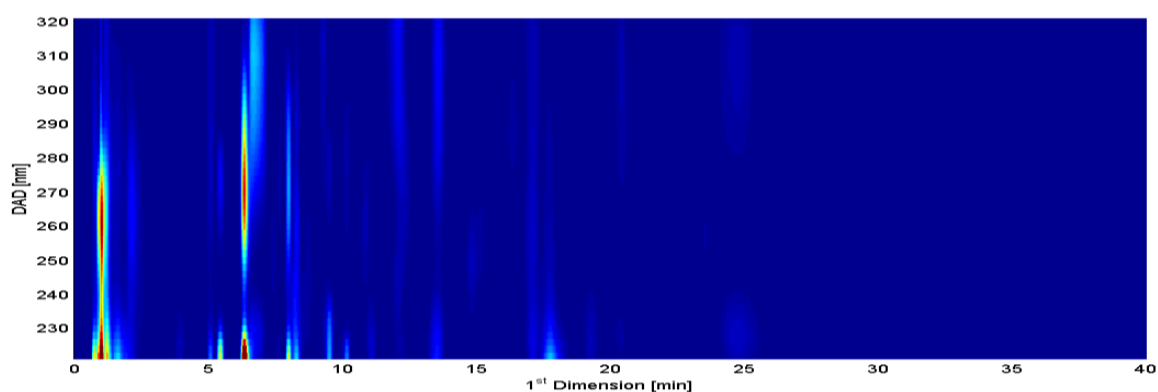


Figure 60: Chromatogram obtained by optimization in the 1D (6.63% of MeOH_i, 40mM [PPB]_i, 2 t_i, 49.22%MeOH_f, 5mM [PPB]_f, and 4 t_f).

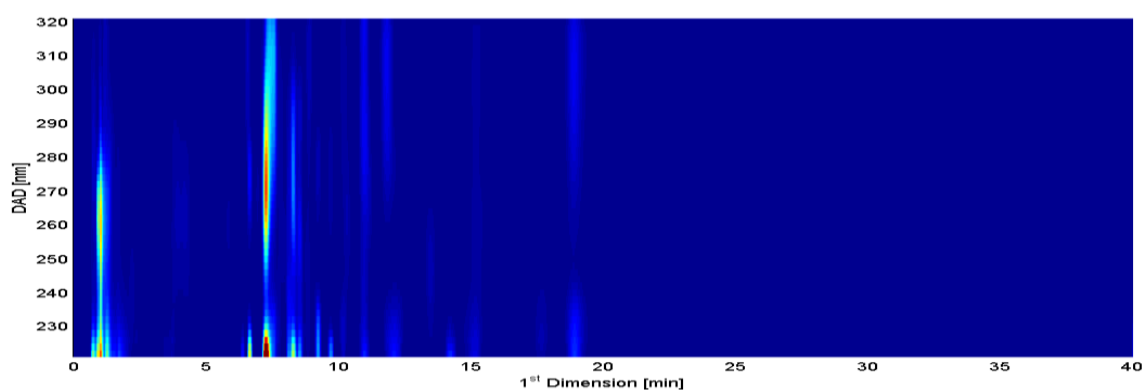


Figure 61: Chromatogram obtained by optimization in the 1D (5% of MeOH_i, 50mM [PPB]_i, 3 t_i, 50%MeOH_f, 10mM [PPB]_f, and 4 t_f).

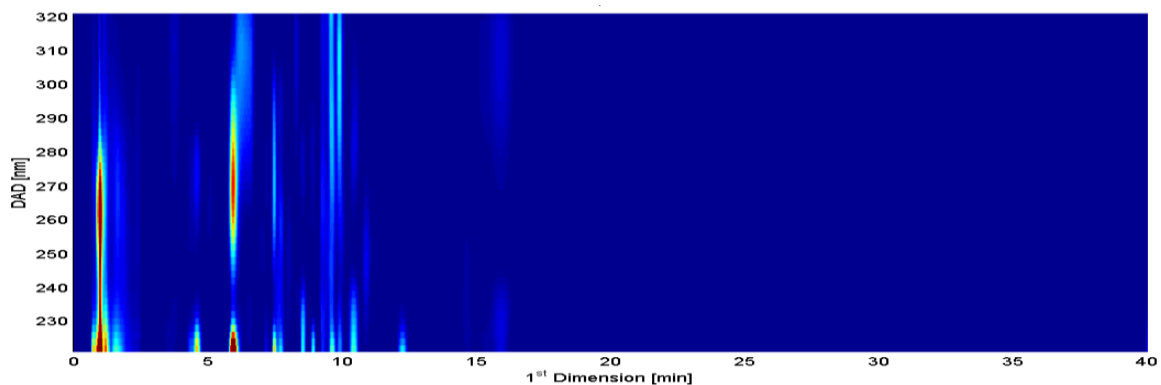


Figure 62: Chromatogram obtained by optimization in the ¹D (10% of MeOH_i, 43.29 mM [PPB]_i, 2 t_i, 40% MeOH_f, 10mM [PPB]_f, and 4.97 t_f).

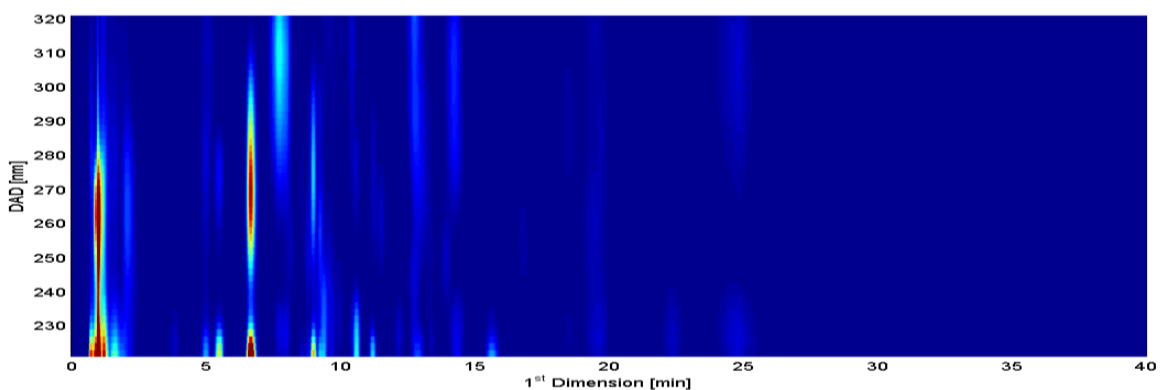


Figure 63: Chromatogram obtained by optimization in the ¹D (6.63% of MeOH_i, 40 mM [PPB]_i, 3 t_i, 40% MeOH_f, 5mM [PPB]_f, and 6 t_f).

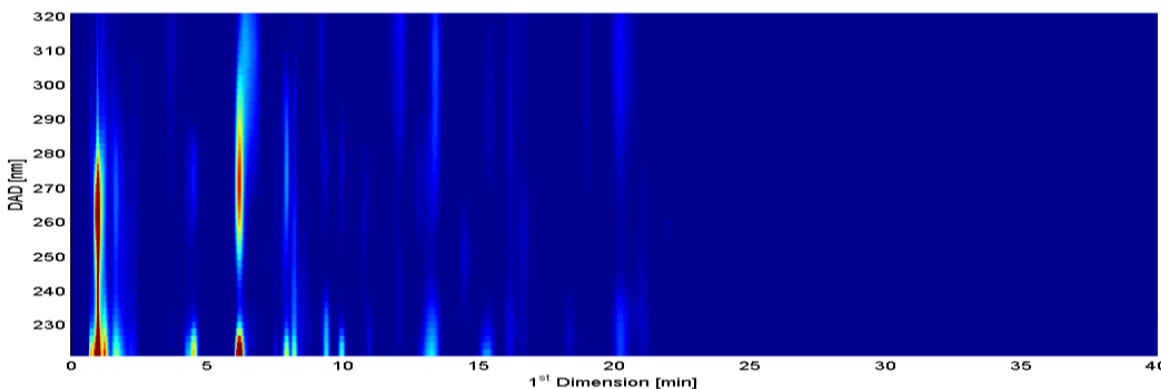


Figure 64: Chromatogram obtained by optimization in the ¹D (10% of MeOH_i, 40mM [PPB]_i, 3 t_i, 50% MeOH_f, 10mM [PPB]_f, and 4 t_f).

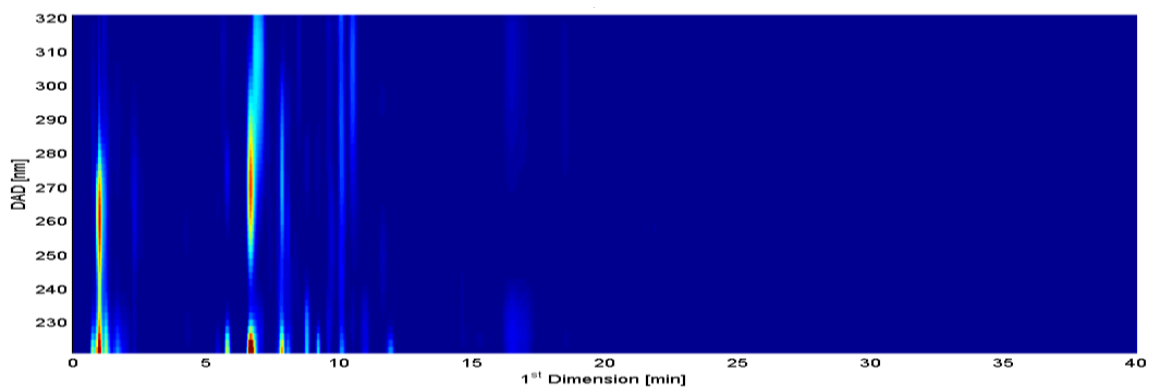


Figure 65: Chromatogram obtained by optimization in the ¹D (5% of MeOH_i, 50mM [PPB]_i, 3 t_i, 48.91%MeOH_f, 5mM [PPB]_f, and 4 t_f).

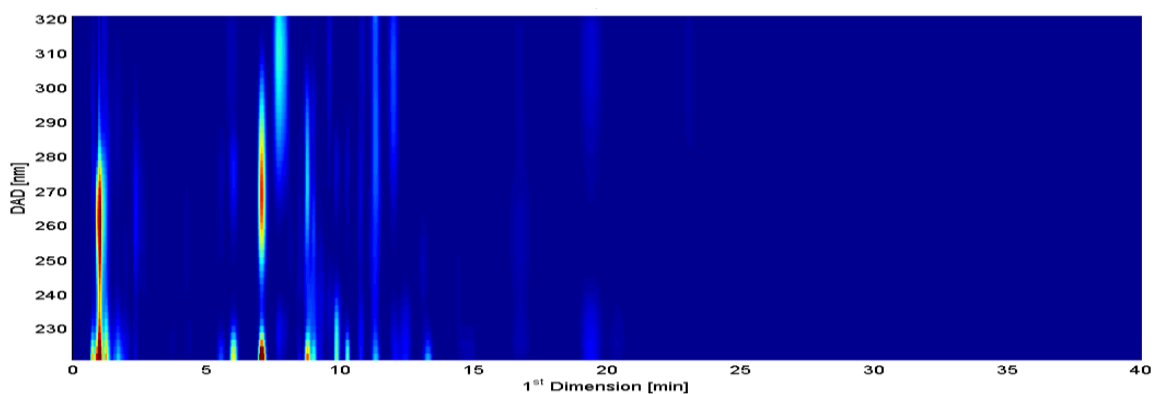


Figure 66: Chromatogram obtained by optimization in the ¹D (5% of MeOH_i, 50mM [PPB]_i, 2.76 t_i, 40%MeOH_f, 10mM [PPB]_f, and 6 t_f).

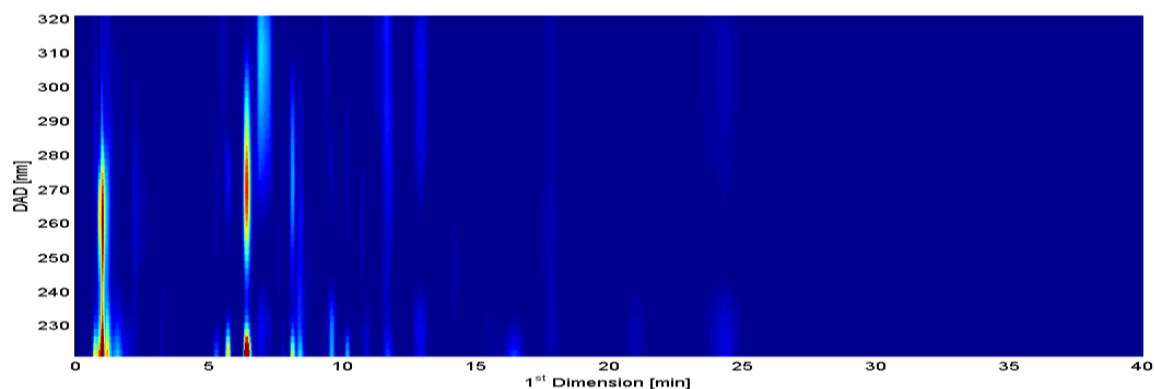


Figure 67: Chromatogram obtained by optimization in the ¹D (5% of MeOH_i, 40 mM [PPB]_i, 2 t_i, 40%MeOH_f, 6.91mM [PPB]_f, and 4.42 t_f).

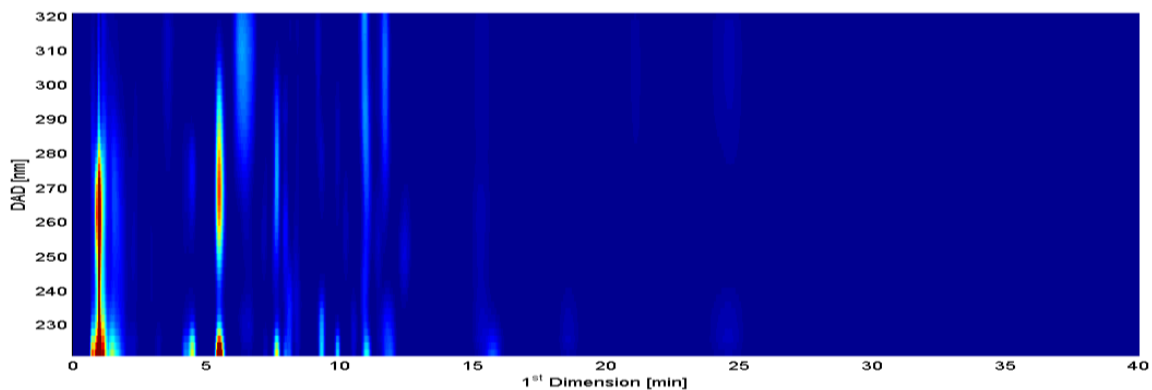


Figure 68: Chromatogram obtained by optimization in the ¹D (10% of MeOH_i, 44.29 mM [PPB]_i, 3 t_i, 40% MeOH_f, 5mM [PPB]_f, and 4 t_f).

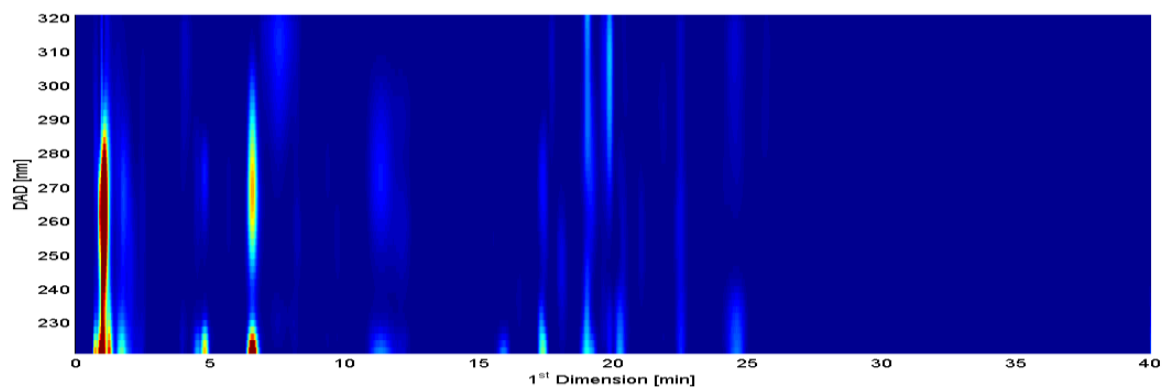


Figure 69: Chromatogram obtained by optimization in the ¹D (8.72% of MeOH_i, 40mM [PPB]_i, 2 t_i, 44.72% MeOH_f, 10mM [PPB]_f, and 6 t_f).

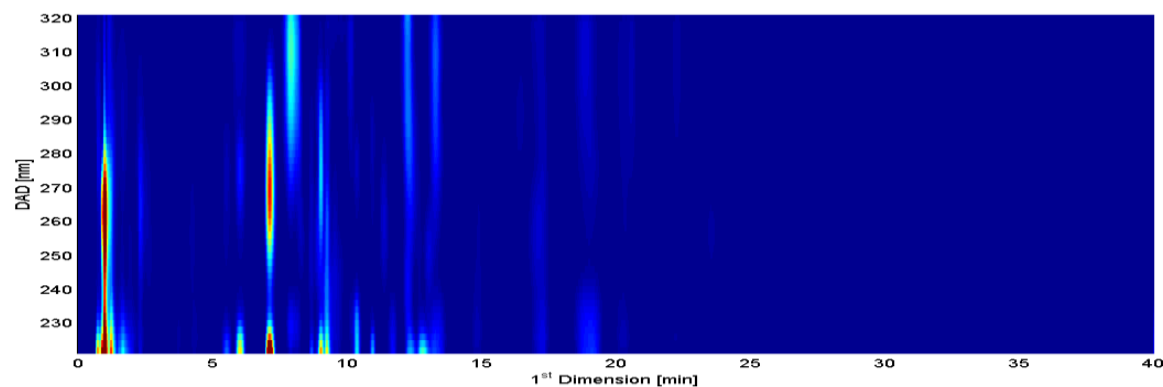


Figure 70: Chromatogram obtained by optimization in the ¹D (5% of MeOH_i, 50mM [PPB]_i, 3 t_i, 50% MeOH_f, 5mM [PPB]_f, and 6 t_f).

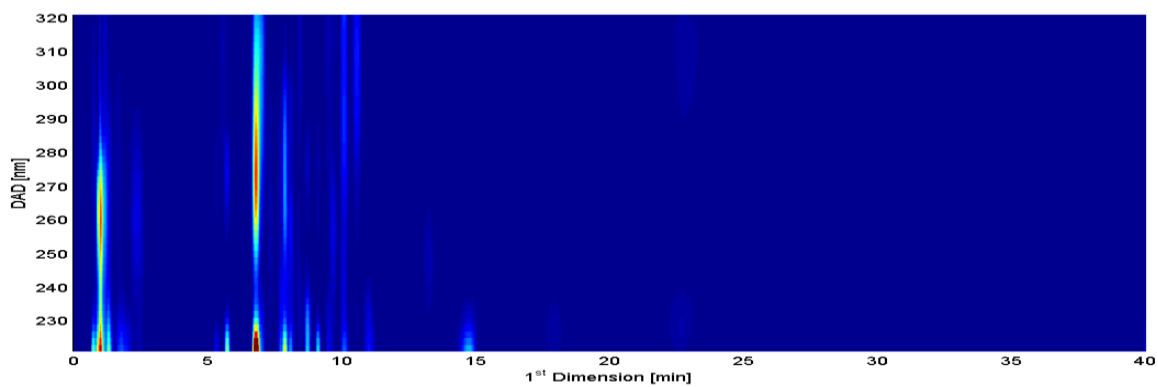


Figure 71: Chromatogram obtained by optimization in the 1^{D} (5.39% of MeOH_i, 40.31mM [PPB]_i, 2.91 t_i, 40%MeOH_f, 5mM [PPB]_f, and 4.03 t_f).

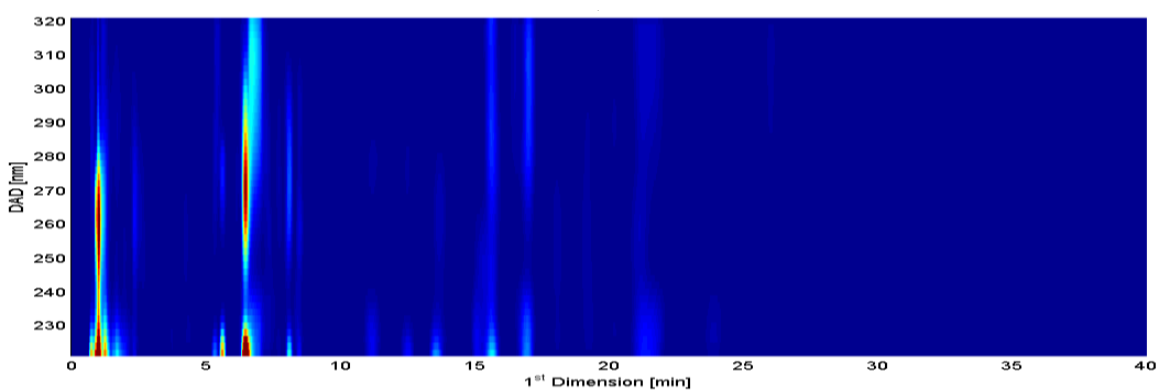


Figure 72: Chromatogram obtained by optimization in the 1^{D} (5% of MeOH_i, 50mM [PPB]_i, 2 t_i, 40%MeOH_f, 10mM [PPB]_f, and 4 t_f).

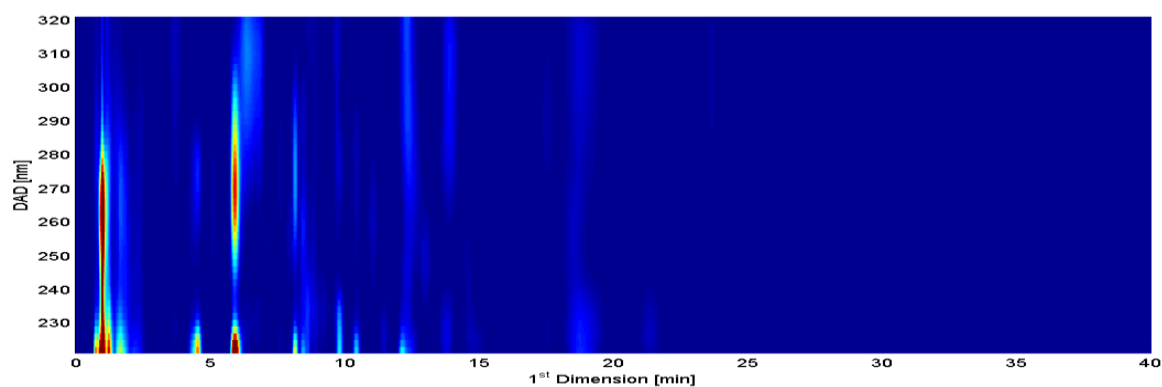


Figure 73: Chromatogram obtained by optimization in the 1^{D} (10% of MeOH_i, 50mM [PPB]_i, 2 t_i, 40%MeOH_f, 5mM [PPB]_f, and 6 t_f).

a

Annex B: Optimization of the 2D for the LC \times LC

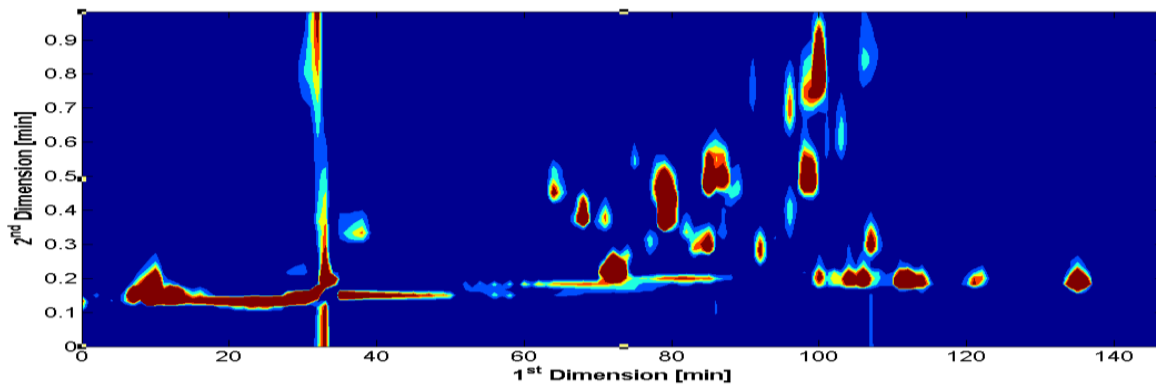


Figure 74: Chromatogram obtained by optimization in the ²D (25% of MeOH_i, and 25% MeOH_f).

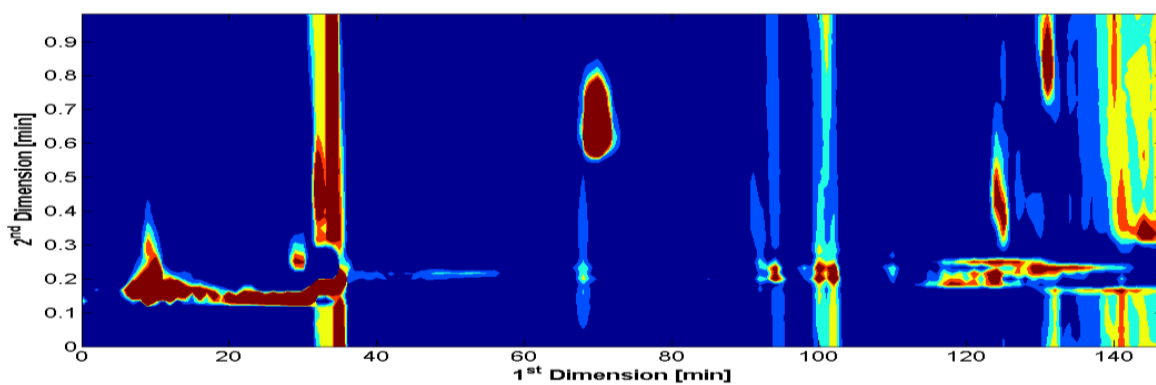


Figure 75: Chromatogram obtained by optimization in the ²D (35% of MeOH_i, and 28% MeOH_f).

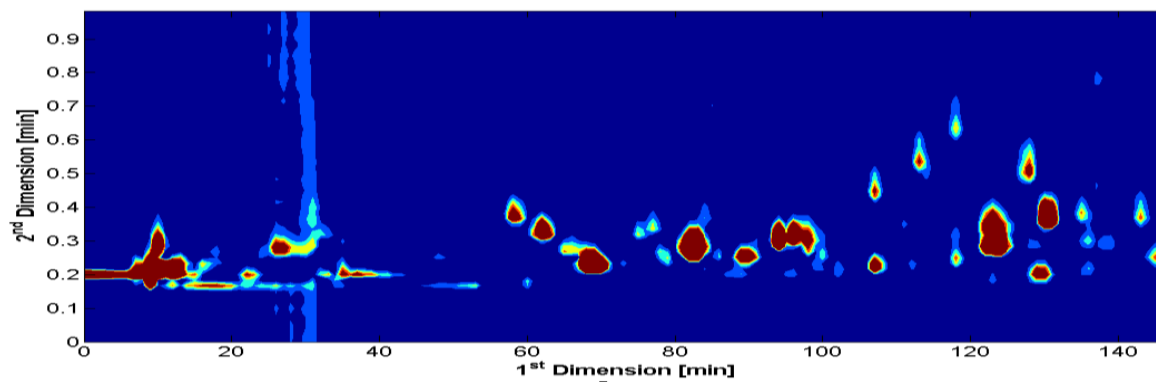


Figure 76: Chromatogram obtained by optimization in the ²D (28% of MeOH_i, and 35% MeOH_f).

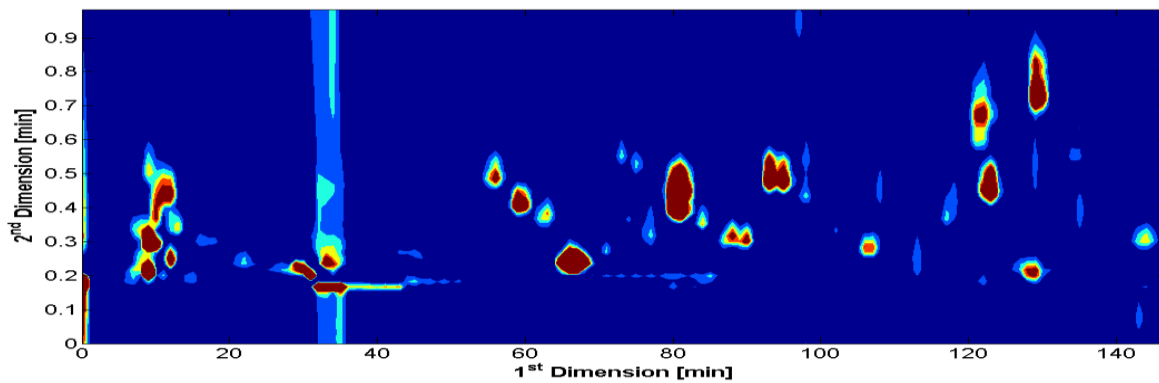


Figure 77: Chromatogram obtained by optimization in the ²D (18% of MeOH_i, and 32% MeOH_f).

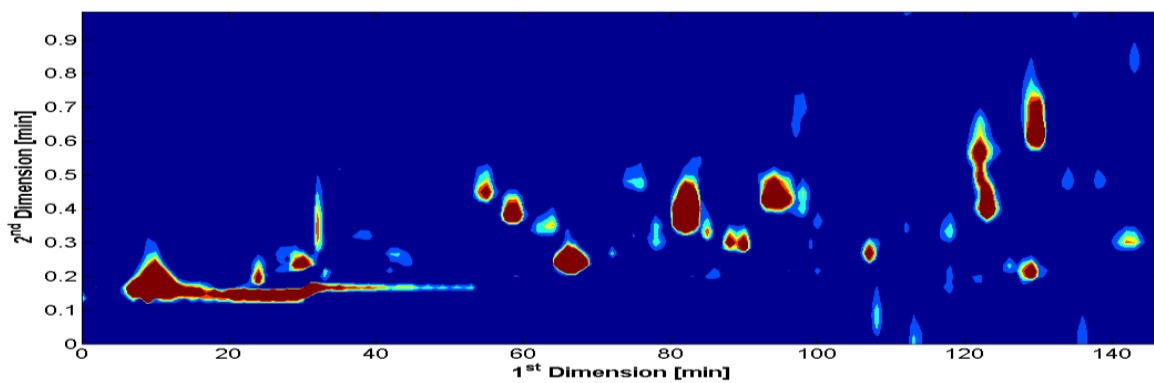


Figure 78: Chromatogram obtained by optimization in the ²D (10% of MeOH_i, and 34% MeOH_f).

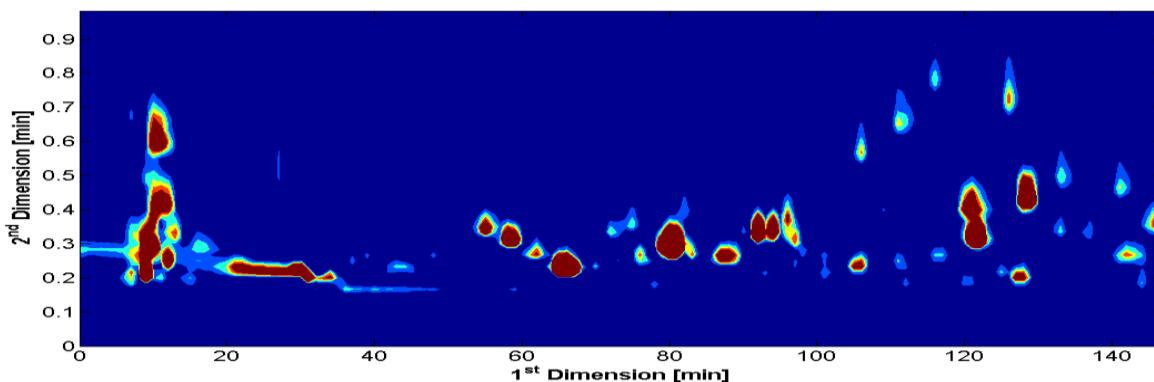


Figure 79: Chromatogram obtained by optimization in the ²D (21% of MeOH_i, and 42% MeOH_f).

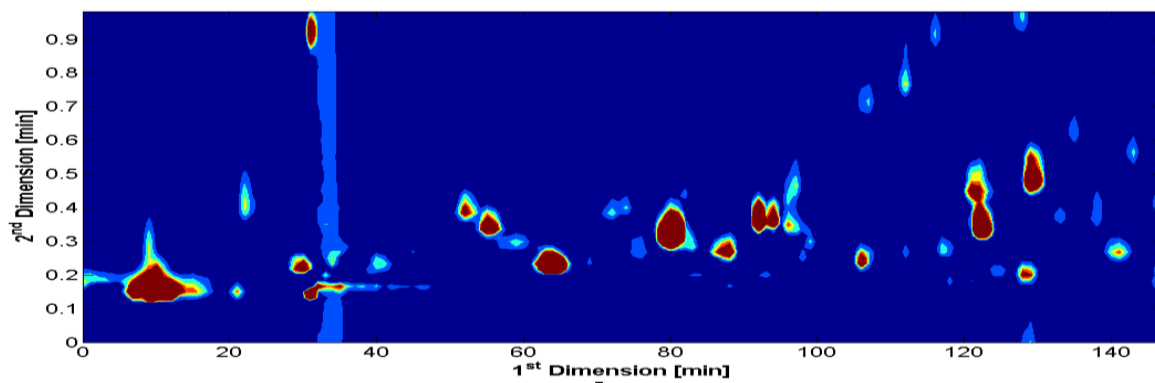


Figure 80: Chromatogram obtained by optimization in the 2D (11% of MeOH_i, and 39% MeOH_f).

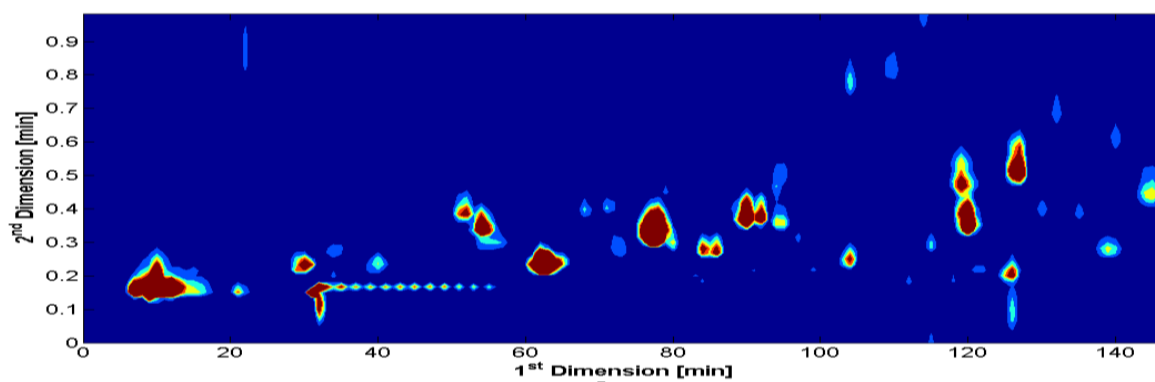


Figure 81: Chromatogram obtained by optimization in the 2D (15% of MeOH_i, and 38% MeOH_f).

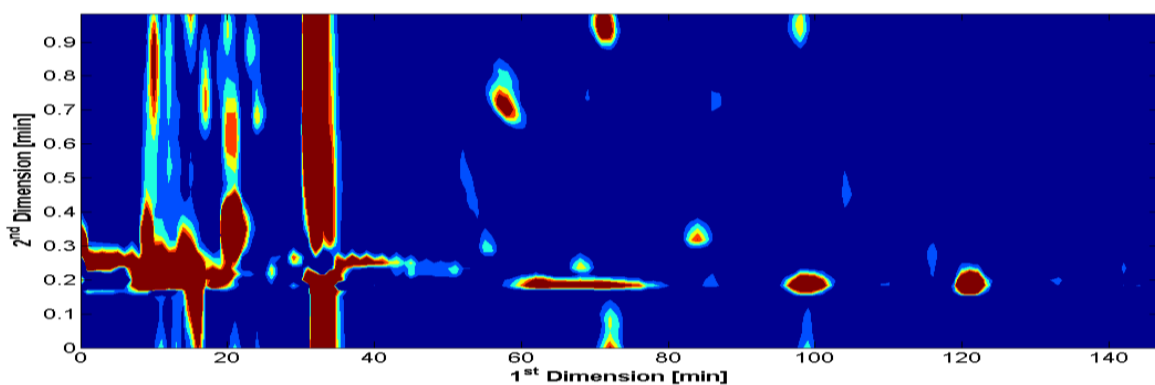


Figure 82: Chromatogram obtained by optimization in the 2D (12% of MeOH_i, and 28% MeOH_f).

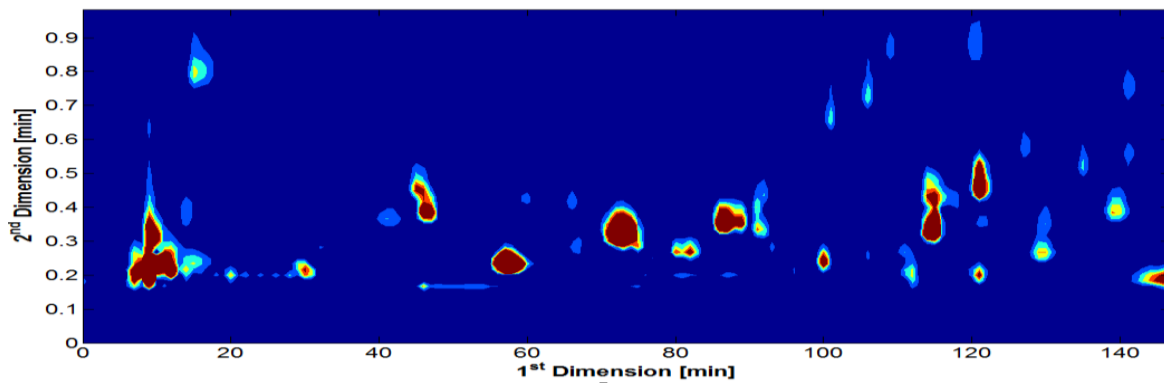


Figure 83: Chromatogram obtained by optimization in the ²D (19% of MeOH_i, and 39% MeOH_f).

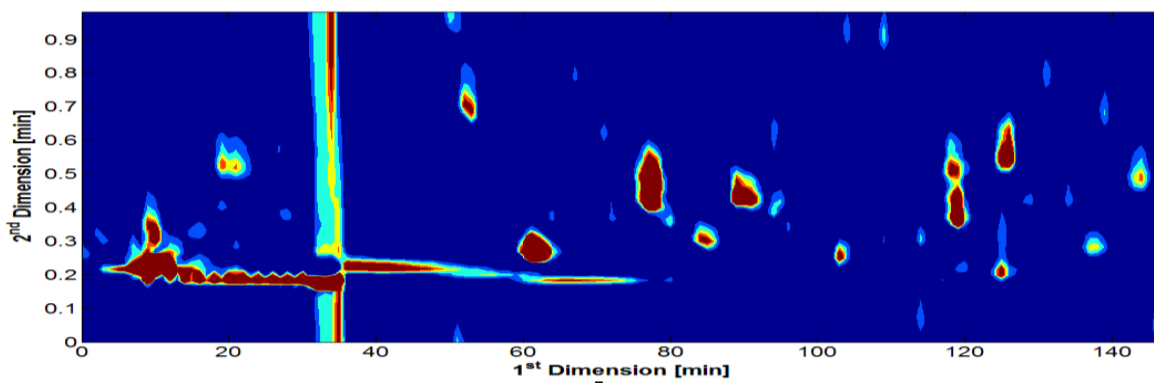


Figure 84: Chromatogram obtained by optimization in the ²D (22% of MeOH_i, and 33% MeOH_f).

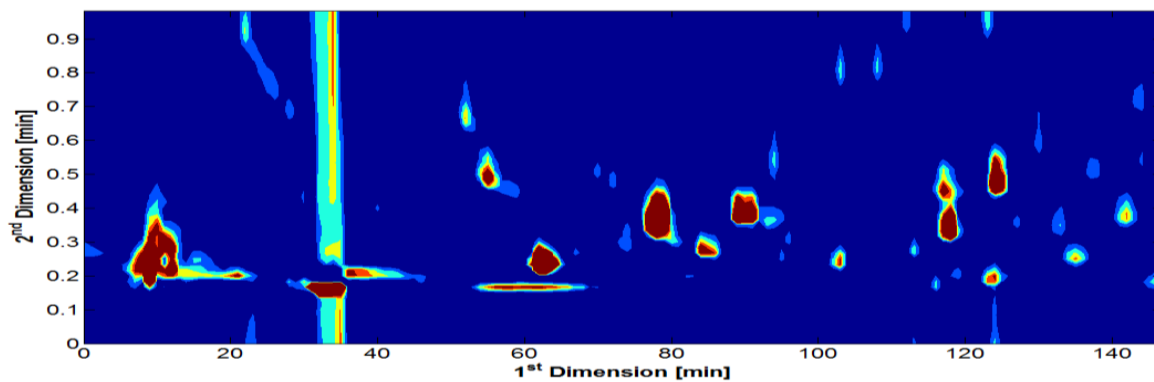


Figure 85: Chromatogram obtained by optimization in the ²D (17% of MeOH_i, and 37% MeOH_f).

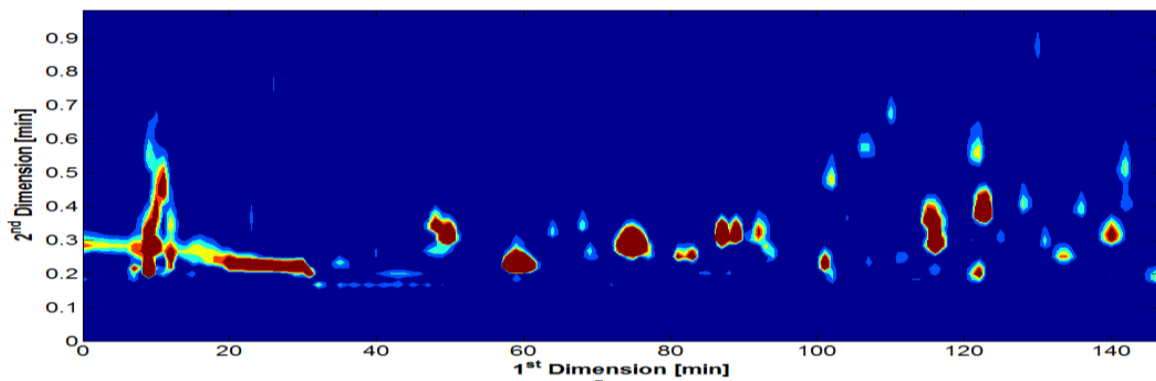


Figure 86: Chromatogram obtained by optimization in the 2D (18% of MeOH_i, and 44% MeOH_f).

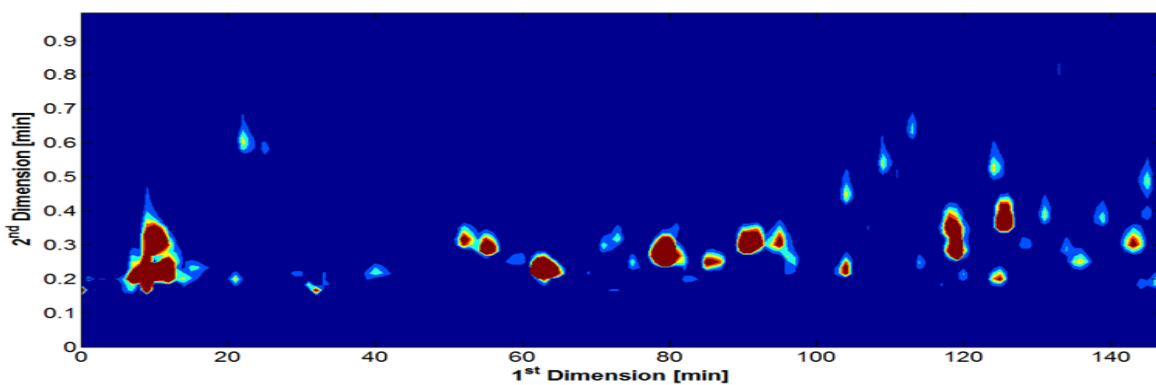


Figure 87: Chromatogram obtained by optimization in the 2D (20% of MeOH_i, and 46% MeOH_f).